Dissertation

submitted to the

Combined Faculties for the Natural Sciences and for Mathematics

of the Ruperto-Carola University of Heidelberg, Germany

for the degree of

Doctor of Natural Sciences

presented by

Master of Science: Godwin Kofi Dogbevia

Born in: Keta, Ghana

Oral-examination: 28th November 2011

Tetracycline-controlled inducible gene expression systems to manipulate neuronal circuits in the mammalian brain

Referees: Prof. Dr. Peter H. Seeburg

Dr. Rolf Sprengel

Erklärung gemäss § 7 (3) b) und c) der Promotionsordnung:

Ich erkläre hiermit, dass ich die vorgelegte Dissertation selbst verfasst und mich dabei keiner anderen als der von mir ausdrücklich bezeichneten Quellen und Hilfen bedient habe. Desweiteren erkläre ich hiermit, dass ich an keiner anderen Stelle ein Prüfungsverfahren beantragt bzw. die Dissertation in dieser oder anderer Form bereits anderweitig als Prüfungsarbeit verwendet oder einer anderen Fakultät als Dissertation vorgelegt habe.

Heidelberg, 29th September 2011. Godwin Kofi Dogbevia

To my mother

ACKNOWLEDGEMENT

This study was done in the laboratory of Prof. Dr. Peter H. Seeburg in the Max Planck Institute for Medical Research Heidelberg and was supported by the Max-Planck Gesselschaft and the University of Heidelberg. My deepest appreciation goes to Prof. Dr. Peter H. Seeburg for giving a working space in his laboratory and also for his supervisory role and scientific guidance. I would like to thank members of my thesis advisory committee; Prof. Dr. Peter H. Seeburg, Dr. Rolf Sprengel and Dr Soojin Ryu for their invaluable contribution to this thesis.

My gratitude goes to Dr. Rolf Sprengel for giving me the opportunity to join his group, for scientific guidance, patience and for providing funding for my stay in the institute.

I would like to sincerely thank Dr. Mazahir Hasan for his direct supervision and the guidance on the direction of this project. His unflinching support and believe that I can make it, even in difficult moments was a great motivation for me. His enthusiasm, dynamism and quest for success were the driving force behind the modest success achieved in this project. For the long hours spent together discussing the project, I say thank you.

My debt of gratitude goes to Dr. Miyoko Higuchi for her support, scientific and personal advice.

My appreciation goes to Dr. Georg Köhr, Dr. Mario Trevino, Dr. Valery Grinevich, Dr. Martin Schwarz, Dr. Günter Giese, Dr. Yair Pilpel, and Dr. Peter Pimpl for their help, support and advice.

My gratitude goes to my colleagues in Dr. Hasans' group: Finn Peters, Matthias Heindorf, Frauke Leitner, Katherina Spieler and Niclas Kneisel for their support and the

friendly atmosphere created in the lab.

I would like to Thank Annette Harold for her technical support, advice and the lovely atmosphere created in the lab.

Thanks to Sabine Grünewald, Simone Hundermer, Martina Lang, Hans Gaugler and Horst Grosskurth for their technical support.

I would like to thank Frau Gwenaëlle Matthies for her assistance with all the administrative works.
My appreciation goes to my lab colleagues: Dr. Wannan Tang, Dr. Verena Bosch, Dr. Liliana Layer, Dr. Simone Giese, Dr. Ilaria Bertocchi, Dr. Ying Yang, Pouya Balaghy-Mobin, Yiwei Chen, Ann-Marie Michalski, Dario Arcos-Diaz, Areej Albariri, Zhen Zeng, Sophie Knobloch, Lena Hoffmann, Inna Benhauser, Ling Zhang, Shi-Bin Li, Dan Du and Horst Obenhaus for the time shared together and the friendly atmosphere in the lab.

My appreciation goes to my African colleagues in Heidelberg for providing a 'home away from home'. And to all my friends who contributed in diverse ways to making my stay in Heidelberg a memorable one. Moments shared together with you will linger on forever.

My heart-felt gratitude goes to my sibling: Emmanuel, Kojo, Kwashie, Maria and Kwame for your support, prayers and encouragement

To my fiancée Adelaide, for your patience, prayers and support.

Lastly, and most importantly my profound gratitude goes to my mother, whose singular contribution to my life cannot be catalogue here. To you I dedicate this thesis.

SUMMARY

Regulatable control of gene expression in the mammalian brain is of tremendous importance in understanding the role of neural circuits in the processing, storage and retrieval of information. To understand the fundamental molecular mechanisms underlying these processes, there is the need to develop diverse molecular genetic tools that allow for conditional gene regulation in the central nervous system.

To address this issue, we have developed recombinant adeno-associated viruses (rAAVs) equipped with tetracycline (Tet)-controlled genetic switches to inducibly and reversibly manipulate neural circuits, in the mammalian brain. The present work focused on three objectives: In the first part, long-term, Tet-controlled gene regulation in neurons was investigated. In this part, the rAAV system was used to study the kinetics of Tet-controlled gene regulation *in vitro* and *in vivo* using the firefly luciferase reporter assay. Furthermore, repeated cycles of gene activation and inactivation *in vivo* were also demonstrated. In the second part, inducible, subregion- and cell type-restricted gene recombination and gene knockout in the mouse brain was investigated by employing the rAAV system expressing the site-specific Cre recombinase enzyme and a red fluorescent marker protein under Tet control. Conditional and region-specific gene recombination in transgenic reporter mice was carried out by either targeting the viruses to the hippocampus, cortex or both. Gene recombination occurred in these regions only upon Doxycycline (Tet derivative) injection. With the rAAV and Tet-controlled inducible gene expression systems, the *N*-Methyl-D-aspartate (NMDA) receptors were knocked out in the barrel field. We clearly demonstrated by electrophysiology that loss of NMDA receptors took place after one week of Dox treatment. With the inducible knockout approach, we are currently investigating the function of NMDA receptors in acquisition and maintenance of associative learning and memory.

In the last part, inducible and reversible silencing of synaptic transmission was investigated with the use of tetanus toxin light chain (TeTxLC). By reversible silencing of synaptic transmission with TeTxLC, the role of neurons from different brain regions in memory consolidation processes and behavior will be investigated. With this approach, we have demonstrated that TeTxLC expression results in silencing of synaptic

transmission. Moreover, by expressing the TeTxLC in the striatum of the mouse brain, a behavioral phenotype was produced, which was reversed by Dox administration. The original TeTxLC has a long half-life thus, very slow off rate. To reduce the half-life of the TeTxLC, new variants of TeTxLC were generated, named fast one (F1-TeTxLC) and fast two (F2-TeTxLC). With these new variants of TeTxLC, we observed that reversible silencing of synaptic transmission took place within 3 weeks with F1-TeTxLC and less than two weeks with F2-TeTxLC *in vivo*. We also demonstrated synaptic silencing in organotypic brain slices 24-48 hours after Dox treatment *in vitro.*

A combination of these newly developed genetic tools will be of great advantage to investigate the role of neural circuits in learning, memory consolidation and behavior.

ZUSAMMENFASSUNG

Um besser verstehen zu können, wie neuronale Schaltkreise Informationen prozessieren, speichern und abrufen, ist es von großer Bedeutung, die Expression bestimmter Gene im Gehirn regulieren zu können. Daher bedarf es der Entwicklung verschiedener genetischer Werkzeuge um konditionale Genexpression zu ermöglichen.

In dieser Arbeit wurden rekombinante adenoassoziierte Viren (rAAV) entwickelt, die mit Tetracyclin (Tet)-regulierten genetischen Sequenzen ausgestattet sind. Mit Hilfe dieser Technik ist es möglich, Neurone oder Netzwerke von Neuronen im Gehirn von Säugetieren reversibel und induzierbar zu manipulieren. Die vorliegende Arbeit beschäftigt sich mit drei Fragestellungen. Im ersten Abschnitt wurde über längere Zeit die Tet-kontrollierte Genregulation in Neuronen untersucht. In diesem Abschnitt wurde das rAAV-System verwendet, um die Kinetik der Tet-abhängigen Genexpression *in vitro* und *in vivo* mit Hilfe des "firefly luciferase" Reporter-Assays zu untersuchen. Dabei konnte gezeigt werden, dass sich die Genexpression zyklisch An-und Abschalten lässt.

Im zweiten Teil dieser Arbeit wurde untersucht, wie sich induzierbare Gen-Rekombination und Gen „Knock-out" auf spezielle Hirnregionen und Zelltypen eingrenzen lassen. Dafür wurde ein Tet-induzierbares rAAV-System entwickelt, welches neben der Sequenz-spezifischen Cre-Rekombinase auch ein rot-fluoreszierendes Protein exprimiert. Für die konditionale Gen-Rekombination wurden der Hippocampus, der Kortex oder beide Hirnregionen von transgenen Reporter-Mäusen mit Viren injiziert. Die Gen-Rekombination erfolgte in diesen Regionen in Abhängigkeit der Zugabe von Doxyciclin, eines Tet-Derivates. Darüber hinaus wurde mit diesem rAAV-System der *N*-Methyl-D-Aspartat (NMDA) Rezeptor im Barrel-Kortex deletiert. Mit Hilfe elektrophyisologischer Studien konnte bereits eine Woche nach Dox-Gabe eine Reduktion des NMDAR-Levels festgestellt werden. Mit diesem System kann die Funktion des NMDAR bei der Erlernung und Aufrechterhaltung assoziativer Gedächtnisinhalte erforscht werden.

Im letzten Abschnitt dieser Arbeit wurde eine Methode entwickelt, mit welcher durch Expression der kleinen Untereinheit von Tetanus Toxin (TeTxLC) die synaptische Transmission reversibel und induzierbar gehemmt werden kann. Dieses System ermöglicht die Erforschung der Funktion spezifischer Neuronenpopulationen bei Prozessen der Gedächtniskonsolidierung und des Verhaltens. Es konnte gezeigt werden, dass die synaptische Transmission durch Expression von TeTxLC gehemmt wird. Durch Expression von TeTxLC im Striatum wurde bei Mäusen ein Verhaltens-Phänotyp erzeugt, welcher durch Gabe von Dox revidiert werden konnte. Das anfänglich entwickelte TeTxLC hat eine lange Halbwertszeit und somit eine sehr langsame Aktivitätsabnahme. Um die Halbswertszeit des TeTxLC-Proteins zu verringern wurden zwei weitere Varianten des TeTxLC-exprimierenden Systems generiert, fast one (F1-TeTxLC) und fast two (F2-TeTxLC). Mit diesen neuen Varianten konnte die Aufhebung der induzierten Hemmung der synaptischen Transmission signifikant verkürzt werden: auf drei Wochen mit F1-TeTxLC und weniger als zwei Wochen mit F2-TeTxLC. Darüber hinaus konnten wir synaptische Hemmung in organotypischen Gehirnschnitten 24-48 Stunden nach Behandlung mit Dox *in vitro* nachweisen.

Die Kombination dieser neu entwickelten genetischen Werkzeuge wird sehr nützlich sein zur Erforschung der Funktion neuronaler Netzwerke beim Lernen, der Gedächtniskonsolidierung und des Verhaltens.

TABLE OF CONTENTS

Symbols and Abbreviations

AMPA	(2-amino-3-(5-methyl-3-oxo-1,2- oxazol-4-yl)propanoic acid)
α	alpha
β	beta
bp	base pair
BSA	Bovine serum albumin
CA1	cornu ammonis 1
CA3	cornu ammonis 3
CNS	central nervous system
CR	condition response
CS	conditioned stimulus
C-terminal	carboxy-terminal
Cy^3	cynine dye 3
Ctx	cortex
DAB	3,3'-Diaminobenzidine
DG	dentate gyrus
DMSO	dimethyl sulfoxide
DNA	deoxyribonucleic acid
dNTPs	deoxynucleotide triphosphate
EDTA	Ethylenediaminetetraacetic acid
EGFP	enhanced green fluorescent protein
et al	and others
FCS	fetal calf serum
FITC	Fluorescein isothiocyanate
g	gram
hr	hour
HP	hippocampus
hSYN	human synapsin
k	kilo

kDa	kilodalton
KO	knockout
LTP	long-term potentiation
m	milli
mA	milliampere
mKO	monomeric kusabira orange
M	molar
min	minute
mRNA	messenger ribonucleic acid
NMDA	N-methyl-D-aspartic acid
P	postnatal day
PAGE	polyacrylamide gel electrophoresis
PBS	Phosphate buffer saline
PBS-T	PBS-Tween
PCR	Polymerase chain reaction
PCP	phencyclidine
PFA	paraformaldehyde
pH	potential hydrogen
P_{tet}bi	bidirectional tetracycline promoter
RPM	Revolutions per minute
rAAV	recombinant adeno-associated virus
RT	room temperature
sec	second
SEM	standard error of mean
SDS	sodium dodecyl sulfate
SG	stratum granulosum
SL	stratum lucidum
tdTOM	tandem dimer tomato
TE	Tris/EDTA buffer
US	unconditioned stimulus
V	volt

VP	viral protein
µ	micro
WT	wild-type

1. INTRODUCTION

The mammalian brain is considered one of the most complex networks of cells on this planet. The cells of these networks are called neurons. In the human cerebral cortex alone, there are about 25 billion neurons (Pelvig et al., 2008, Herculano-Houzel, 2009). Each of these neurons makes up to tens of thousands of synaptic connections to other neurons. The central goal of neuroscience today is no longer the investigation of a single neuron but an ability to comprehend networks of cells that interact with each other to form circuits and to link these circuits to information processing and behavior. Brain circuits are composed of different neuronal types with diverse functions (Callaway, 2005). At the functional level, a large number of synaptic and extra-synaptic proteins controls communication between synapses. With trillions of connections, the brain has a tremendous computational capacity to engage dedicated neuronal circuits in learning and memory and behavior. To understand how activity-regulated genes control the function of neuronal circuits at a molecular and cellular level, it is imperative to develop methods to inducibly inactivate any gene-of-interest in specified neuronal types, for example, by using the Cre-*lox*P-mediated gene recombination (Sauer and Henderson, 1989). Alternatively, dominantly acting mutant protein variants and siRNAs can be used to interfere with protein activity and expression levels, respectively (Gaur, 2006). To dissect the functional role of specific neuronal types embedded in neuronal circuits, methods are also needed for reversible silencing of synaptic transmission.

To understand the functional roles of neural circuits, we have developed recombinant adeno-associated viruses (rAAVs) equipped with tetracycline (Tet)-controlled genetic switches to inducibly and reversibly manipulate neurons, and thereby circuit function in the mammalian brain. The present study focused on three main goals: (1) Long-term, Dox-controlled, tTA- and rtTA-dependent regulated gene expression in neurons, (2) Inducible, subregion- and cell type–restricted gene expression and gene knockout in the mouse brain and (3) Inducible and reversible silencing of synaptic transmission with tetanus toxin light chain (TeTxLC).

1.1 Tetracycline-controlled inducible gene expression systems

1.1.1 Genetic components of the Tet system

Controlling individual gene activity in the mammalian brain is the ultimate requirement for correlating gene function to neuronal physiology and animal behavior (Strand et al., 2007). From a list of different inducible gene expression systems (Gingrich and Roder, 1998), the tetracycline (Tet)-controlled genetic switches have shown superior performance in different biological preparations and model animals (Gossen and Bujard, 2002, Berens and Hillen, 2004, Sprengel and Hasan, 2007). Tet is a powerful antibiotic, which kills bacteria through inhibition of translation (Epe and Woolley, 1984, Hillen and Berens, 1994). The bacteria can mount resistance to Tet by expressing TetA resistance protein, a proton-$[Tet.Mg]^{+}$antiporter (Yamaguchi et al., 1990). TetA is not expressed under regular conditions because its expression is blocked by the Tet repressor (TetR). Tet repressor (TetR) of the Tn*10* Tet-resistance operon of *Escherichia coli* is a protein composed of 208 amino acids with 10 α-helices that make up the interaction surfaces for TetR dimerization, binding to the Tet operator DNA sequence (tetO) and an inducer, Tet or one of its derivatives such as doxycycline (Dox) (Hillen and Berens, 1994, Orth et al., 2000). In the absence of Tet, TetR dimmer binds in the TetR and TetA promoter regions to the operators tetO1 and tetO2 respectively (Hillen and Berens, 1994, Sprengel and Hasan, 2007). The binding physically hinders transcriptional initiation at the TetR and TetA promoters, leading to down regulation of the expression of these two genes (Hillen and Berens, 1994, Sprengel and Hasan, 2007).

Tet and Dox are the ideal inducers for controlling gene expression because they can rapidly distribute in different tissues *in vivo* (Bocker et al., 1981, Michel et al., 1984). Tetracyclines are widely used antibiotics with well-studied pharmacokinetics in different mammalian species. However, Tet derivative Dox, is preferred because it is more hydrophobic than Tet and can rapidly cross the blood-brain-barrier (Bocker et al., 1981, Michel et al., 1984). Dox concentrations required to control gene expression *in vivo* are

largely within the non-toxic range (Bocker et al., 1981, Michel et al., 1984). TetR binds to Tet and Dox with high affinity with the following binding constants: $[Tet.Mg]^+$ (Ka ~10^9 M^{-1}) and $[Dox.Mg]^+$ (Ka ~10^{10} M^{-1}), which are about two to five orders of magnitude higher than the affinity of these drugs to the prokaryotic ribosome (Lederer et al., 1996). The affinity of the TetR to the tetO (Ka ~6x 10^9 M^{-1}) is reduced by nearly 9 orders of magnitude when an inducer, Tet, binds to TetR (Lederer et al., 1996). TetR also has a very low affinity for non-specific DNA sequences (Ka ~4x10^5 M^{-1}). These biophysical and biochemical features make the bacterial Tet system an ideal choice for the reversible control of gene expression in living cells (Hillen and Berens, 1994).

1.1.2 Tet-controlled gene expression in eukaryotic systems

The basic genetic components of the Tet system as mentioned above consist of three essential components; TetR, tetO and Tets. These components have been modified in various ways for the control of gene expression in eukaryotes. For the reversible control of gene expression in eukaryotic cells and organisms, the C-terminal region of the TetR was fused to a potent transcription activation domain (VP16) derived from the herpes simplex virus (HSV) (Gossen and Bujard, 1992, Sprengel and Hasan, 2007). The hybrid protein, TetR-VP16, named the tetracycline transactivator (tTA), binds to the tetO sequences through the TetR domain, while the VP16 participates in the recruitment of the RNA polymerase II transcription initiation complex to initiate transcription (Gossen and Bujard, 1992, Sprengel and Hasan, 2007). In the absence of Tet, or its derivatives such as Dox, tTA binds to the P_{tet} and drives the expression of downstream genes (Tet-ON) (Fig. 1.1 A). However, in the presence of Tet, tTA is unable to bind to P_{tet} (Fig. 1.1 B) resulting in the termination of transcription initiation at Ptet (Tet-OFF).

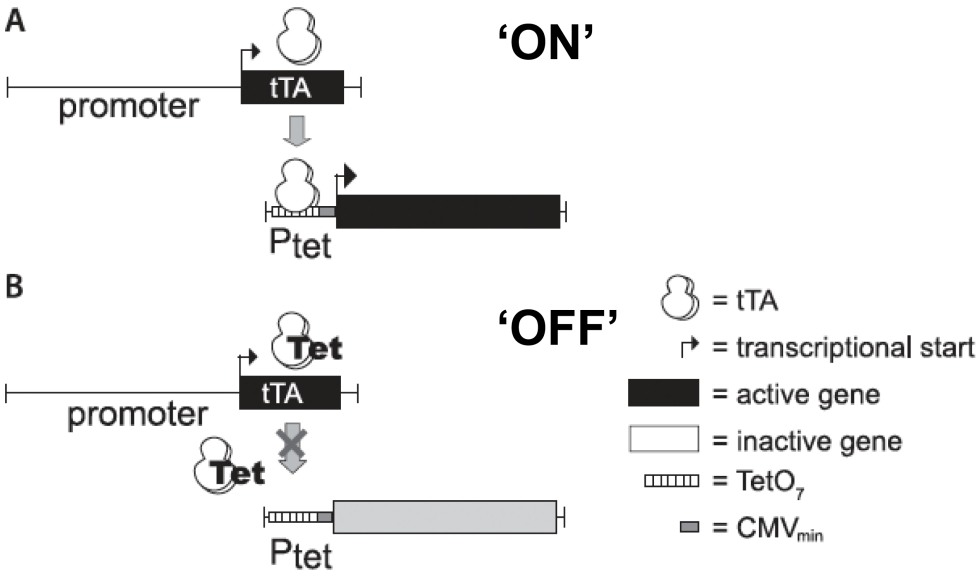

Figure 1.1 Principles of the Tet-OFF-system. (A) When the constitutively expressed tTA binds to P_{tet}, tTA activates transcription. (B) In the presence of Tet, tTA is unable to bind to P_{tet}, and P_{tet}-controlled gene transcription is turned-off (Tet-OFF). (From Sprengel and Hasan 2007).

1.1.3 tTA- and rtTA-dependent P_{tet}/P_{tet}bi promoters

To control the expression of a gene-of-interest, a tTA-responsive promoter, also called the Tet-promoter (P_{tet}), was engineered by linking seven Tet-operator sequences $(tetO)_7$ upstream to a human cytomegalovirus minimal promoter ($hCMV_{min}$) containing the transcription start sites with a TATA box to express gene(s) (also called Tet-responder genes). In addition, to simultaneously co-express two different genes, a bi-directional Tet-promoter (P_{tet}bi) was constructed by placing $(tetO)_7$ in between two oppositely oriented $hCMV_{min}$ (Baron et al., 1995) (Fig. 1.2). In the absence of Dox, tTA binds to P_{tet}/P_{tet}bi and activates gene transcription. To inactivate gene transcription, Dox binds to tTA, which strongly reduces the binding between tTA and tetO. Thus, in all tissues *in vivo,* gene expression can be turned "ON" and "OFF" with the tTA system by the removal or addition of Dox to the system respectively (Fig.1.1).

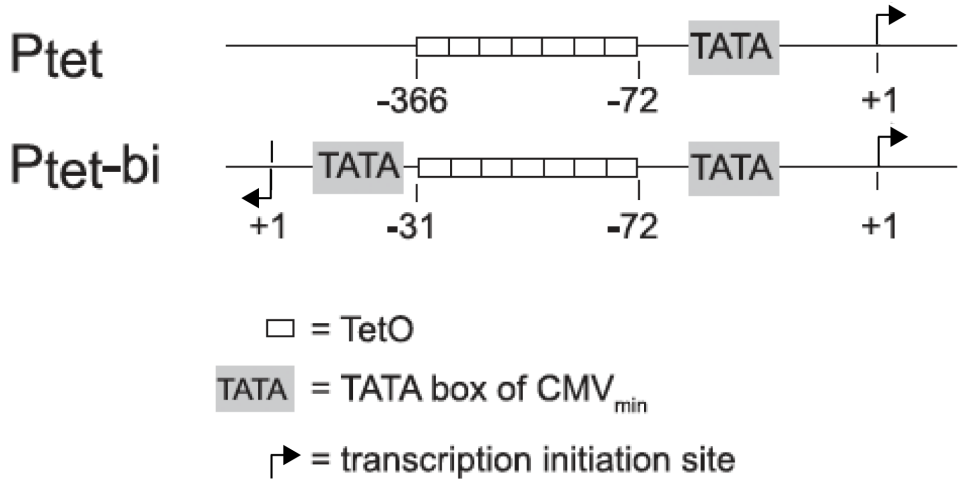

Figure 1.2 Schematic drawing of P_{tet} and P_{tet}bi promoters. The different promoter elements of the two tTA/rtTA-controlled promoters are shown. Nucleotide positions relative to the transcriptional start sites (position +1) are depicted (Sprengel and Hasan, 2007).

However, tTA-dependent gene expression during early embryonic and postnatal development can interfere with cellular physiology and early development. To switch-off tTA-dependent gene expression prenatally, pregnant mice can be treated with Dox in drinking water at doses, which are appropriate for brain and non-brain tissues. Successful re-activation of gene expression can be achieved upon Dox removal. However, this procedure for gene re-activation is not without problems, especially with studies related to the nervous system. First, it was found that wild-type mice prenatally treated with Dox were impaired in fear-related associative learning and memory (Mayford et al., 1996), which might be related to Dox-induced toxicity in neurons during prenatal development (Mayford et al., 1996). Second, when gene expression was kept in the off state, by administering Dox during embryonic development, re-activation of tTA-dependent gene expression in the adult brain was very slow (several weeks to months). Interestingly, even after re-activation, gene expression levels in neurons were variable and gene expression patterns in brain slices were highly mosaic (Bejar et al., 2002, Lindeberg et al., 2002,

Krestel et al., 2004). The slow gene reactivation kinetics can be largely due to the slow Dox efflux from the brain tissues after it is absorbed in lipid tissues. However, it was very puzzling why gene re-activation levels were variable and gene expression patterns were highly mosaic.

1.1.4 The reverse tTA (rtTA) system

To overcome these difficulties, an ideal inducible system was desired that would activate and inactivate gene expression with Dox addition and removal, respectively. This would overcome the biological problems associated with Dox-controlled, tTA-dependent inactivation of gene expression during prenatal and early postnatal development. A reverse TetR (rTetR) variant was identified that was used to generate the reverse tTA (rtTA) system (Gossen et al., 1995). This new variant was generated by four point mutations in the TetR, E71K, D95N, L101S and G102D, which lead to the reversal of the pharmacology of TetR (Hecht et al., 1993, Gossen et al., 1995). Only when bound to Dox can the rtTA bind to P_{tet}/P_{tet}bi to activate gene transcription and gene expression is switched-off when Dox unbinds rtTA (Gossen et al., 1995). Subsequently, an improved rtTA variant, rtTA-M2 (Urlinger et al., 2000) was generated which, compared to the original rtTA , requires nearly ten-times lower Dox concentration for full gene activation (Gossen et al., 1995).

Both tTA and rtTA have been successfully applied in different mouse tissues (Kistner et al., 1996) including the brain (Mayford et al., 1996, Mansuy et al., 1998).

1.1.5 Improvement of the tTA/rtTA systems

The original tTA/rtTA systems were equipped with the VP16 as an activation domain. It was found that high VP16 levels in cells have toxic side effects (Berger et al., 1992), largely due to ‘squelching’ which is a consequence of titrating components of the transcriptional machinery from their respective intracellular targets (Gill and Ptashne,

1988). To reduce the toxicity, a 12 amino acids minimal transcriptional activation domain (F-domain), incapable of interacting with various cellular transcriptions factors, was derived from VP16 (Fig. 1.3) (Baron et al., 1997, Kim, 2001). When compared to the originally described transactivator (Gossen and Bujard, 1992, Gossen et al., 1995), the new Tet transactivator variant with minimal activation domains was well tolerated at higher intracellular concentrations (Baron et al., 1997). Additionally, a nuclear localization signal inserted at the N-terminus of the tTA improved the binding efficiency of tTA to the P_{tet} responder in the nucleus (Urlinger et al., 2000, Hasan et al., 2001, Kim, 2001, Krestel et al., 2004). It appears that the use of three F-domains is an optimal trade-off for minimal cellular toxicity and robust gene activation.

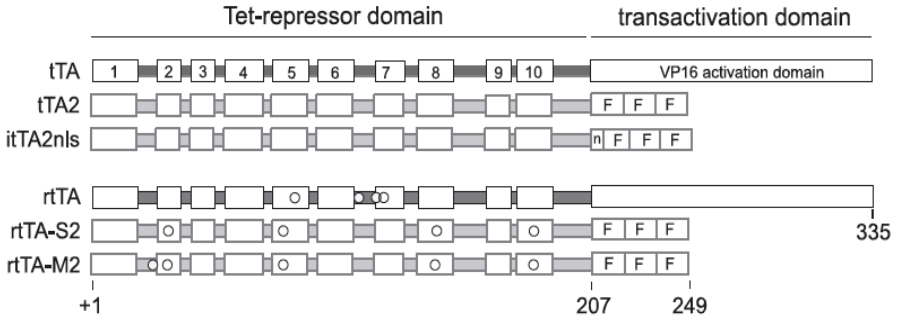

Figure 1.3 Schematic drawings for some currently available tTA and rtTA variants. The TetR core region with 10 α-helices (1-10) contains sites for tetO binding, Tet binding and homodimerization. VP16 or minimal F-domains make up the transactivation domains. The position of the nuclear localization domain (n) is indicated. Amino acid exchanges in different rtTAs are indicated by circular dots. Codon improved tTA and rtTA variants are in light grey, original tTA and rtTA are in black. Amino acid positions are numbered starting with the first amino acid (position +1). (From Sprengel and Hasan, 2007).

One great advantage of the binary transcriptional systems including the tTA/rtTA system is that even a weak promoter driving the activator allows for expression amplification of

a responder gene (Iyer et al., 2004). With rAAV-tTA/rtTA systems, gene expression can be targeted to any brain region and neuron-types. For functional analysis of network activity, one could, for example use genetically encoded Ca^{2+} indicator proteins (FCIPS) (Wallace et al., 2008). By light-induced uncaging of Dox, the rAAV-rtTA system allows for rapid and local rtTA-dependent gene activation in neurons, even down to a single neuron within a microcircuit (Cambridge et al., 2009). As previously demonstrated (Zhu et al., 2007), the combinatorial use of transgenic tTA/rtTA-mice and P_{tet}/P_{tet}bi in rAAV can help to achieve cell-type specificity, and it is a versatile approach for precisely controlled, reversible genetic manipulation of neuronal microcircuits.

1.2 The Tet-systems and recombinant adeno-associated viruses (rAAV)

Even though the rtTA system has been explored in a variety of biological tissues, the performance of this system in the mammalian brain has been, with few notable exceptions, somewhat disappointing. Even after the construction of the improved rtTA variant (rtTA-M2), which has nearly 10 times higher affinity for tetO, it was still not possible to reliably and robustly activate gene expression with Dox in neurons. Previous studies showed that the rtTA system was poorly inducible in a majority of neurons in the postnatal mouse brain (Yu et al., 2005, Beard et al., 2006, Eckenstein et al., 2006, Uchida et al., 2006, Zhu et al., 2007, Zeng et al., 2008, Wortge et al., 2010). It was discovered that the Tet responder genes under the control of P_{tet}/P_{tet}bi introduced into the mouse germ-line become functionally silenced and thus unresponsive to tTA/rtTA, when kept in the inactive state during early development (Zhu et al., 2007). However, it was found that the deficiencies were overturned by the introduction of episomal recombinant adeno-associated virus (rAAV) carrying appropriate P_{tet}-controlled responder genes (Zhu et al., 2007).

1.2.1 Recombinant adeno-associated viruses

Adeno-associated viruses (AAV) are nonpathogenic viruses, which infect humans and other primates and causes very mild immune responses. The successful cloning of the AAV in the early 80's enables the cloning of foreign genes into the AAV vector for subsequent expression in mammalian cells (Samulski et al., 1982, Laughlin et al., 1983). The nonpathogenic nature of the AAV makes it a very attractive tool for gene therapy.

1.2.2 AAV genome and proteome

AAV is a small (~26 nm) replication-defective, non-enveloped virus belonging to the genus *Dependovirus* and the family of parvoviridae (Blacklow, 1988). The virus was initially discovered as a contaminant in adenovirus preparations (Atchison et al., 1966, Hoggan et al., 1966). The AAV genome is about 4.7 kb in size and is composed of single-stranded DNA (ssDNA), either positive- or negative-sensed (Grimm et al., 2003). The genome comprises inverted terminal repeat (ITRs) sequences of 145 bases at both ends of the DNA strand. ITRs are required for efficient multiplication of the viral genome and though AAV is mainly episomal, it occasionally integrates into the host genome using the ITR (Bohenzky et al., 1988). ITRs are required in *cis*- to the genes of interest, which replaces structural (*cap*) and packaging (*rep*) genes (Mendelson et al., 1986). The AAV genome consists of two major open reading frames, which encode replication (*rep*) and capside (*cap*) proteins (Mendelson et al., 1986).

There are four different Rep proteins (Rep78, Rep68, Rep52 and Rep40) generated from two different promoters through alternate splicing (Mendelson et al., 1986). The Rep proteins are required for the AAV life cycle. The capsid proteins (VP1, VP2 and VP3) on the other hand are generated from one promoter called p40. The molecular weight of these capsid proteins are 87, 72 and 62 kDa respectively (Jay et al., 1981). The capside proteins are also generated via alternate splicing and alternate start codon usage (Figure 1.4 A) (Mendelson et al., 1986, Trempe and Carter, 1988, Russell and Kay, 1999). These proteins self-organize to form a capsid of icosahedral symmetry

(Buning et al., 2008). The virion particle has a molecular weight of about 6.2 x 10^3 kDa (Buller and Rose, 1978, Muzyczka, 1992, Linden and Berns, 2000).

In order to use the AAV for more general applications, the recombinant adeno-associated virus (rAAV) was developed by replacing the Rep and Cap genes from the vector with genes of interest (Fig. 1.4 B). The ITR, which is the most important viral component in rAAV has GC rich sequences (Fig. 1.4 C) (Russell and Kay, 1999). Also included in the ITR sequence are two motifs, a terminal resolution site (TRS) and a Rep binding site (RBS), which are necessary for replication and encapsidation of the viral genome.

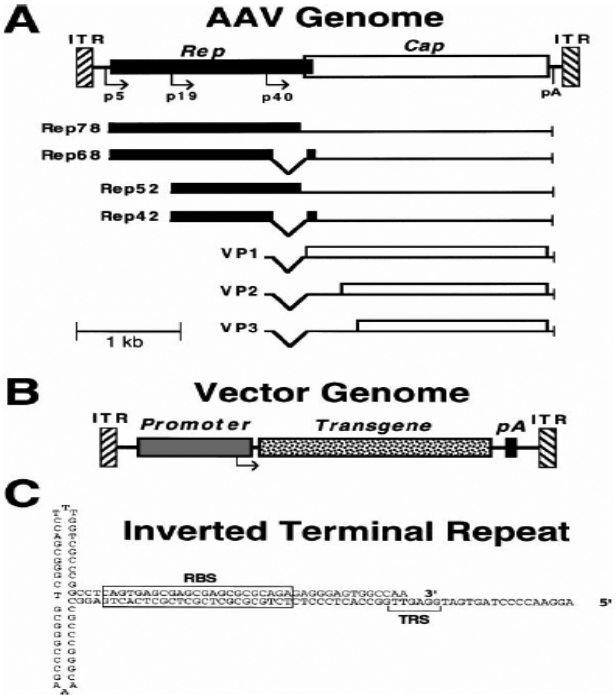

Figure 1.4 Structure of wild-type and vector AAV genomes. (A) A map of the wild-type AAV genome, including Rep (solid) and Cap (open) reading frames, promoters (p5, p19 and p40), polyadenylation site (pA), and inverted terminal repeats (ITR). The viral transcripts encoding the different Rep and Cap (VP1-3) proteins are shown below the genome. The smaller Rep proteins, VP2 and VP3, are translated from internal initiation sites. (B) Map of a typical AAV vector, showing replacement of the viral Rep and Cap genes with a transgene cassette (promoter, transgene cDNA, and polyadenylation site). (C) Secondary structure of the AAV ITR, with the locations of the Rep binding site (RBS) and terminal resolution site (TRS) indicated. (From Russell and Kay, 1999).

1.2.3 AAV serotypes

As of 2008, more than 110 distinct primate AAV capsid sequences have been isolated (Gao et al., 2005, Schultz and Chamberlain, 2008). And there are 12 characterized primate serotypes (Rutledge et al., 1998, Xiao et al., 1999, Mori et al., 2004). AAVs have been found in many animal species, including nonhuman primates, canines, fowl, and humans (Xiao et al., 1999). All the characterized AAV serotypes are known to infect diverse tissues and cell types (Summerford and Samulski, 1998, Qing et al., 1999, Summerford and Samulski, 1999, Di Pasquale et al., 2003). Because the various serotypes infect cells via different and distinct cell surface receptors, it has been suggested that different serotypes will target different cell types. AAV serotype 2 (AAV2) the most commonly used serotype is known to have tropism towards skeletal muscles, neurons, vascular smooth muscles and hepatocytes (Koeberl et al., 1997, Bartlett et al., 1998, Richter et al., 2000, Manno et al., 2003). AAV 2 uses three different cell surface receptors for transduction, namely heparan sulfate proteoglycan (HSPG), $a_V\beta_5$ integrin and fibroblast growth factor receptor 1 (FGFR-1). The HSPG functions as a primary receptor while the other two act to enable the entry into the cell by AAV through receptor-mediated endocytosis (Fig. 1.7) (Summerford and Samulski, 1998, Qing et al., 1999, Summerford et al., 1999).

Different AAVs have been tested in the nervous system including AAV1, AAV2, AAV4, AAV5, AAV6, AAV7 and AAV8 (Alisky et al., 2000, Davidson et al., 2000, Yang et al., 2002, Burger et al., 2004). Although AAV2 has been used predominantly, AAV1 and AAV5 have demonstrated higher infectivity in the CNS in regions such as hippocampus, striatum, globus pallidus, substantia nigra and spinal cord (Wang et al., 1998, Alisky et al., 2000, Burger et al., 2004). However, in my PhD work, a cross-packaging of AAV1 and AAV2 were used (Zhou and Muzyczka, 1998, Hasan et al., 2004, Tang et al., 2009).

1.2.4 rAAV production and delivery system

Since AAVs are replication defective viruses, they require genes of a helper virus, such as adenovirus or herpes virus (Hermonat and Muzyczka, 1984). Originally, adenovirus and herpes simplex virus were used for producing rAAVs (Hermonat and Muzyczka, 1984, Flotte and Carter, 1995, Conway et al., 1997, Zhou and Muzyczka, 1998). However, for *in vivo* application, it is important to avoid the use of adenovirus or the herpes virus. To overcome this, the required helper genes E4, E2A and VA from adenovirus were used to construct a helper plasmid named pDG plasmids (Fig. 1.5) (Grimm et al., 2003). This plasmid also contains *rep* gene derived from AAV2 and *cap* genes from serotypes 1-6 (Grimm et al., 1998, Grimm et al., 2003). This cross-packaged rAAV vector plasmid and the different helper plasmids (pDG) were found to be about 10 times more efficient than the traditional adenovirus used (Grimm et al., 1998, Grimm et al., 2003).

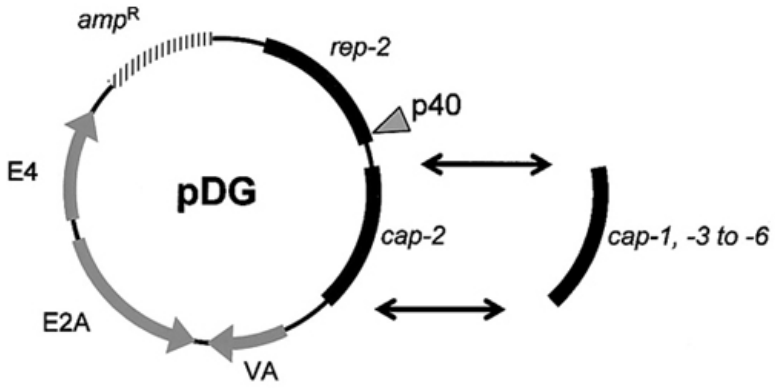

Figure 1.5 Map of pDG plasmid. Plasmid pDG carries all essential genes for packaging of AAV-2 vectors into capsids of AAV-2, i.e., AAV-2 *rep* and *cap* genes and VA, E2A, and E4 genes of adenovirus 5. Five novel helper constructs were derived from pDG by exchanging the AAV-2 *cap* gene with *cap* of AAV serotype 1, 3, 4, 5, or 6 (from Grimm et al., 2003).

By transfecting HEK293 cells with pDG plasmids together with an AAV plasmid in a heterologous expression system, virus particles with high infectivity can be packaged (Fig. 1.6) and purified (Hermens and Verhaagen, 1998, Auricchio et al., 2001, Zolotukhin et al., 2002, Hauck et al., 2003, Sun et al., 2003, Zeltner et al., 2010).

1.2.5 Cellular entry and trafficking of rAAV

Entry of AAV into the cell is by the attachment of the virus to the cell surface receptor followed by internalization. The primary receptor for AAV2 is heparan sulfate proteoglycan, but it has also been found that interaction with other co-receptors is of importance for virus internalization (Schultz and Chamberlain, 2008). Fibroblast-growth factor receptor-1 and $\alpha_v\beta_5$ integrin can act as co-receptors (Qing et al., 1999, Summerford et al., 1999, Sanlioglu et al., 2000, Schultz and Chamberlain, 2008). There are other receptors for other serotypes as well, such as O-linked 2,3-sialic acid for AAV4 and N-linked sialic acids for AAV5 (Kaludov et al., 2001, Walters et al., 2001). Internalization of AAV occurs through receptor-mediated endocytosis through clathrin-coated pits (Fig. 1.7) (Bartlett et al., 2000, Seisenberger et al., 2001).

Once internalized, the AAV is processed in the endosome, trafficked into the nucleus via lysosomes and the Golgi apparatus (Fig. 1.7). Inside the nucleus, the virus is uncoated and forms episomal concatamers (Chen et al., 2001). In non-dividing cells, these concatamers remain intact throughout the life of the cell. Random integration of AAV DNA into the host genome is rare (McCarty et al., 2004). In dividing cells, AAVs are diluted by every cell division because the episomal DNA is unable to replicate in host cells lacking *cap* and *rep* genes.

Another major advantage of the rAAVs is that they can target gene expression into selected cell types at any time in the animal's life (During, 1997) by using cell-type specific promoters. That allows detailed investigation of gene function without interference during development, as is the case with traditional transgenic mice derived by pronuclear DNA microinjections (Gordon and Ruddle, 1982, Mann and McMahon, 1993). This not only obviates the use of conditional transgenics, but also readily expands

the use of transgenesis to species other than rodents. With multiple viruses, it is possible to deliver and thus express multiple genes simultaneously, even in different spatially defined locations (Shevtsova et al., 2005). Co-infectivity of viral particles can be as high as >85 % (Shevtsova et al., 2005). Maximum transgene expression can be observed in a matter of weeks and typically persists throughout life (Klein et al., 2002).

The rAAV-vectors equipped with tetracycline-dependent genetic switches have been engineered for inducible gene expression in the mouse nervous system (Zhu et al., 2007). We used a two-virus approach: the first virus expresses either tTA or rtTA under the control of a ubiquitous or a cell-type-specific promoter. The second virus, the responder virus, is equipped with a P_{tet}bi to express at least two genes simultaneously.

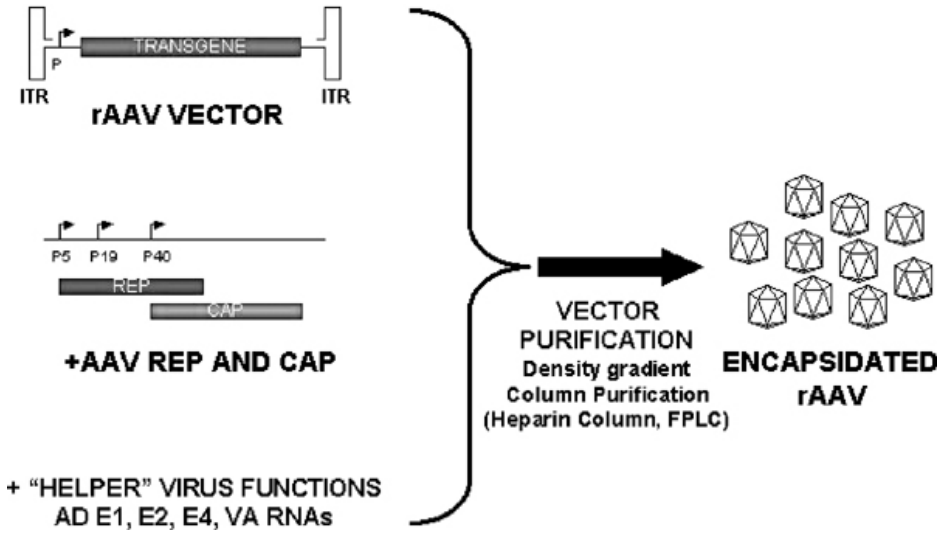

Figure 1.6 General scheme of rAAV2 vector production. The rAAV vectors have been constructed by the removal of endogenous viral genes, and the insertion of an expression cassette(s) between flanking ITRs. The rAAVs are generally encapsidated by transfection of a plasmid containing the rAAV vector into cells with provision of AAV rep and cap (as either plasmids or by using cells expressing them) and 'helper' virus functions such as Adenovirus E1, E2, E4, and VA RNAs (either as a plasmid or by viral infection). The resulting vector is then purified for use using density gradient centrifugation ($CsCl_2$ or Iodixanol) and/or column purification (from Sun et al., 2003).

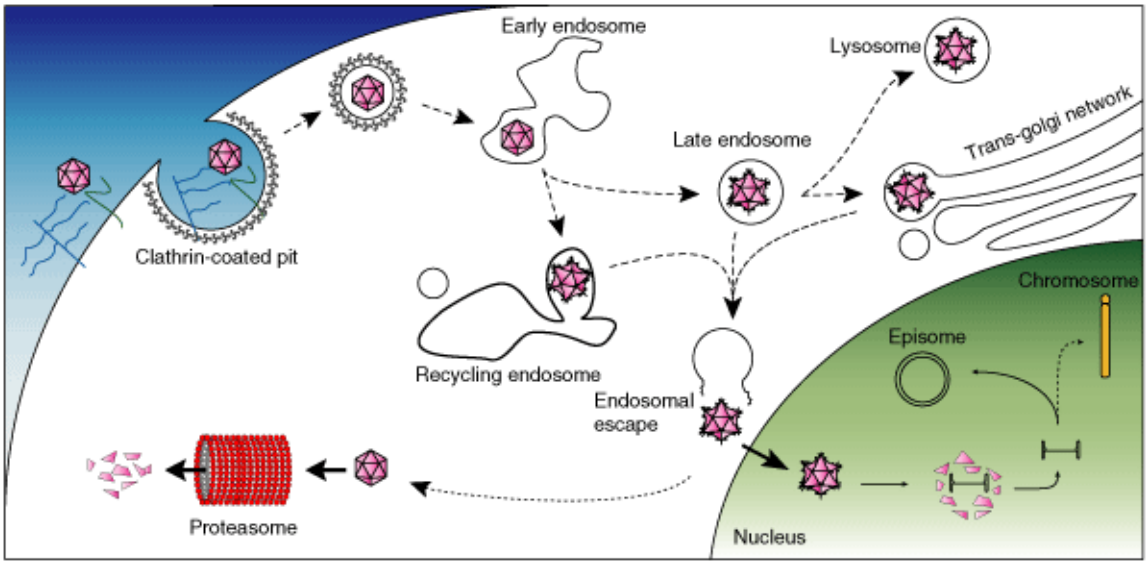

Figure 1.7 Schematic representation of cell entry and trafficking of recombinant adeno-associated virus (rAAV). Stages and various cellular events during AAV cell transduction. The process starts with the viral binding to the cell surface receptor and entry by receptor-mediated endocytosis, followed by trafficking to the nucleus, uncoating and viral gene expression (Schultz and Chamberlain, 2008).

1.3 The Cre /*lox*P recombinase system

Cre recombinase (Cre) is an enzyme from the P1 bacteriophage, which catalyzes site-specific DNA recombination between *lox*P sites (Abremski and Hoess, 1984, Hamilton and Abremski, 1984, Sauer and Henderson, 1989, Nagy, 2000). The *lox*P site is a 34 bp consensus sequence, consisting of spacer sequence of 8 bp and two 13 bp palindromic flanking sequences (Nagy, 2000). Recombination takes place within the spacer area of the *lox*P sites. Introduction of the Cre/*lox*P sites into the mammalian (eukaryotic) system by transgenesis serves as a powerful tool to study gene functions in a conditional knockout mouse model. The system is of tremendous importance to neuroscience because it allows for region- and cell-type specific gene knockout in the mouse brain. In the present study, I employed the rAAV system expressing the Cre recombinase enzyme to

conditionally and inducibly knockout the NMDA receptor subunit NR1 in a region specific manner in NR1-2*lox* mice (Niewoehner et al., 2007). I also used the same system to investigate site-specific gene recombination in the Rosa26R mice (Soriano, 1999).

1.4 NMDA receptors in learning and memory

The notion that information is stored in the brain has been with us for more than a century following the demonstration by Cajal that networks of neurons communicate with each other at specialized junctions called synapses. Neurons are therefore thought to communicate with each other through various neurotransmitters mediated by receptors (Bliss and Collingridge, 1993). One of these receptors is the *N*-methyl-D-aspartate (NMDA) receptor. The NMDA receptor is a heterotetrameric ionotropic glutamate receptor consisting of two obligatory NR1 and two regionally localized NR2 subunits (Fig. 1.8) (Monyer et al., 1992, Witt et al., 2004, Stephenson, 2006). NMDA receptors require the co-binding of both L-glutamate and glycine and the relief of a voltage-dependent blockade by magnesium ions. NMDA receptor is a non-specific cation channel which is permeable to Na^+, K^+ and Ca^{2+}. At physiological levels, the receptor is blocked by Mg^{2+} and can be unblocked by depolarization of the postsynaptic cell (Witt et al., 2004).

NMDA receptor dependent synaptic plasticity is thought to underlie some types of learning and memory (Bliss and Collingridge, 1993, Bannerman et al., 1995). In support of this argument, it has been demonstrated that hippocampal long-term potentiation (LTP) and spatial learning in watermaze are impaired by blocking NMDA receptors with D(-)-2-amino-5-phosphonovaleric acid (AP5), a selective antagonist of NMDA receptor (Morris et al., 1986).

NMDA receptors have also been implicated in associative memory. An example is the classical conditioning of the eyeblink reflex to neutral stimulus, which is a form of an associative learning and is known to involve NMDA receptors in the cerebellum, hippocampus, neocortex, neostriatum septum and amygdala (Christian and Thompson, 2003). It has been shown that pharmacological manipulation of NMDA receptor by

agonists facilitated the acquisition of the behavioral trace eyeblink condition response (Thompson et al., 1992, Christian and Thompson, 2003). Systemic administration of other noncompetitive NMDA antagonists MK801 and phencyclidine (PCP), blocked acquisition of trace conditioned response at doses which caused slowing of delay acquisition but did not impair performance of the learned conditioned response (Thompson and Disterhoft, 1997). The above observations point to the role of NMDA receptors in memory acquisition and memory retrieval.

A mutation in one of the receptor subunits has also been reported to produce similar memory deficits (Sakimura et al., 1995). It has also been demonstrated in transgenic mice that region specific deletion of the NMDA receptor subunit NR1 in the dentate gyrus (DG) of the hippocampus produced behavior phenotype with impairment in spatial working memory but intact hippocampus-dependent reference memory (Niewoehner et al., 2007). It was shown in the same transgenic mice that there is a severe impairment of LTP in both medial and lateral perforant path input to the DG (Niewoehner et al., 2007). Colchicine lesion and other lesion studies of the DG of the hippocampus have shown severe impairment in both spatial working memory and spatial reference memory (O'Keefe and Nadel, 1978 , Sutherland et al., 1983, Xavier et al., 1999, Jeltsch et al., 2001). It was also demonstrated that ablation of NMDA receptor gene in CA3 pyramidal cells lead to impairment in pattern completion (Nakazawa et al., 2002).

The role of NMDA receptors in the motor cortex in acquisition and maintenance of associative learning and memory was therefore investigated. With the inducible knockout approach, we knocked out the NR1 subunit in the motor cortex and together with our collaboration partners, we subjected these mice to various behavioral paradigms such as the Skinner box test (operant conditioning), classical conditioning of vibrissae responses and *in vivo* LTP study(Thompson and Disterhoft, 1997).

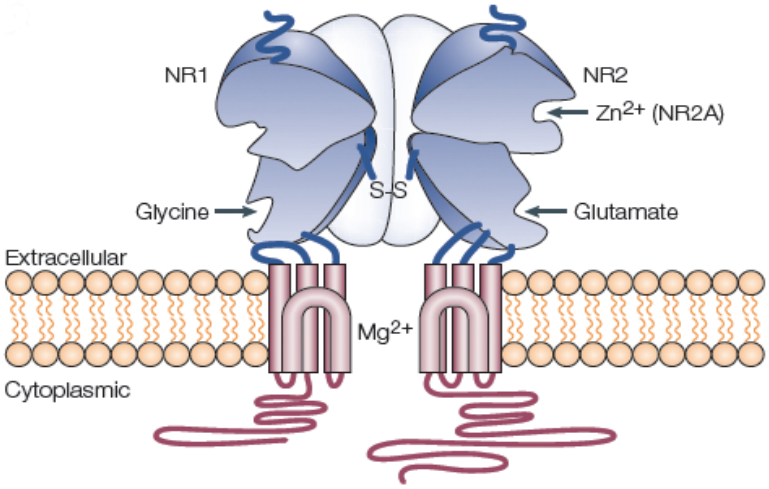

Figure 1.8 Model of NMDA receptor activation: The integral ion channel is blocked by magnesium in a voltage-dependent manner. Depolarization of the neuron removes the Mg^{2+} block. The binding of both L-glutamate and glycine results in the opening of the channel, allowing Na^{+} and Ca^{2+} to enter and K^{+} to move out (from Witt et al., 2004).

1.5 Neurotoxins and synaptic transmission

A neurotoxin is a toxin which specifically acts on nerve cells by either interacting with ion channels or membrane proteins. Many of these neurotoxins are naturally occurring and are used by some predatory organisms for defense. Examples include toxins from scorpions, bees and spiders. Many of these toxins act by affecting voltage dependent ion channels, examples include tetrodotoxin which acts on sodium channels and agitoxin on potassium channels (Kao and Levinson, 1986). Bungarotoxin on the other hand binds irreversibly to the acetylcholine receptor at the neuromuscular junction, causing paralysis and respiratory failure (Chang, 1999). Botulinum neurotoxins are another group of potent neurotoxins produced by different strains of *Clostridium botulinum* and they are metalloproteases. Examples include botulinum toxin from *Clostridium botulinum* and tetanus toxin from *Clostridium tetani.* They cleave the synaptic vesicle protein

synaptobrevin in the case of tetanus toxin and SNAP-25 in the case of botulinum toxin (Schiavo et al., 1992a, Foran et al., 2003).

1.5.1 Reversible silencing of synaptic transmission with tetanus toxin light chain (TeTxLC)

Tetanus toxins belong to a family of *Clostridial* neurotoxins (Niemann et al., 1994). In their native form, these toxins are produced as single chain polypeptides and subsequently are cleaved into two chains linked by a single disulphide bond (Fig 1.9A) (Schiavo et al., 1992a). The heavy chain (HC, 100 kDa) mediates neuron-selective binding, internalization, intraneuronal sorting and the translocation of the 50 kDa light chain (LC) to the cytosol (Niemann et al., 1994, Sweeney et al., 1995). This is achieved by the interaction of the HC with disialogangliosides in the neuronal membrane. The tetanus toxin light chain (TeTxLC) is a zinc endopeptidase that proteolytically cleaves the synaptic vesicle protein synaptobrevin 2 (VAMP2) (Schiavo et al., 1992a, Schiavo et al., 1992b, Sweeney et al., 1995).

The cleavage of VAMP2 (a 19 kDa protein) takes place between Gln 76 and Phe 77 (Schiavo et al., 1992a). Synaptobrevins are part of a core complex of proteins involved in vesicle fusion. Some of these proteins are the N-ethylmaleimide-sensitive fusion protein (NSF), α-soluble NSF attachment protein (α-SNAP), and γ-SNAP involved in vesicle fusion processes (Sudhof, 1995, Sweeney et al., 1995). The vesicle proteins are collectively called v-SNAREs for vesicle membrane and t-SNAREs for target membrane. Synaptobrevins are considered v-SNAREs, which target vesicles to the plasma membrane using syntaxin and SNAP-25. (Trimble et al., 1988, Sollner et al., 1993, Sweeney et al., 1995). The cleavage of VAMP2 by tetanus toxin light chain therefore results in the prevention of Ca^{2+}-induced fusion of synaptic vesicles to the presynaptic membrane and, subsequently, in the suppression of evoked synaptic transmission (Fig. 1.9 B) (Schiavo et al., 1992a, Sudhof, 1995, Sweeney et al., 1995).

To study reversible silencing of synaptic transmission, we have deployed the tetanus toxin light chain (TeTxLC) (Martin et al., 2002) under the control of the Tet-

inducible systems. In previous studies, TeTxLC has been elegantly used to silence synaptic transmission in specific neuronal cell types in mice, and functional changes in neuronal circuits were directly correlated to changes in learning and memory and behavior (Sweeney et al., 1995, Yamamoto et al., 2003, Nakashiba et al., 2008). It has also been demonstrated that the toxin acts exclusively at the presynaptic terminal and does not produce any detectable morphological changes (Sweeney et al., 1995). The postsynaptic response was found to be normal when exogeneous glutamate was applied (Sweeney et al., 1995). With TeTxLC, tTA-dependent reversibility of synaptic silencing was observed approximately 3 weeks after Dox treatment (Yamamoto et al., 2003, Nakashiba et al., 2008).

There are other systems of reversibly silencing synaptic transmission, such as the use of MIST (Molecules for Inactivation of Synaptic Transmission). MIST induces dimerization of VAMP2 and synaptophysin, leading to a blockade of synaptic transmission (Karpova et al., 2005). However, MIST has to be delivered intracerebroventricularly (ICV), a highly invasive procedure, and this might be too stressful for the mice in behavior studies (Karpova et al., 2005, Lerchner et al., 2007). Other methods include the use of membrane-tethered toxins that bind sodium channels but also have their own limitations (Ibanez-Tallon et al., 2004). Silencing has also been achieved with the transgenic expression of the allatostatin receptor in mammalian brain. However, expression of the allatostatin receptor results in membrane hyperpolarization through endogenous G-protein-coupled inward rectifier K^+ channels, making firing of action potentials less likely (Wehr et al., 2009).

The use of TeTxLC as a tool for reversible silencing of synaptic transmission is therefore more advantageous in many ways as presented above.

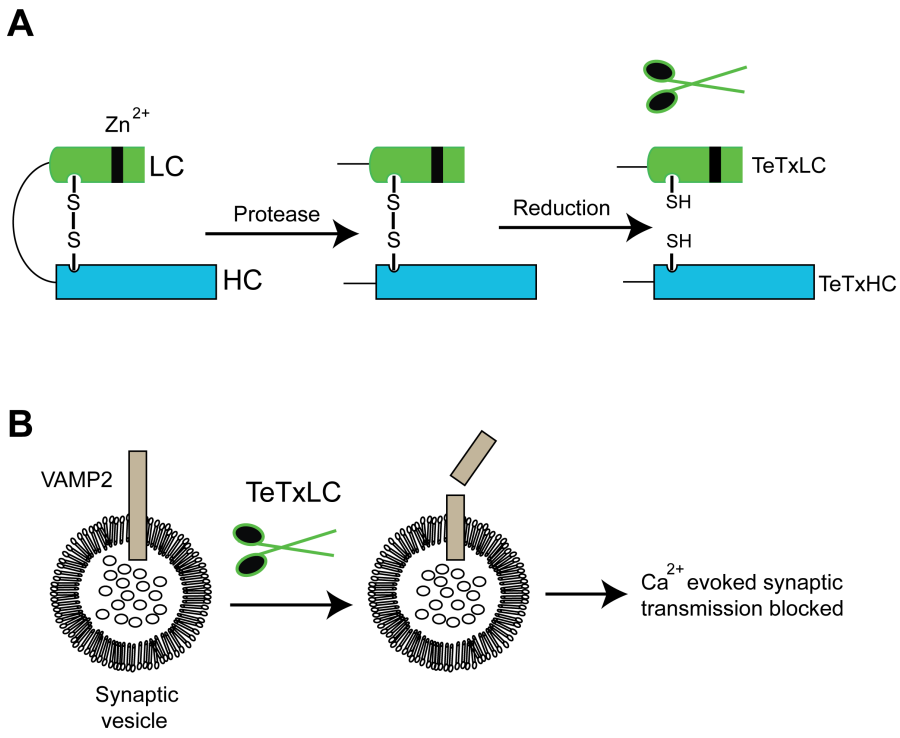

Figure 1.9 Mechanism of action of the *Clostridial* neurotoxin (tetanus toxin)

(A) Tetanus toxin is produced as a single chain polypeptide which is cleaved by protease to generate the 100 kDa heavy chain (HC) and the 50 kDa light chain (LC) held together by a disulphide bond. (B) The HC mediate the translocation and endocytosis of the LC into the cytosol and into the presynaptic terminus. The LC then selectively cleaves VAMP2 leading to abrogation of Ca^{2+}-evoked synaptic vesicle release of neurotransmitters (modified from Schiavo et al., 1992 and Yamamoto et al., 2003).

2. RESULTS

2.1 Long-term, Dox-controlled, tTA- and rtTA-dependent regulated gene expression in neurons *in vitro* and *in vivo*

2.1.1 Dox-controlled, tTA- and rtTA-dependent regulated gene expression *in vitro*

To test whether the rAAV-Tet (Dox) systems can be used for rapid gene activation and inactivation in a Dox-dependent manner, dissociated primary neurons and rat organotypic brain slices were co-infected with three viruses: (a) a Tet-responder virus (rAAV-P_{tet}bi-fLUC/tdTOM) to express the firefly luciferase gene and a red fluorescent protein variant tdTomato (tdTOM) under the control of a P_{tet}bi promoter, (b) an activator virus (either rAAV-hSYN-tTA or rAAV-hSYN-rtTA) for neuron specific expression of either tTA or rtTA under the control of the human synapsin promoter and (c) a control reporter virus (rAAV-hSYN-rLUC) to express the renilla luciferase gene under a human synapsin promoter. rLUC allows for normalization of variability in transfection/infection efficiency and sample handling during luciferase activity measurements (Fig. 2.1 A).

Organotypic slices and dissociated primary neurons were infected with virus cocktail for two weeks. Robust tTA- and rtTA-dependent gene activation was observed in organotypic slices as visualized by tdTOM fluorescence (Fig. 2.1 B). With the rtTA system, gene activation was observed only in the presence of Dox after forty-eight hours (Fig. 2.1 B, middle). To quantify gene expression, luciferase assays were performed. Robust gene activation was observed with both, the tTA- (150 fold) and the rtTA-systems (200 fold) (Fig. 2.1 C). Luciferase activity was basal without tTA or rtTA (Fig. 2.1 C, see asterisk) indicating minimal leakiness of P_{tet}bi, thus making the rAAV-Tet systems applicable for gene expression studies. In rtTA infected slices there was no discernible gene expression in the absence of Dox when visualized by fluorescence imaging or quantified by firefly luciferase activity measurement (Fig. 2.1 B and C). A time course of

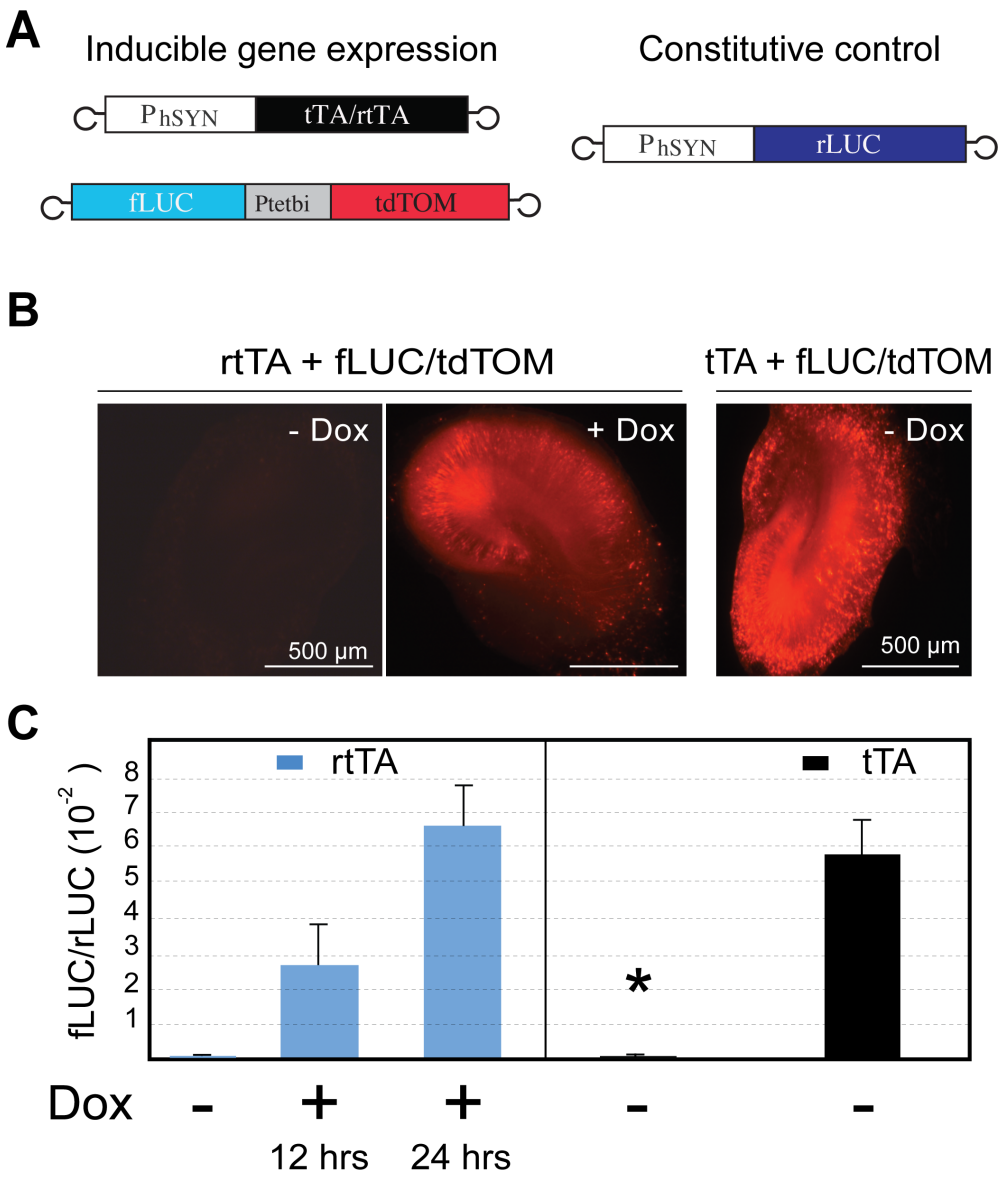

Figure 2.1 Kinetics of Tet-dependent gene regulation (continued below)

(A) Schematics of rAAV vectors for inducible gene expression studies. A virus equipped with a human synapsin promoter (hSYN) to express tTA or rtTA (left upper panel), a P_{tet}bi virus to express two different reporter genes encoding the firefly luciferase (fLUC) and a red fluorescent protein variant, tdTomato (left lower panel) and a virus equipped with an hSYN to express renilla luciferase (rLUC) (right panel). (B) Dox-controlled, rtTA- (left panel) and tTA- (right panel) dependent gene activation in rat organotypic hippocampal slices infected with rAAV-hSYN-tTA + rAAV-P_{tet}bi-fLUC/tdTOM and rAAV-hSYN-rtTA + rAAV-P_{tet}bi-fLUC/tdTOM, respectively. (C) Firefly luciferase activity measurements in organotypic hippocampal slices. The asterisk (*) shows measurements in which tTA virus was not included in the infection mixture.

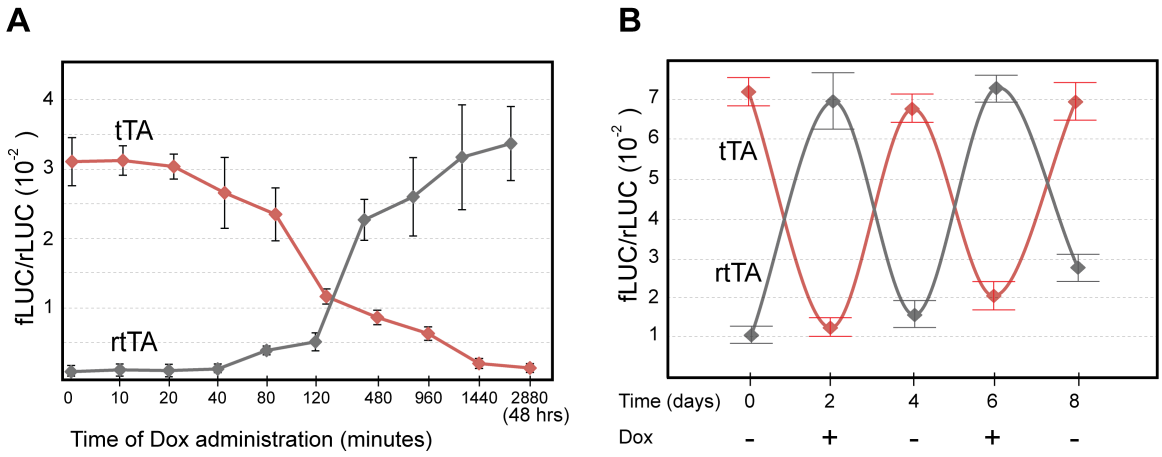

Figure 2.2 Kinetics of Tet gene regulation (continued from above)

(A) Time course of Dox-controlled, tTA- and rtTA-dependent luciferase activity in infected dissociated primary neurons. The cells were incubated with Dox (1 µg/ml) and harvested at different time points. Luciferase activities were measured from cell lysates at different time points after Dox treatment, ranging from 10-2880 minutes. (B) Repeated cycles of gene activation and inactivation in dissociated primary neurons upon Dox administration. Cells were harvested every 48 hours after Dox addition or withdrawal and the lysates were used for luciferase activity measurements.

Dox-induced gene activation and inactivation was performed in dissociated neurons with viruses that express either tTA or rtTA in combination with the firefly luciferase under the control of P_{tet}bi promoter and a virus containing a renilla luciferase construct under the control of a constitutive promoter, hSYN. With the rtTA and the tTA systems, gene activation and inactivation by Dox (1 µg/ml of medium) was maximum or minimum, respectively, after 48 hours (Fig. 2.2 A). Since Dox-controlled, tTA-dependent gene inactivation or rtTA-dependent gene activation was nearly complete after 48 hours (Fig. 2.2 A), a 48 hour period was chosen for recording repeated cycles of Dox-controlled gene activation and inactivation *in vitro*.

Over a period of eight days, the firefly luciferase gene was turned "ON" and "OFF" in a Dox-dependent manner (Fig. 2.2 B). Residual luciferase activity was observed at the end of an "OFF" cycle. With a left-over residual luciferase activity, the subsequent cycle of gene activation thus started out with a higher basal level of luciferase

activity. From these results, it was estimated that the firefly luciferase has a half-life of approximately eight hours. Therefore, with the firefly luciferase as a reporter, an activation time of 48 hours and an inactivation time of 72 hours would be appropriate choices. It should be noted, however, that the inactivation time course should be determined for different proteins which might differ in their respective half-lives. With these findings with the rAAV-Tet systems, it should be possible to study various biological features by controlling gene expression in a cyclic manner *in vitro*.

2.1.2 Dox-controlled, tTA- and rtTA-dependent regulated gene expression *in vivo*

As the above kinetics of Dox-induced gene expressions were done *in vitro*, these results may not be the same *in vivo*. Therefore in order to perform such a kinetic study *in vivo*, the first thing was to determine the optimal Dox concentration required for tTA- and rtTA-dependent gene activation and inactivation. To achieve this, three viruses (rAAV-P_{tet}bi-fLUC/tdTOM + rAAV-hSYN-tTA/rtTA and rAAV-hSYN-rLUC) were injected bilaterally into the cortices and the hippocampi of 10 wild-type mice. Two weeks after virus injection, mice were injected with different concentrations of Dox (3, 10, 30, and 100 µg/g body weight, n=1 per group). Two days after Dox injection, firefly luciferase and renilla luciferase activities were measured from brain lysates derived from virus infected brain regions (four sampling points per mouse).

With the tTA system, it was observed that 10 µg/g body weight of Dox was sufficient to strongly reduce gene expression (Fig. 2.3 A). When this same experiment was repeated with the rtTA system, it was found that 30 µg/g body weight of Dox was sufficient for gene activation (Fig. 2.3 B). After determining the optimal Dox concentration for tTA- and rtTA-dependent gene activation, the next experiment was to determine the number of days required to complete one cycle of gene activation and inactivation. To achieve this goal, 10 wild-type mice were injected into the cortices and the hippocampi of both brain hemispheres with the three viruses (rAAV-P_{tet}bi-fLUC/tdTOM + rAAV-hSYN-tTA/rtTA and rAAV-hSYN-rLUC). Two weeks after virus injection, a single dose of Dox (10 µg/g body weight for tTA injected mice and 30 µg/g

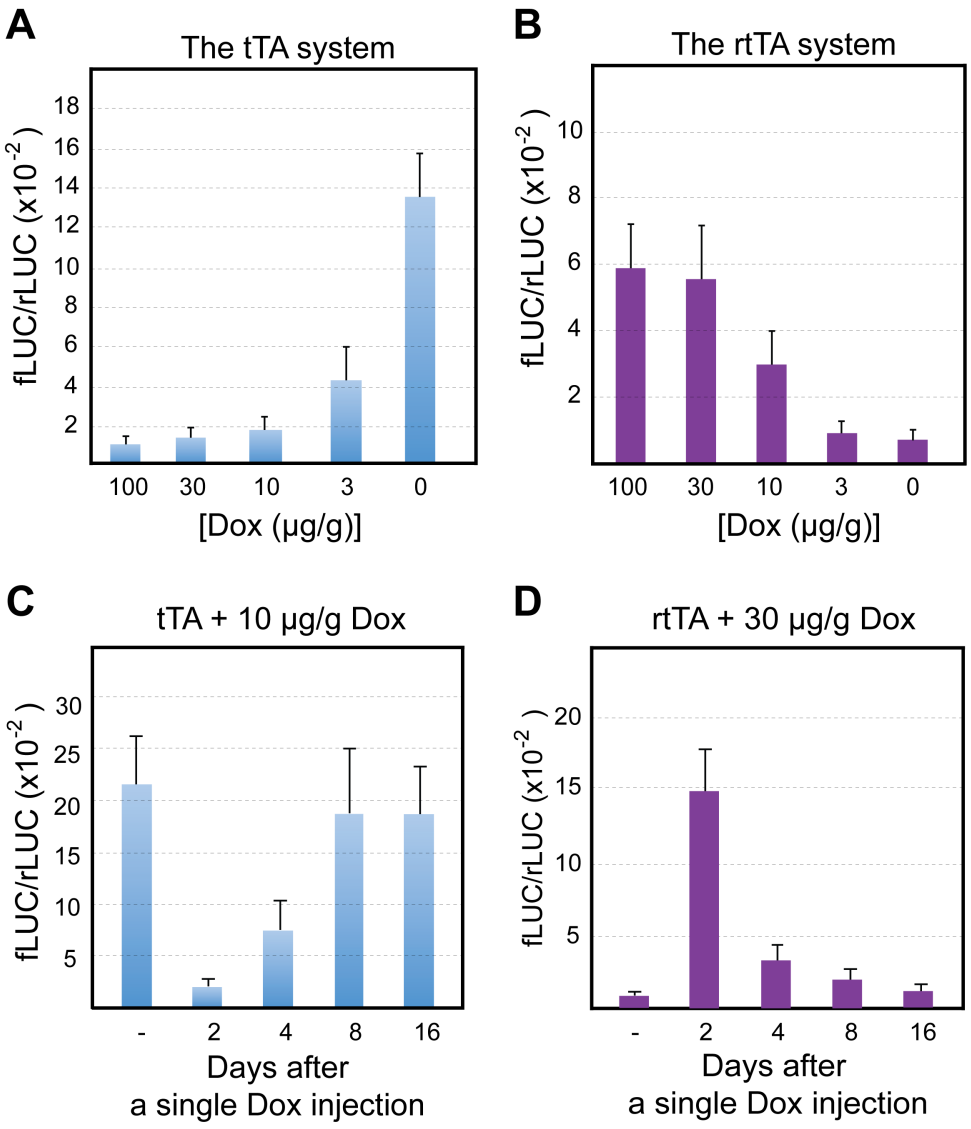

Figure 2.3 Optimal concentration of Dox for *in vivo* gene regulation in the mouse brain

(A) Luciferase activities measured from mouse brain extracts infected with rAAV-P_{tet}bi-fLUC/tdTOM + rAAV-hSYN-rLUC + rAAV-hSYN-tTA and later injected with different concentrations of Dox. 10 µg/g body weight of Dox was sufficient for a strong reduction in tTA dependent gene activation. (B) Luciferase activities from brain extracts injected with rtTA virus, followed by Dox injection. 30 µg/g body weight of Dox was found to be sufficient to induce optimal gene activation. (C) Time course of complete cycle of Dox-controlled tTA-dependent gene activation and inactivation. A single i.p. injection of Dox (10 µg/g) showed that gene inactivation took two days and reactivation took six days. (D) Time course of complete cycle of rtTA-dependent gene regulation *in vivo*. Luciferase activities were measured from rtTA injected mice, which were injected with a single dose of Dox (30 µg/g body weight). It showed that a complete cycle of gene activation /inactivation required 8 days.

body weight for rtTA injected mice) was delivered by intraperitonial injection (i.p.). Two mice from each group (tTA/ rtTA) were without Dox (control).

Firefly and renilla luciferase activities were measured from brain extracts derived from the cortices and the hippocampi of both brain hemispheres (Fig. 2.3 C and D). The brain extracts were obtained from 4 different regions per mouse. It was observed with the tTA system that two days were required to observe robust gene inactivation by a single Dox injection (10 µg/g body weight) and six days for reactivation (Fig. 2.3 C). The rtTA system on the other hand, required two days after a single Dox (30 µg/g body weight) injection to observe optimal gene activation and six days for inactivation (Fig. 2.3 D). One could therefore conclude from these experiments that a complete cycle of Dox-controlled tTA/rtTA-dependent gene activation and inactivation can be done in eight days (Fig. 2.3 C and D).

Based on the above results, repeated cycles of gene activation and inactivation *in vivo* were performed. To do this, 10 wild-type mice were injected with three viruses (rAAV-P_{tet}bi-fLUC/tdTOM + rAAV-hSYN-tTA and rAAV-hSYN-rLUC) and 10 other mice with the other three viruses (rAAV-P_{tet}bi-fLUC/tdTOM + rAAV-hSYN-rtTA and rAAV-hSYN-rLUC) into the cortices and the hippocampi of both brain hemispheres. tTA injected mice were all (except 2) injected with 10 µg/g body weight of Dox at different time points for sixteen days (i.e 2 days of Dox injection for inactivation, followed by 6 days of withdrawal for reactivation) (Fig. 2.4 A). Two complete cycles of gene regulation were achieved in 16 days.

Mice injected with the firefly luciferase, renilla luciferase and rtTA viruses were also injected with 30 µg/g Dox at different time points for 16 days (2 days of Dox injection for activation and 6 days of Dox withdrawal for gene inactivation). At the end of two cycles of gene regulation, luciferase activities were measured from brain extracts from all virus-infected mice (Fig. 2.4 B). There was about 3-fold gene regulation in both the tTA and the rtTA gene expression systems. These findings were in agreement with previous studies using transgenic mice where a 4 fold increase in *in vivo* gene regulation was observed (Hasan et al., 2001). The results also show that the *in vitro* kinetics is faster than the *in vivo*. Based on these *in vivo* and *in vitro* findings, it was concluded that

rAAVs equipped with the tetracycline genetic switches can allow for repeated cycles of gene activation and inactivation *in vitro and in vivo.*

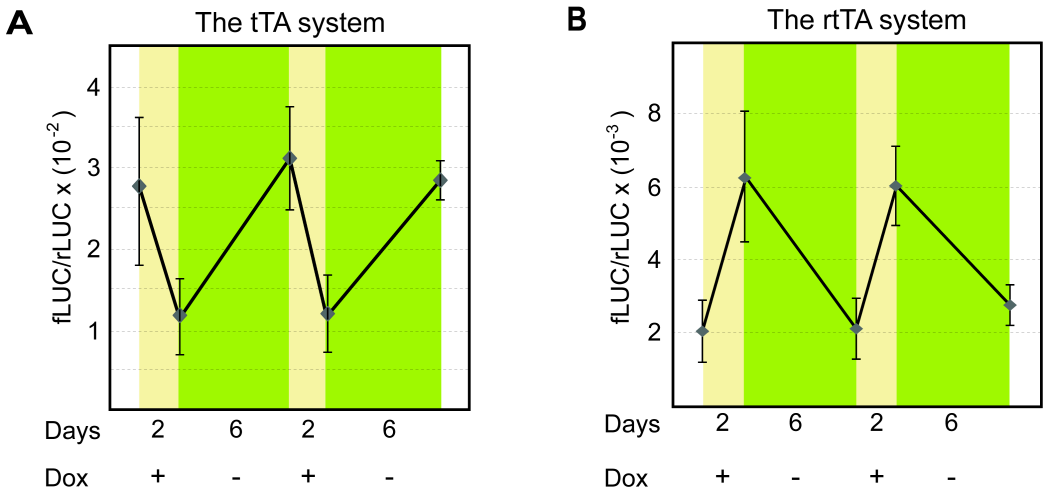

Figure 2.4 Repeated cycles of Tet-controlled gene regulation *in vivo*

(A) Dox-controlled tTA-dependent repeated cycles of gene activation and inactivation *in vivo.* 10 wild-type mice were injected with a mixture of firefly luciferase, renilla luciferase and tTA viruses. These mice were later injected with Dox for 2 days and withdrawn from Dox for 6 days. At the end of 2 cycles of gene regulation covering 16 days, luciferase activities were measured from brain extracts from the cortices and the hippocamppi. (B) Dox-controlled rtTA-dependent cyclic gene regulation. 10 wild-type mice were injected with firefly luciferase, renilla luciferase and rtTA viruses. After two cycles of gene regulation, covering 16 days, luciferase activities were measured from brain extracts.

2.1.3 Comparison between firefly luciferase (*Photinus pyralis*) and the Brazilian luciferase *(Cratomorphus distinctus)*

One of the objectives of the Dox-controlled tTA/rtTA dependent gene regulation kinetic study is to apply it to study *in vivo* noninvasive bioluminescence imaging. For the *in vivo* bioluminescence imaging, it is possible to capture photons emitted in living mouse brain

injected with the firefly luciferase viruses using the photon capturing device called Intensified Charged Coupled Device (ICCD) and an image processor (Sweeney et al., 1999). In order to achieve this, the Brazilian luciferase *(Cratomorphus distinctus*) which has been reported to be 50 times better at emitting photons than the *Photinus pyralis* (fLUC) was used. Two new constructs were therefore generated of the Brazilian luciferase (bLUC). The first construct is under the control of P_{tet}bi promoter expressing bLUC and Venus (a green fluorescent protein variant), named rAAV-P_{tet}bi-bLUC/Venus for inducible expression and the constitutive construct rAAV-hSYN-bLUC under the human synapsin promoter (Fig. 2.5 A).

To compare the activity of bLUC and fLUC under the inducible promoter, rat organotypic slices were infected with rAAV-P_{tet}bi-bLUC/Venus + rAAV-hSYN-tTA/rtTA + rAAV-hSYN-rLUC and rAAV-P_{tet}bi-fLUC/tdTOM + rAAV-hSYN-tTA/rtTA + rAAV-hSYN-rLUC (Fig. 2.5 B). Two weeks after virus infection, rtTA infected slices were either treated with Dox or without (control) for forty-eight hours. After the Dox treatment, slices were harvested for luciferase assay (Fig. 2.5 B). With both the tTA and the rtTA systems, it was observed that bLUC is about 60 times better in the relative values of firefly luciferase activities. It was also observed that there was about a 1000 fold in gene regulation of bLUC compared to fLUC, which was about 300 fold. These results confirmed that bLUC is better suited for *in vivo* bioluminescence imaging.

Based on the *in vitro* luciferase assay data, 5 NMRI mice were injected with rAAV-P_{tet}bi-bLUC/Venus + rAAV-hSYN-tTA + rAAV-hSYN-rLUC and 5 NMRI mice with rAAV-P_{tet}bi-bLUC/Venus + rAAV-hSYN-rtTA + rAAV-hSYN-rLUC (NMRI mice were used for the *in vivo* bioluminescence imaging because their white fur, allow more photons to pass through than the C57BL/6). These viruses were injected into the medial parietal associative cortex (Fig. 2.5 C, pink arrow) and the constitutive rAAV-hSYN-bLUC was injected to the motor cortex (Fig. 2.5 C, white arrow). The extent of virus infection is indicated with the Venus expression, which is about 1.5 mm in diameter. The two coordinates were chosen to be far apart to allow for the separation of the photons coming from the inducible expression and the constitutive expression. The inducible expression system should exhibit an “ON/OFF” cycles of gene regulation by the observation of photons, which should disappear/appear on Dox injection or withdrawal.

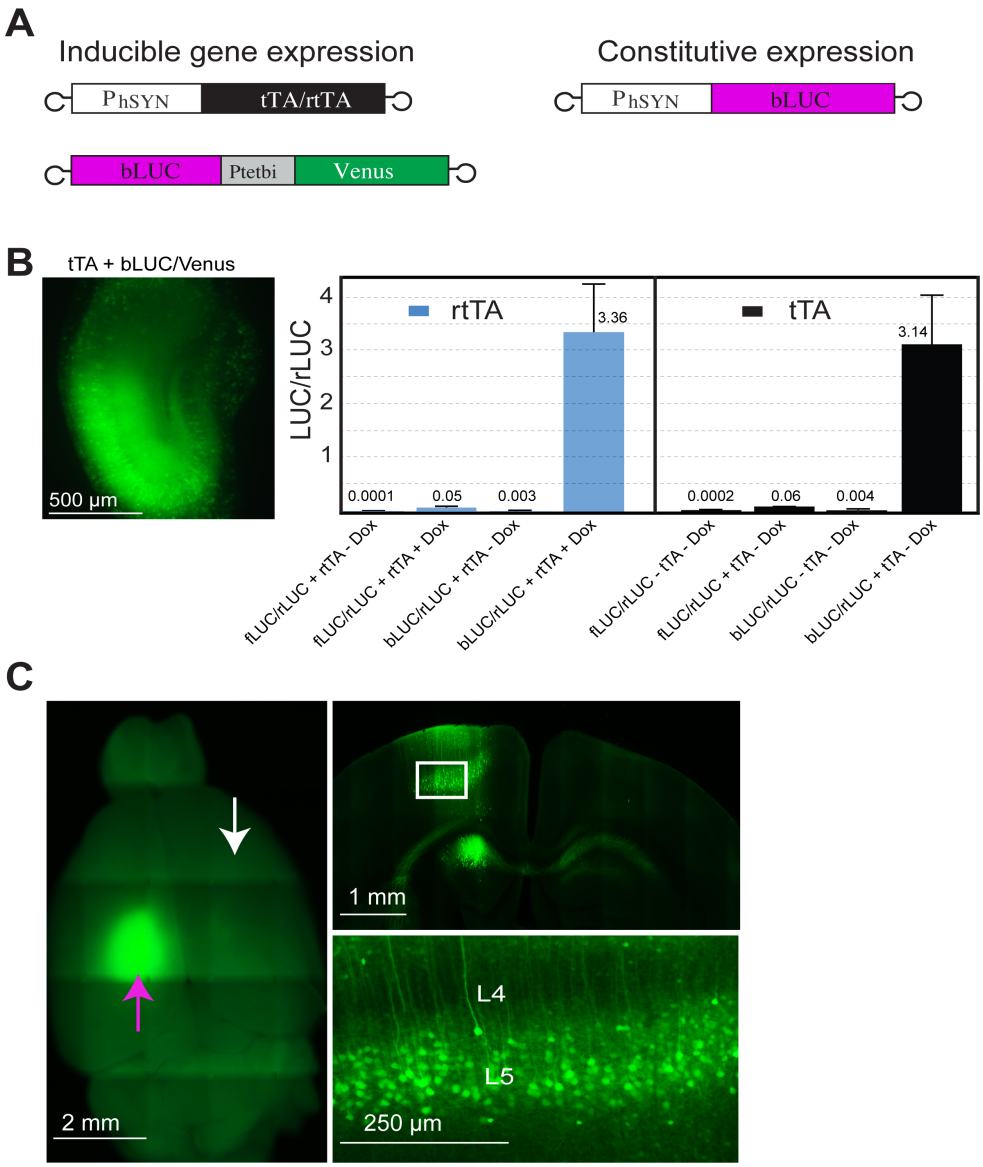

Figure 2.5 Brazilian luciferase *(Cratomorphus distinctus)* and firefly luciferase activities *in vitro*

(A) Schematics of the Brazilian luciferase (bLUC) constructs under the P_{tet}bi promoter (left) and under the constitutive human synapsin promoter**.** (B) Organotypic slice infected with rAAV-P_{tet}bi-bLUC/Venus + rAAV-hSYN-tTA (left). Firefly luciferase activity measurements from organotypic slices infected with rAAV-P_{tet}bi-bLUC/Venus + rAAV-hSYN-tTA/rtTA + rAAV-hSYN-rLUC and rAAV-P_{tet}bi-fLUC/tdTOM + rAAV-hSYN-tTA/rtTA + rAAV-hSYN-rLUC. The findings indicate that bLUC is better regulated and shows higher luciferase expression compared to fLUC. (C) *In vivo* expression of rAAV-P_{tet}bi-bLUC/Venus + rAAV-hSYN-tTA (pink arrow) injected into the medial parietal associative cortex and the constitutive rAAV-hSYN-bLUC (white arrow) injected to the motor cortex. Right panel is a coronal section of the viral injected site expressing the inducible rAAV-P_{tet}bi-bLUC/Venus.

However, the constitutive bLUC should be "ON" throughout the investigation.

2.2 Inducible, subregion- and cell-type restricted gene expression and gene knockout in the mouse brain

To investigate whether Tet-inducible gene expression can be achieved *in vivo* in the mouse brain, different brain regions of wild-type mice were injected with a mixture of activator (rAAV-hSYN-rtTA) and responder (rAAV-P_{tet}bi-iCre/tdTOM) viruses (Fig. 2.6 A) (Zhu et al., 2007). To test the virus for expression, six rat hippocampal organotypic slices were infected with the two viral cocktail (rAAV-hSYN-rtTA and rAAV-P_{tet}bi-iCre/tdTOM). Two weeks after virus infection, four slices were incubated with 1 μg/ml Dox in the medium for 48 hours while the remaining two were without Dox (control). Robust gene activation was observed in all Dox treated slices after forty-eight hours (Fig. 2.6 B, right panel). Slices without Dox showed undetectable expression of tdTOM (Fig. 2.6 B, left panel), indicating that the system is tight and leakiness is minimal.

After the *in vitro* experiment with organotypic slices, viruses (rAAV-hSYN-rtTA and rAAV-P_{tet}bi-iCre/tdTOM) were injected stereotaxically into different brain regions of wild-type mice (cortex, the hippocampus or both). In total, eight mice were injected (two were injected into only hippocampus, two into the cortex and four into both cortex and the hippocampus). Two weeks after virus injection, six mice were injected with a single dose of Dox (100 μg/g body weight), the remaining two served as a control (without Dox). Two days after Dox injection, mice were perfused and 100 μm thick coronal slices were imaged for gene expression. Dox injected mice showed robust gene expression in virus-infected areas of the brain (Fig. 2.6 C, upper and lower panels). The viral spread was about 0.5-1.5 mm in diameter. Layer 2, 3 and 5 of the cortical pyramidal neurons were massively infected by the rAAV with the soma and dendrites showing strong expression while layer 4 and 6 neurons were largely spared of infection. This phenomenon has been observed in all instances of virus injection into the cortex (Fig. 2.6 C and Fig. 2.8 A). Granule cells of the dentate gyrus and CA1 pyramidal neurons were

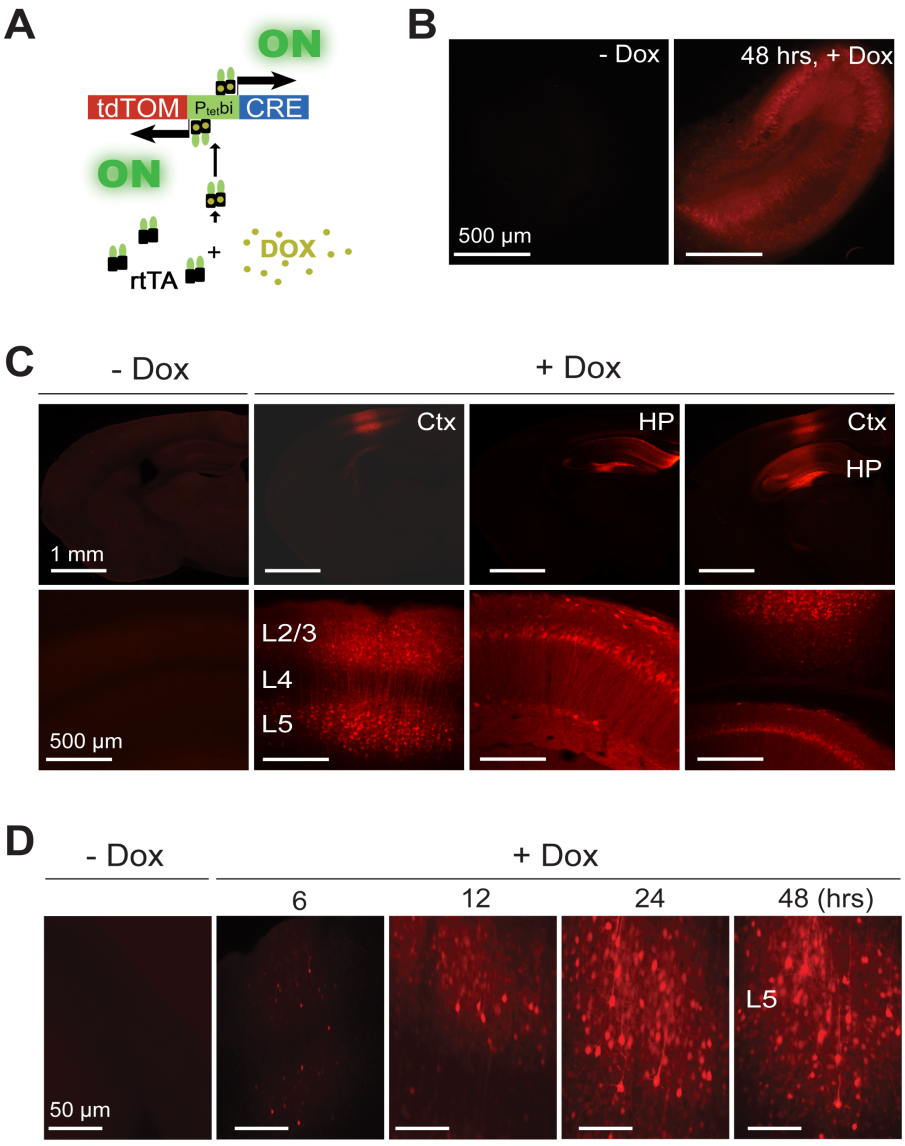

Figure 2.6 Dox-induced, rtTA-dependent brain region- and cell type-specific gene activation *in vivo*
(A) Schematics of rAAV-rtTA system, a virus with a human synapsin promoter for constitutive rtTA expression and a second virus containing P_{tet}bi to express two different genes, the Cre recombinase and a red fluorescent protein variant, tdTOM. Binding of Dox to rtTA enables the rtTA to bind to P_{tet}bi, thus activating gene expression. (B) Rat organotypic slices were infected with rAAV-hSYN-rtTA and rAAV-P_{tet}bi-iCre/tdTOM and gene expression was imaged in the absence and presence of Dox. (C) Fluorescent images of 100 µm thick coronal sections from mouse brain infected with rAAV-hSYN-rtTA and rAAV-P_{tet}bi-iCre/tdTOM. Gene expression was imaged in the absence and presence of Dox. Abbreviations: hippocampus (HP), cortex (Ctx), layer (L). (D) Time course of Dox-induced gene activation *in vivo*. Images of wild-type mice injected with rAAV-hSYN-rtTA + rAAV-P_{tet}bi-iCre/tdTOM into the cortex, followed by Dox injection at different time points over 2 days.

also robustly infected including the mossy fibers (Fig. 2.6 C). Dox untreated mice showed basal expression, indicating marginal leakiness (Fig. 2.6 C, left).

To investigate the time course of Dox-controlled, rtTA dependent gene activation *in vivo*, viruses (rAAV-hSYN-rtTA and rAAV-P_{tet}bi-iCre/tdTOM) were injected into the cortex of 10 wild-type mice. Two weeks after virus infection, mice were put into five groups (two mice per group). The first group was without Dox but only viruses (control), while the other four groups were injected with Dox (100 µg/g body weight) at different time points (6-48 hours). After Dox injection, gene activation was monitored by fluorescence imaging of tdTOM (Fig. 2.6 D). Mice injected with viruses but without Dox showed no observable tdTOM expression (Fig. 2.6 D, left panel). On the other hand, mice injected with both virus and Dox showed robust tdTOM expression. Expression of tdTOM was observed as early as six hours after Dox injection (Fig. 2.6 D, left). The expression of tdTOM increases with time, reaching maximum at 24 hours after Dox injection and remained stable after 48 hours.

After demonstrating Dox-induced, rtTA-dependent gene activation *in vivo*, and also demonstrating region specific gene induction, the same system was applied to test for Cre/*lox*P-mediated gene recombination in specific brain regions in the Rosa26R mice (Fig. 2.7 A and B) (Soriano, 1999). Different brain regions (either cortex, hippocampus, or both) of eight Rosa26R mice were injected with a mixture of two viruses: (rAAV-hSYN-rtTA and rAAV-P_{tet}bi-iCre/tdTOM). Two weeks after virus injection, six mice were injected with a single dose of Dox (100 µg/g body weight) via intraperitonial injection (i.p.) while the remaining two were without Dox (control). Forty-eight hours after Dox injection, all mice including the control were sacrificed. Coronal sections (100 µm thick) were stained for β-galactosidase activity (LacZ staining) (Fig. 2.7 B). Cre/*lox*P gene recombination was observed in virus and Dox injected mice indicating the expression of the Cre enzyme. However, in the control group of mice (without Dox), expression was at basal level (Fig. 2.7 B, left panel). This could be due to the low basal activity of the P_{tet}bi. With multiple viruses infecting each neuron, low basal activity by P_{tet}bi also accumulates. The basal P_{tet}bi activity could also be due to the viral ITR, which act as an enhancer (Hatfield and Hearing, 1991).

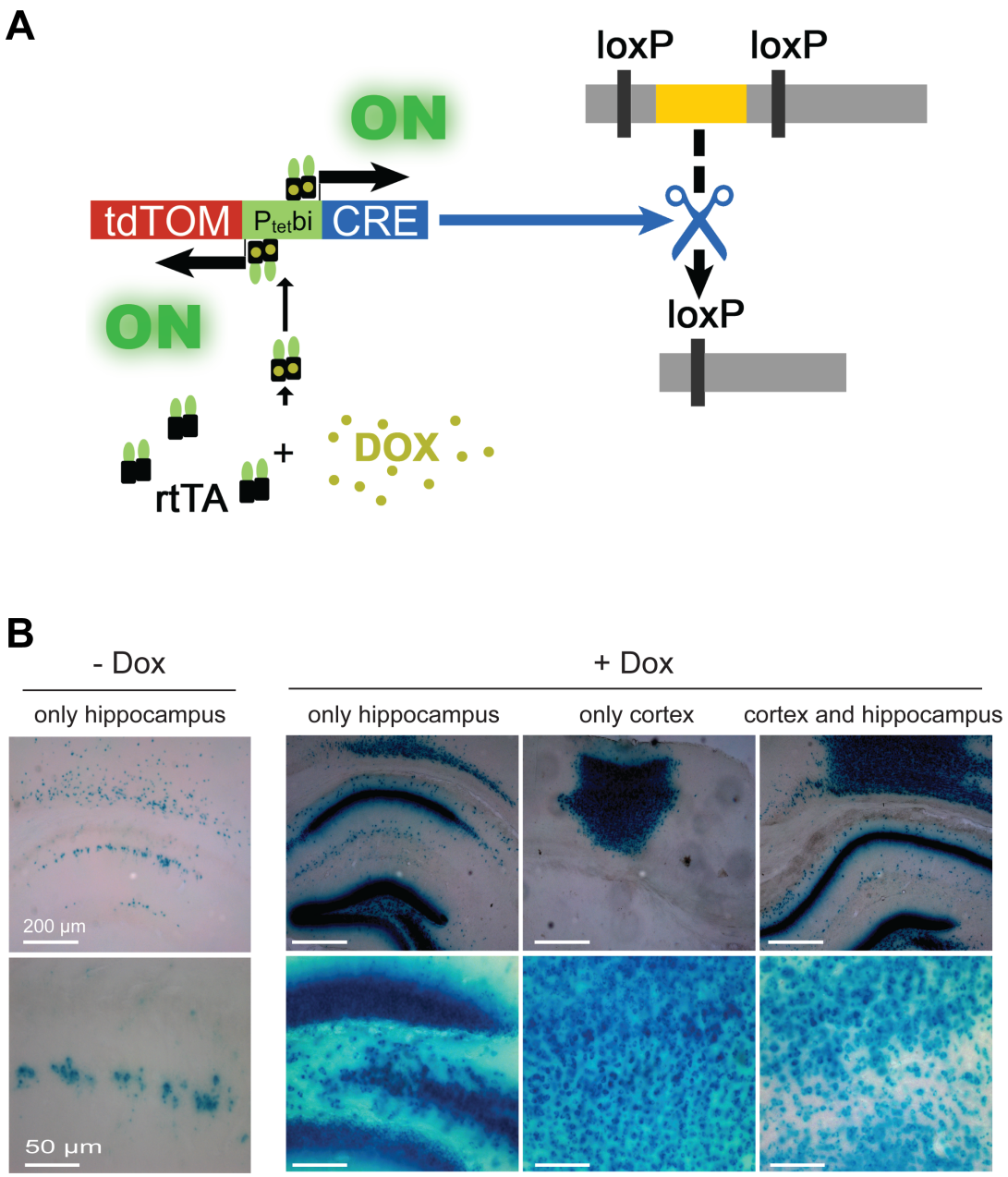

Figure 2.7 Region-specific gene recombination: Dox-induced Cre-mediated gene recombination in Rosa26R mice

(A) Schematics of Dox-controlled, rtTA-dependent Cre gene expression (left panel) and Cre-mediated gene recombination (right panel). (B) rAAV-hSYN-rtTA + rAAV-P_{tet}bi-iCre/tdTOM were injected into specific brain regions (cortex, hippocampus or both) of Rosa26R reporter mice and either treated with Dox or left untreated. β-galactosidase staining was used to monitor Cre-mediated gene recombination.

In order to reduce the level of leakiness due to the responder, the responder virus (rAAV-P_{tet}bi-iCre/tdTOM) stock was diluted by 1:1 and 3:1 with respect to the activator virus. The diluted responder virus was injected together with hSYN-Venus into cortical brain regions of Rosa26R mice. The infectious titer determined in dissociated primary neurons was found to be 5 x10^8 transducing units per milliliter. With a 1:1 and 3:1 dilution of activator to Tet-responder, leakiness was reduced to undetectable levels when investigated by fluorescence imaging of tdTOM (-Dox, Fig. 2.8 A). Interestingly, with an activator-to Tet-responder dilution of 3:1, it was observed that infection was primarily restricted to layer 5 cortical neurons (Fig. 2.8 A, right panel). However, the constitutively expressed Venus also included in the same virus cocktail showed strong expression in both layer 2/3 and layer 5 cortical neurons (Fig. 2.8 A). This is an indication that the targeting/expression of the Tet-responder virus is high in layer 5 cortical neurons (Fig. 2.8 A). When alternate slides from the same virus injected Rosa26R mice were stained for Cre recombinase activity by β-galactosidase staining, the leakiness was reduced significantly in the 3:1 dilution of the responder compared to the undiluted responder virus in the absence of Dox (Fig. 2.8 B, -Dox). The advantage provided by this experiment is that it is possible to precisely target layer specific neurons to investigate cortical circuitry.

2.2.1 Region-specific Dox-mediated rtTA-dependent gene knockout in NR1-2*lox* mice

The NMDA receptor 1 gene (NR1) was chosen to investigate the role of the NMDA receptor in cortical map plasticity and fear-related learning and memory. Based on the result of the Cre-virus titration, Dox-dependent gene knockout in NR1-2*lox* mice was performed. The barrel cortex of six NR1-2*lox* mice (3 months old) was infected with rAAV-hSYN-rtTA and rAAV-P_{tet}bi-iCre/tdTOM for 2-3 weeks. To precisely register the time point of Dox delivery, four mice were treated with Dox by a single i.p. injection and also continuously treated with Dox in the drinking water for 1 week. Two virus infected NR1-2*lox* mice were not treated with Dox (control). The extent of virus infection in the

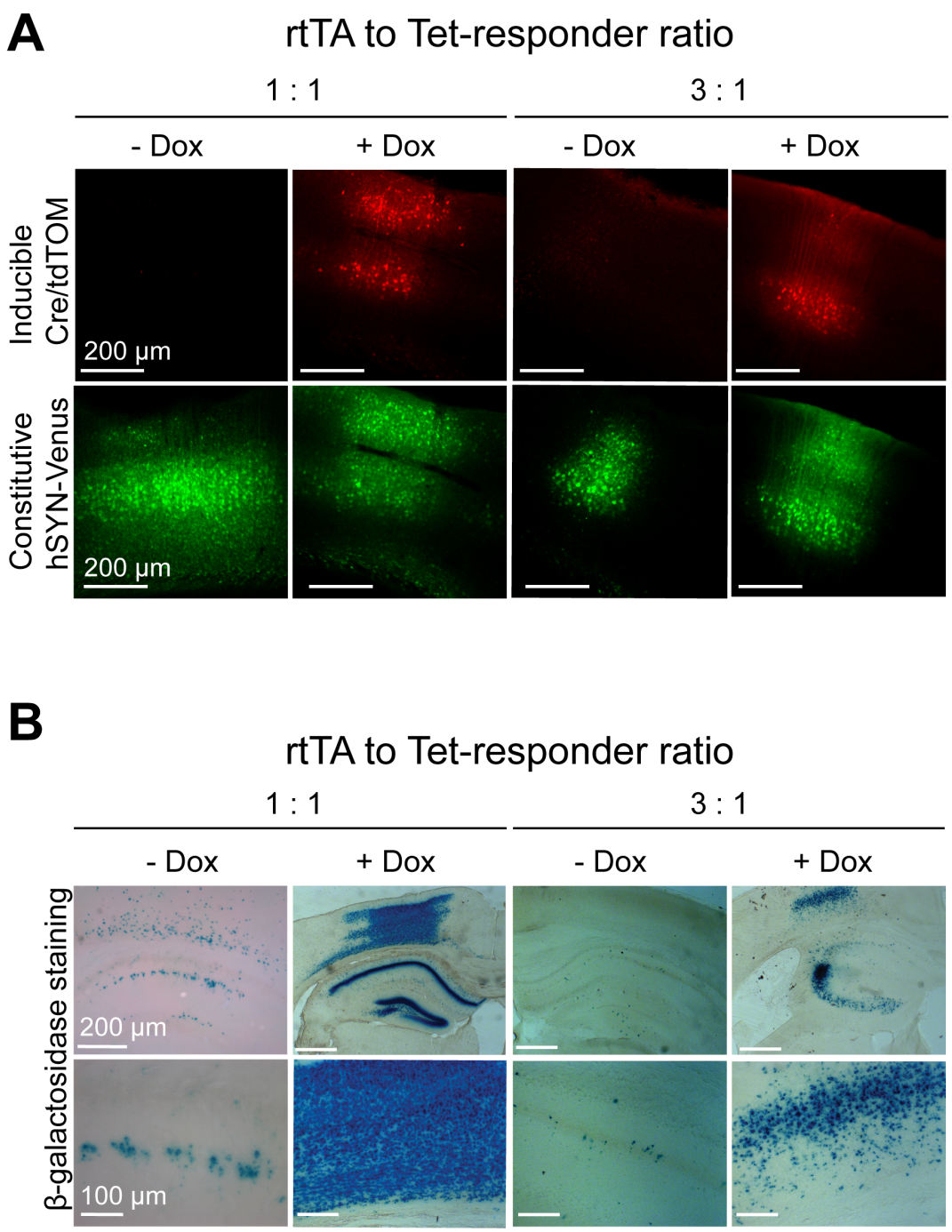

Figure 2.8 Titrating Tet responder viruses to reduce leaky expression

(A) rAAV-hSYN-rtTA, rAAV-P_{tet}bi-iCre/tdTOM and rAAV-hSYN-Venus were injected into the brain of Rosa26R mice. Two weeks after virus injection, Dox-controlled expression was visualized by tdTOM, with rtTA to Tet-responder virus ratio of 1:1 and 3:1. The lower panel is a constitutive Venus expression. (B) ß-galactosidase activity reports Cre/*lox*P recombination under conditions as in (A).

cortex was observed by tdTOM fluorescence. Without Dox, tdTOM-fluorescence was undetectable (Fig. 2.9 A, left panel). In Dox treated mice, gene expression was largely restricted to cortical layer 2/3 and 5 with layer 4 neurons largely uninfected (Fig. 2.9 A, right panel). Immunostaining with mouse monoclonal Cre-specific antibody revealed same layer specific expression (Fig. 2.9 B).

Electrophysiological recordings were performed with 300 µm thick coronal cortical acute slices of layer 2/3 pyramidal neurons of the barrel cortex. Spontaneous NMDA-mediated miniature excitatory postsynaptic currents (NMDA-mEPSCs) were normal in brain slices derived from wild type and virus-infected NR1-2*lox* mice (without Dox) (Fig. 2.9 C). Virus-infected NR1-2*lox* mice (with Dox, 1 week) showed strongly reduced NMDA-mEPSCs. Additionally, an NMDA receptor specific antagonist (2-amino-5-phosphonopentanoic acid, APV) strongly reduced charge transfer in control brain slices (Fig. 2.9 C), but there was virtually no further decrease in NR1 knockout slices. These results provide strong support for complete NR-1 gene knockout in the barrel cortex.

2.2.2 Improving rAAV gene expression by co-injection with D-mannitol

One limitation of the rAAV gene delivery system is that of expression. In order to improve the expression of the rAAV gene delivery system *in vivo*, a new viral delivery protocol was adopted. In this approach, the virus cocktail was mixed with 20-25 % D-mannitol in 0.9 % NaCl. D-mannitol is a simple monosaccharide derived from fructose. It is generally used as osmotic diuretic agent, which causes temporal relaxation of the blood brain barrier (Mastakov et al., 2001, Carty et al., 2010). To enhance virus delivery with this method, rAAV-P_{tet}bi-iCre/tdTOM + rAAV-hSYN-rtTA were injected into the motor cortex of eight C57BL6 wild-type mice under different conditions (Fig. 2.10). The eight mice were put into four different groups (two mice per group). The first group was injected with 300 nl of virus only (Fig. 2.10, far left), the second group had intraperitonial injection of D-mannitol (3 ml of sterile 25 % mannitol in 0.9 % saline per 100 g body weight) (Louboutin et al., 2010) at least 20 minute prior to 300 nl of only virus injection

(Fig 2.10, middle left). The third group was injected with a mixture of virus (150 nl) and D-mannitol (150 nl). Meaning in this case, the volume of virus particle is half that of groups one and two (Fig. 2.10, middle right).

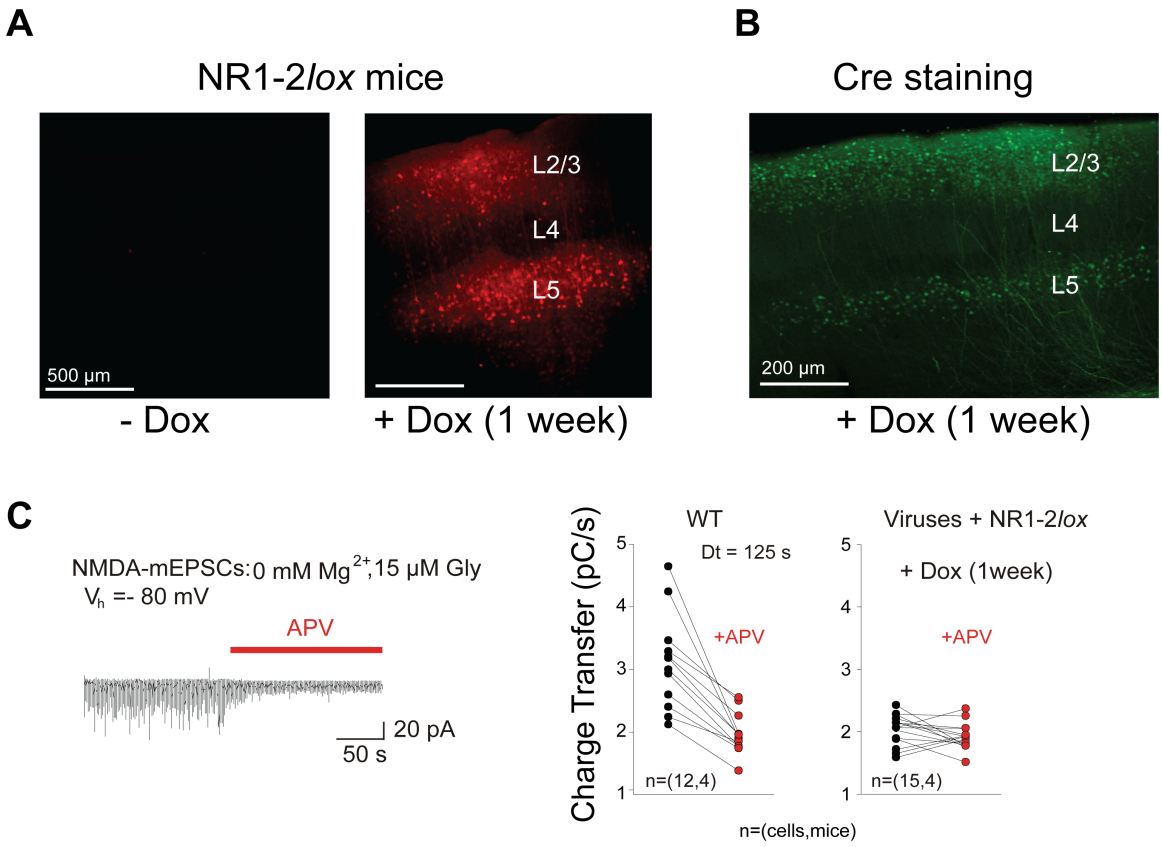

Figure 2.9 Inducible knockout of the NMDA receptor 1 gene

(A) Tet-inducible Cre-viruses delivered to the barrel cortex of NR1-2*lox* mice. Mice were either Dox-treated (1 week) or left untreated. Expression was visualized by tdTOM fluorescence imaging. (B) Mouse monoclonal anti-cre-immunostaining (primary antibody) followed by FITC secondary antibody in Dox-treated NR1-2*lox* mice. (C) Spontaneous NMDA-mediated miniature excitatory postsynaptic currents in acute brain slices of wild type (WT) and viruses/NR1-2*lox* treated with or without Dox (1 week). An NMDA receptor specific antagonist (APV) was used to blocked NMDA-mediated charge transfer. Abbreviation: n= number of mice or cells.

The last group was injected with D-mannitol by i.p. and a 1:1 mixture of virus and D-mannitol (Fig. 2.10, far right). Two weeks after virus injection, all mice were injected with 100 µg/g body weight of Dox and after 48 hours, mice were analyzed for tdTOM expression pattern. It was observed from this experiment that the virus infection was mainly in layer 5 in the first group of mice analyzed and the spread was about 0.9 mm in diameter, while in the second group, infection was observable in almost all layers (layer 2/3, layer 4 and layer 5) and the spread was about 1 mm in diameter. In the third group of mice, infection was mainly in layer 2/3 and layer 5, however, virus spread was about 0.8 mm. In the last group, despite the fact that the actual volume of virus delivered was half of group 1 and group 2, the virus spread was the largest observed, covering about 2 mm in diameter. This observation confirmed an earlier observation (Betz et al., 1998). These findings therefore indicate that prior i.p. injection of D-mannitol and a combination of virus D-mannitol mixture vastly improve virus delivery by increasing the number of neurons infected *in vivo* and also widening the virus spread (Fig. 2.10). NeuN staining on same slides indicates virus infected cells were mainly neurons (Fig. 2.10, lower panels).

2.2.3 The role of NMDA receptors in the motor cortex in associative learning and memory

To investigate the role of NMDA receptors in the motor cortex in associative learning and memory, 20 NR1-2*lox* mice and 20 wild-type mice were injected into the motor cortex at 6 different spots with rAAV-P_{tet}bi-iCre/tdTOM + hSYN-rtTA (Fig. 2.11 B). The motor cortex covers about 3 mm of the mouse's forebrain and the diameter ranges from 05-1.5 mm (Fig. 2.10 A). To ensure that the virus spreads across more than 70 % of this region, the injection was done using the mannitol protocol described above (Fig. 2.10, far right).

The mice were later put on Dox for three weeks to enable expression of the Cre gene and the deletion of the NMDA receptor 1 gene (from the previous experiment, we were able to delete the NMDA receptor within a week after placing the mice on Dox (Fig. 2.9 C). Figure 2.11 B showed an overview of the virus injections (white arrows).

This indicates that the virus spread covers more than 2 mm of the motor cortex. 100 µm coronal sections from a representative mouse brain indicate that the lateral spread of the

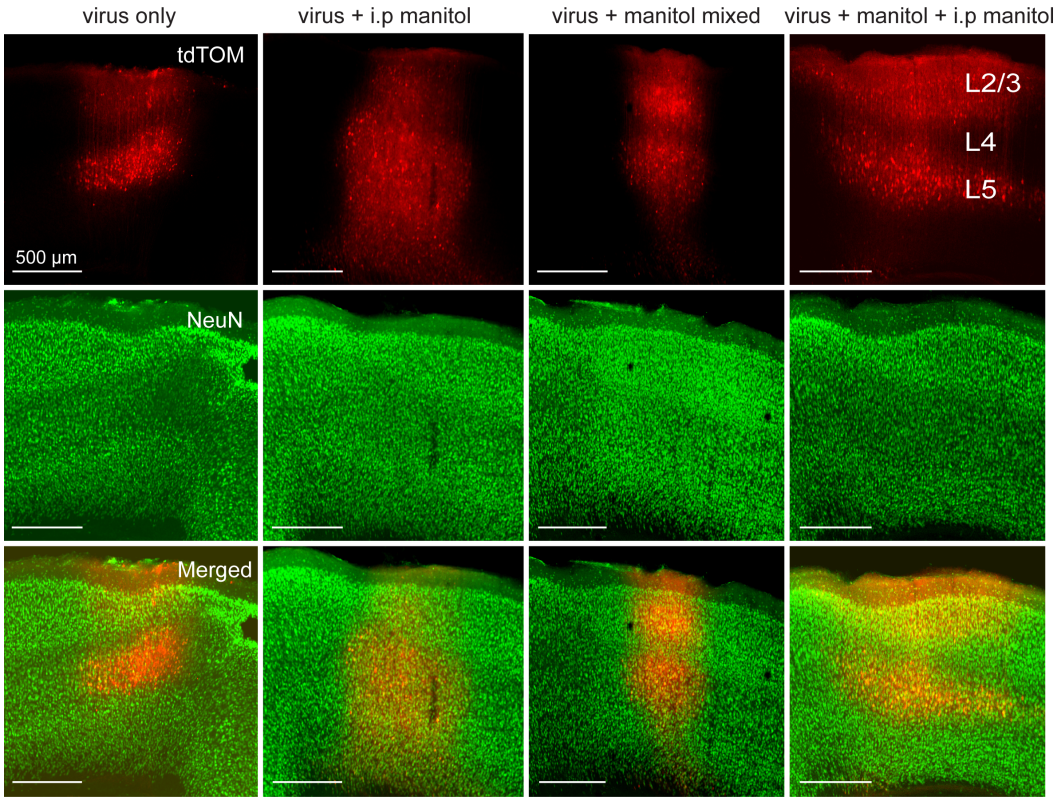

Figure 2.10 Effect of D-mannitol on *in vivo* virus expression pattern

Wild-type mice infected with rAAV-P_{tet}bi-iCre/tdTOM + hSYN-rtTA with or without D-mannitol in the motor cortex. The first group of mice was injected with virus only (300 nl). The observed virus spread was mainly in layer 5 and about 0.9 mm wide. In the second group (second image from left) mice were injected with viruses and i.p injection of D-mannitol. Virus spread mainly in all layers and the spread is about 1mm. In the third group, (3rd image from left), mice were injected with virus and mannitol mixture (1:1). Infection was mainly in layer 2/3 and 5 and the viral spread was 0.8 mm. In the last group, mice were injected with virus/mannitol mixture (1:1), and i.p. mannitol: Infection was mainly in layer 2/3 and 5. This group also showed the widest virus spread of about 2 mm. NeuN staining also indicated more neurons are labeled in the last group.

virus is 1mm or more in diameter (Fig 2.11 C and D). It was observed that more than 70 % of the motor cortex expressed the viruses. Cell counts using confocal images of 100 µm coronal sections indicated that within the infected regions, more than 90 % of NeuN positive cells expressed tdTOM. Viral infection was observed in layer 2/3 and 5 excluding layer 4. Immunostaining with mouse monoclonal Cre antibody showed that most (> 80 %) of all tdTOM positive neurons were also Cre positive (Fig. 2.11 E). This implies that the P_{tet}bi promoter drove the expression of both genes, to nearly equal extent. The wild-type mice and the NR1-2*lox* mice injected with the viruses are currently being analyzed to assess the role of the motor cortex NMDA receptors in associative learning and memory.

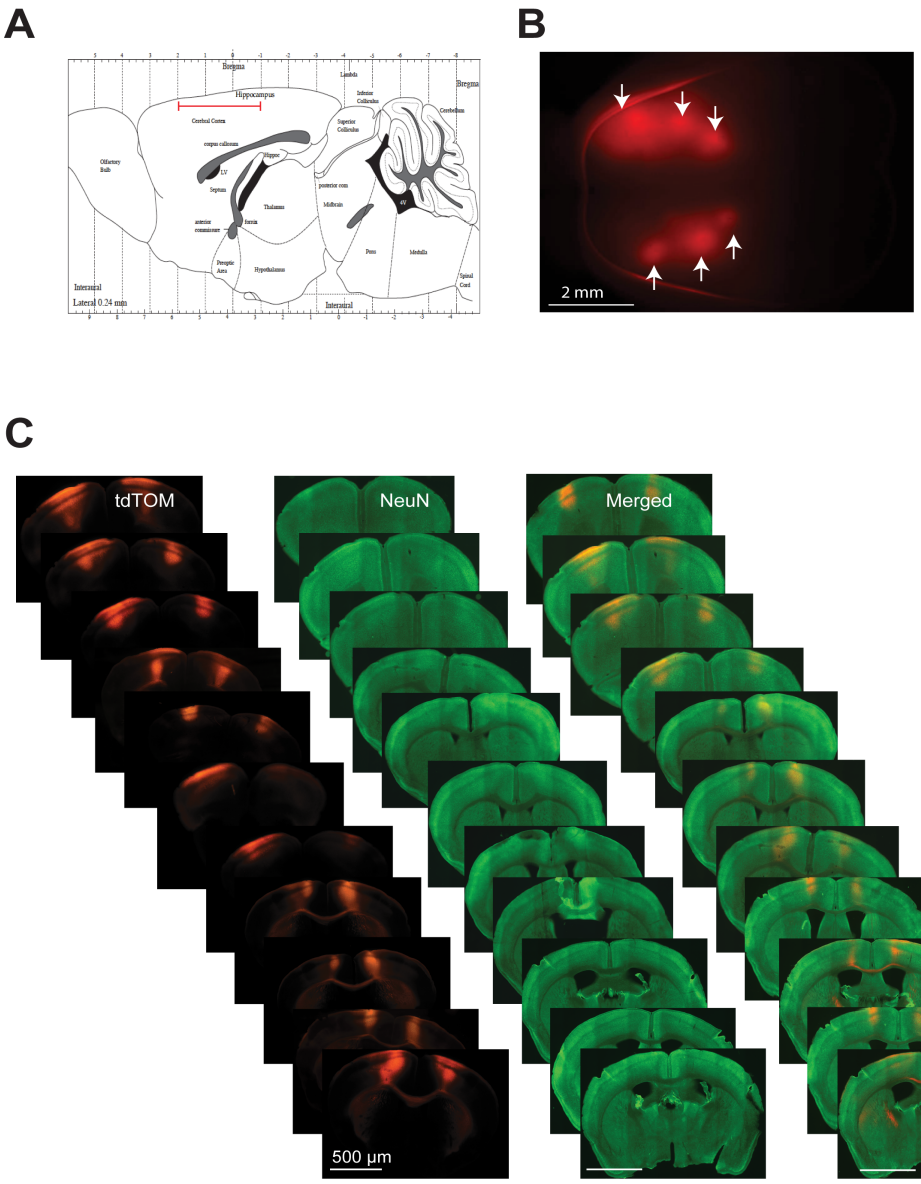

Continued on next page

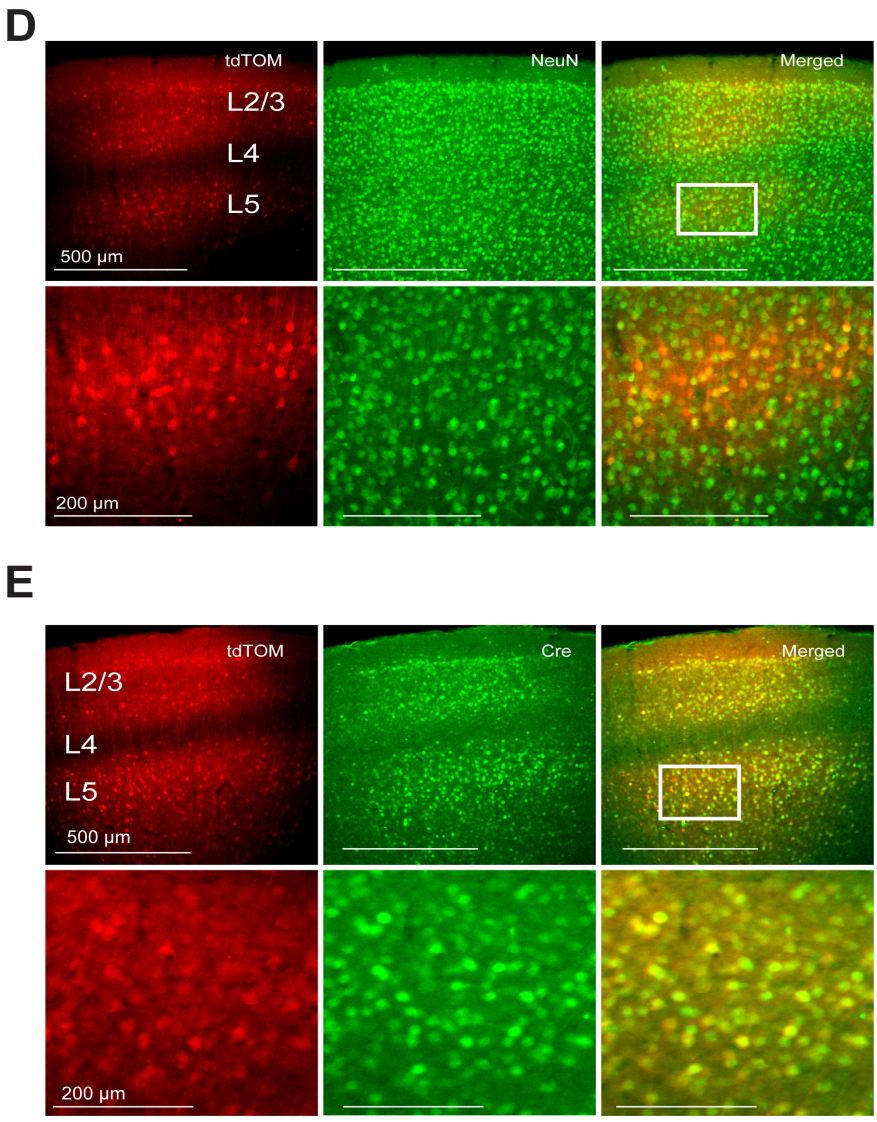

Figure 2.11 Viral mediated Cre expression in the motor cortex.

(A) An overview of the mouse brain showing the dimension of the motor cortex indicated by the pink bar (from Paxinos and Franklin, 2001). (B) An overview of the adult mouse brain injected with rAAV-P_{tet}bi-iCre/tdTOM + rAAV-hSYN-rtTA into the motor cortex followed by one week of Dox treatment. (C) 100 µm coronal sections expressing tdTOM (left) and immunostained with mouse anti NeuN primary antibody and an FITC coupled secondary antibody (right) arranged in a chronological order from the forebrain to the midbrain (D) Confocal images of tdTOM expressing regions overlaid with FITC NeuN immunostained regions indicate that all tdTOM expressing cells are neurons. The lower panel is a higher magnification of the highlighted region (rectangular box) showing a near 100 % overlay of tdTOM and NeuN. (E) Immunostaining with mouse monoclonal anti-Cre antibody followed by FITC secondary antibody indicates that most tdTOM positive cells are also Cre positive**.**

2.3 Inducible and reversible silencing of synaptic transmission with tetanus toxin light chain (TeTxLC)

In order to dissect the role of different neuron types in circuit function, the tetanus toxin light chain (TeTxLC) gene was placed under the control of rAAV-tTA/rtTA systems for inducible and reversible silencing of synaptic transmission (Fig. 2.12 A). TeTxLC is known to selectively cleave the synaptic vesicle protein synaptobrevin-2 (VAMP2) (Fig. 1.9) (Schiavo et al., 1992a, Yamamoto et al., 2003). To detect TeTxLC expression, rAAV equipped with a human synapsin promoter was used to express the TeTxLC gene that was linked to the monomeric kusabira orange (mKO) via a 2A peptide (Tang et al., 2009). The rAAV from this construct (TeTxLC-2A-mKO), was used to infect four rat organotypic hippocampal slices for two weeks. Strong expression of mKO was detected by fluorescence imaging in infected slices (Fig. 2.12 B, top-left). A protein with an apparent molecular weight of 55 kDa that matches the molecular weight of the TeTxLC-2A fusion protein was detected by Western blot analysis using a 2A-specific antibody (rabbit polyclonal) (Fig. 2.12 B, top-right).

To confirm the *in vivo* expression of TeTxLC-2A fusion proteins by immunostaining with a 2A-specific antibody, the rAAV-hSYN-TeTxLC-2A-mKO was injected into wild-type mice into the CA1 region of the hippocampus. Immunostaining two weeks after virus infection with the 2A antibody in acute brain slices correlated well with mKO expression (Fig. 2.12 B, lower panels). To demonstrate that TeTxLC cleaves synaptobrevin-2 (VAMP2), tissue lysates from TeTxLC- infected organotypic slices were analyzed by Western blot for the expression of different synaptic vesicle proteins: VAMP1 (rabbit polyclonal), VAMP2 (rabbit polyclonal), synaptophysin (goat polyclonal), synaptotagmin (goat polyclonal) and cellubrevin (rabbit polyclonal). β-tubulin (mouse monoclonal) served as a loading control. As expected, TeTxLC-infected slices showed strong reduction in the expression of the 19 kDa synaptobrevin-2 protein levels, without detectable changes in the levels of the other synaptic vesicle proteins (Fig. 2.12 C). Surprisingly, the 15 kDa VAMP1 protein was equally undetectable in TeTxLC infected slices. These results showed that TeTxLC selectively cleaves VAMP2 and also has an impact on VAMP1 (Fig. 2.12 C).

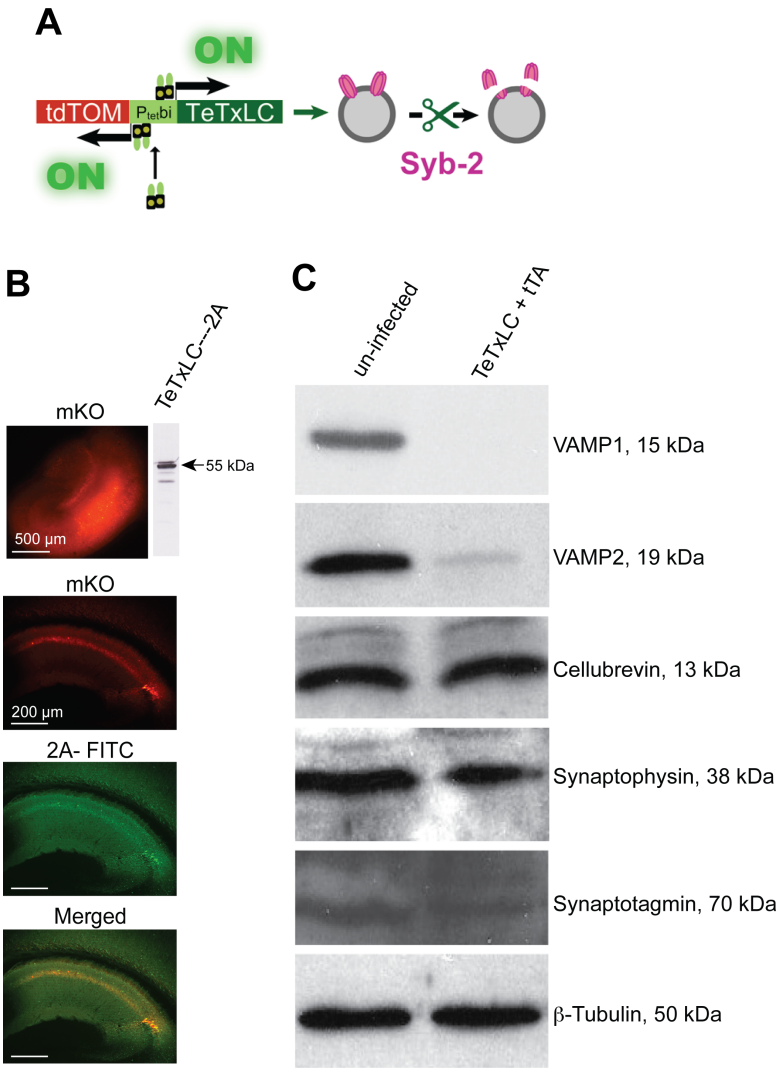

Figure 2.12 Detecting TeTxLC expression

(A) Schematics of TeTxLC expression under control of the Tet-inducible system. TeTxLC cleaves synaptobrevin-2. (B) Rat organotypic hippocampal slices were infected with rAAV-hSYN-TeTxLC-2A-mKO and analyzed for the expression of a monomeric orange fluorescent protein (mKO) (top-left). The TeTxLC protein was detected by Western blot using a rabbit polyclonal 2A-specific antibody (top-right). Coronal sections from brain slices infected with rAAV-hSYN-TeTxLC-2A-mKO were immunostained with 2A antibody coupled to FITC secondary antibody and fluorescently imaged for mKO and TeTxLC-2A expression. (C) Rat organotypic hippocampal slices were infected with rAAV-hSYN-tTA and rAAV-P_{tet}bi-TeTxLC/tdTOM and lysates were blotted using antibodies against different synaptic vesicle proteins: rabbit polyclonal antibodies against VAMP1, VAMP2 and cellubrevin, goat polyclonal antibodies against synaptophysin and synaptotagmin. β-tubulin (mouse monoclonal) served as a loading control.

2.3.1 Silencing of synaptic transmission with TeTxLC in acute hippocampal slices

To provide electrophysiological evidence that TeTxLC can silence synaptic transmission *in vivo*, six wild-type mice were infected with viruses (rAAV-hSYN-tTA and rAAV-P_{tet}bi-TeTxLC/tdTOM) by stereotaxic injection into the hippocampus CA3 region. Robust tdTOM expressions were observed in CA3 pyramidal neurons and in the mossy fibers two weeks after virus injection (Fig. 2.13 B). Electrophysiological recordings were performed on virus-infected slices with tdTOM expression serving as a guide. The stimulation was done in the stratum granulosum (SG) of the dentate gyrus (GD) and the recording at stratum lucidum of CA3 (Fig. 2.13 A). Six virus-infected and seven un-infected wild-type mice were used for field-post synaptic potential recordings (f-PSP).

The red fluorescent protein (tdTOM) indicates the extent of viral infection in the hippocampus (Fig. 2.13 B). Infection was observed widely in the CA3 pyramidal neurons (Fig 2.13 B, insert) and also in the mossy fibers of the DG. In a single trial, field postsynaptic potentials (f-PSP) were strongly reduced in TeTxLC-infected slices compared to non-infected slices (Fig. 2.13 C, left panel). In response to increasing stimulation intensities, the f-PSP slopes remained strongly reduced in TeTxLC infected slices compared to uninfected slices (Fig. 2.13 C, right panel). These results clearly demonstrate that TeTxLC blocked synaptic vesicle release by cleaving VAMP2 and therefore silenced synaptic transmission. It was also observed that the postsynaptic response remained intact when exogenous glutamate was applied into the recording chamber (data not shown). This is a confirmation that the action of TeTxLC is presynaptic and that the cells are viable.

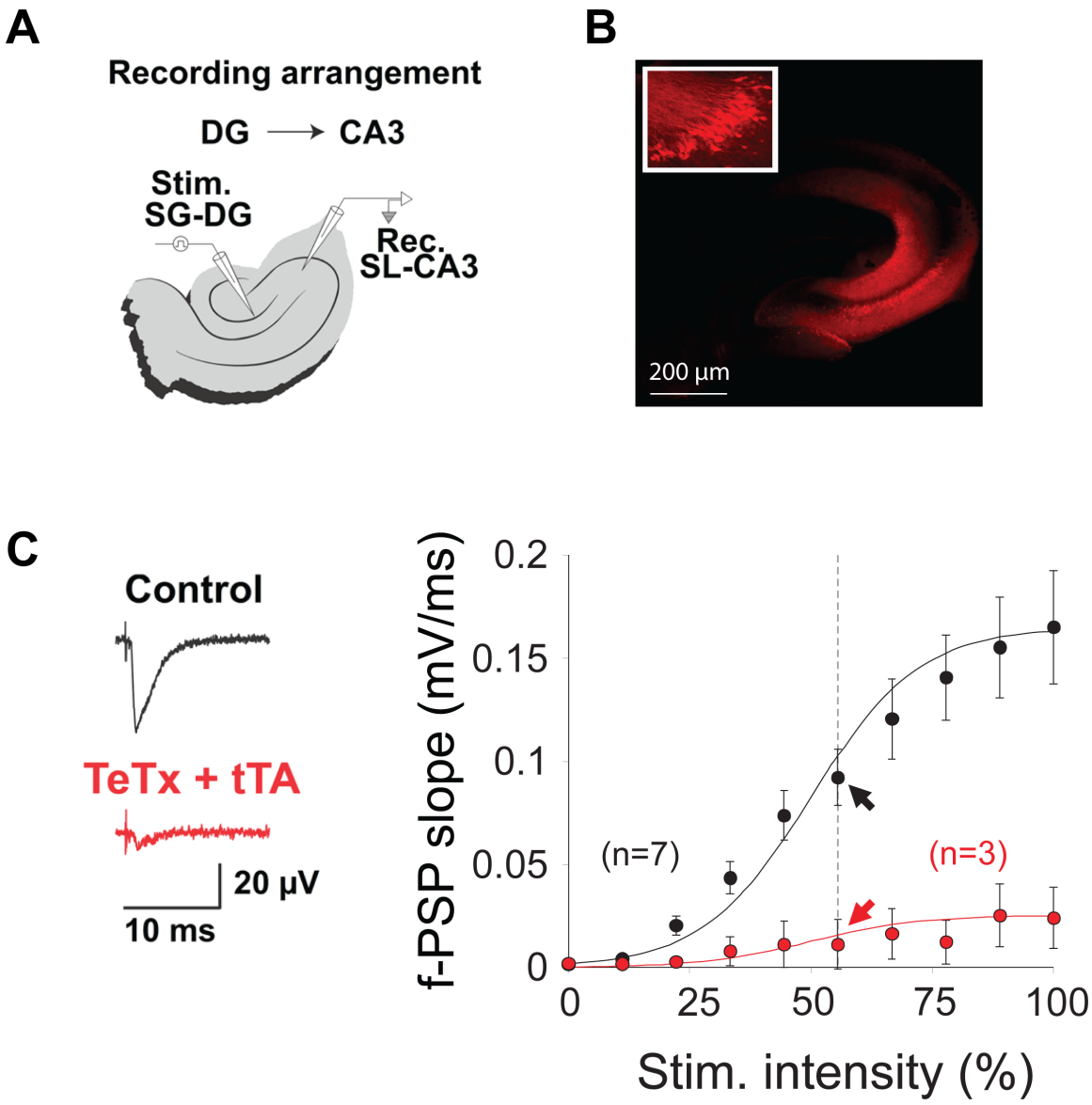

Figure 2.13 Silencing of synaptic transmission in acute brain slices

(A) A diagram of the electrophysiological recording arrangement. The stimulating electrode was placed in the stratum granulosum of dentate gyrus (SG-DG) and recording electrode in the stratum lucidum of CA3 (SL-CA3). (B) Sample image of tdTOM fluorescence expression in a hippocampal slice of a mouse infected with rAAV-hSYN-tTA and rAAV-P_{tet}bi-TeTxLC/tdTOM. Infection was robust in the CA3 pyramidal neurons (insert) and also in the mossy fibers. (C) A single trial field potential from control (upper left column) and TeTxLC-infected slices (lower left panel). Plot of field potential slope with increasing stimulation intensities in uninfected (black trace) and in virus-infected slices (red trace). Abbreviations: n= number of mice, f-PSP= field postsynaptic potential.

2.3.2 Mice constitutively expressing TeTxLC in the striatum show ipsilateral rotation behavior in open field and contralateral behavior in tail suspension test

To find out whether synaptic silencing could alter behavior in mice, the nigro-striatal pathway was chosen as a model system to investigate locomotor behavior. This pathway plays a crucial role in relaying dopaminergic signals from the *substantia nigra* to the motor and sensory neurons. Unilateral disruption of this pathway is known to affect motor coordination (Schwarcz et al., 1979, Lerchner et al., 2007). However, the effect of this disruption is subtle and difficult to quantify. To overcome this limitation, a previous study used amphetamine to boost motor activity in mice, and demonstrated that unilaterally virus-infected mice in the striatum rotated ipsilaterally (Schwarcz et al., 1979, Lerchner et al., 2007).

To demonstrate this behavior test with TeTxLC, a constitutively expressed rAAV-hSYN-TeTxLC-2A-mKO was injected into the striatum of wild-type mice (10) for two weeks. As a control, rAAV-hSYN-Venus was also injected into the striatum of wild-type mice (five). To assess rotational behavior, all infected mice were injected with a single intraperitonial dose of amphetamine (5 mg/kg) and placed in a square open-field box (50 cm x 50 cm) for 10 minutes. The locomotor activity with and without amphetamine treatment (Fig. 2.14 A, upper-left) was video-recorded (Movies M2A and B). A mouse is considered to have made one rotation if it turned round in a circle, turns made circling the periphery of the box were not counted as rotation scores (M 1B and M 2B). Post-hoc analysis of both TeTxLC-2A-mKO and Venus injected mice indicate expression of mKO and Venus in the striatum respectively and also no visible damage to tissues in the striatum as a result of the virus injection (Fig. 2.14 A, right panel). These mice (rAAV-hSYN-TeTxLC-2A-mKO) in a tail suspension test (TST) also displayed preferential turning into the contralateral direction to the virus-infected hemisphere (Fig. 2.14 B, M 4). TST is one of the most common tests used to access antidepressant-like activity in mice (Cryan et al., 2005). This test takes advantage of the fact that animals subjected to short-term inescapable tail suspension will develop an immobile posture (Cryan et al., 2005). In this test, virus-injected mice were suspended by the tail for one minute. TeTxLC-2A infected mice turned to the right direction (injected into the left hemisphere).

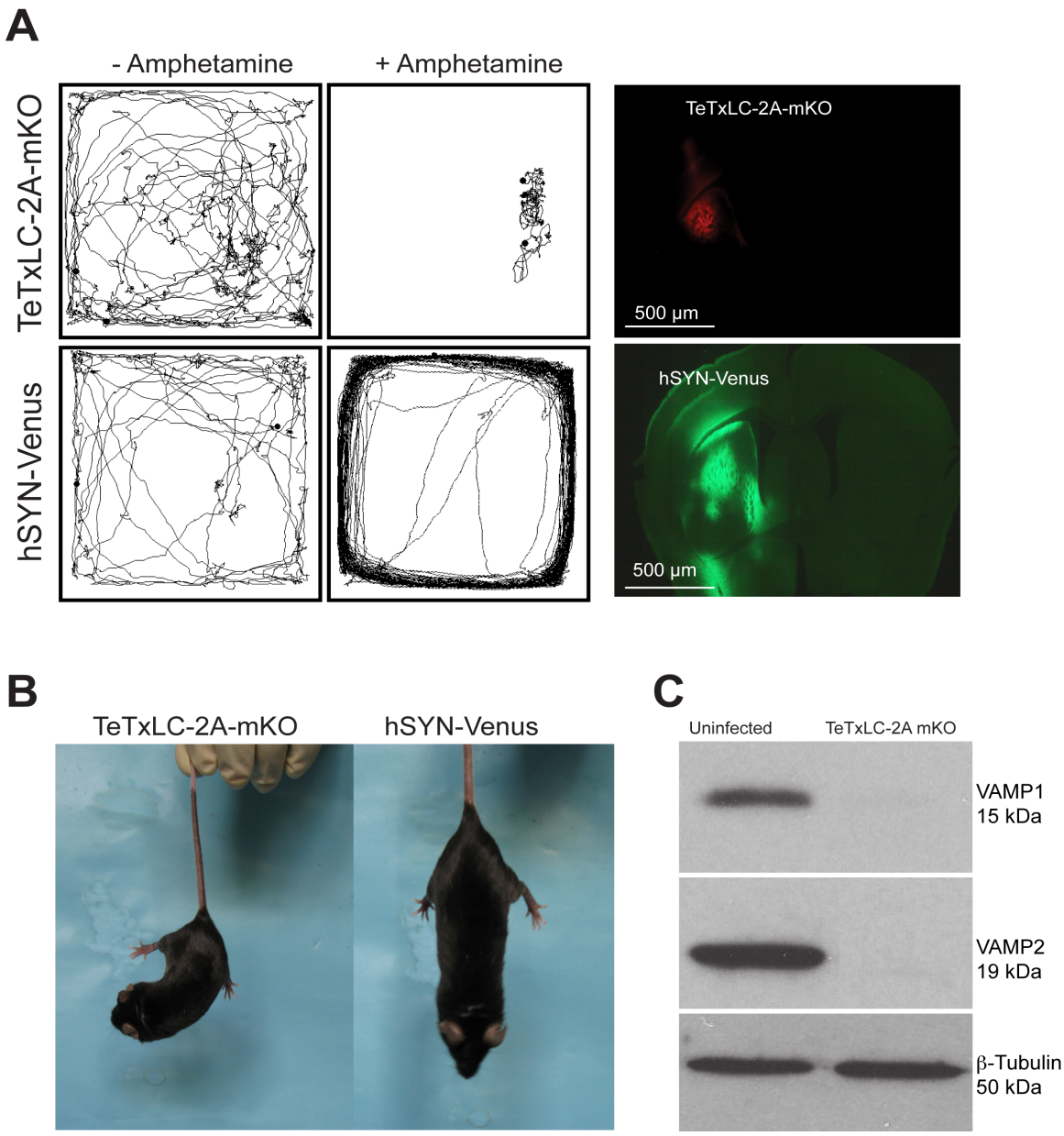

Figure 2.14 rAAV-hSYN-TeTxLC-2A-mKO produced behavioral phenotypes

(A) rAAV-hSYN-TeTXLC-2A-mKO was injected into the striatum followed by amphetamine induce rotational behavior studies. Virus injected mice displayed ipsilateral rotational behavior. Post-hoc analysis of the injected hemisphere showed expression of mKO. (B) In a tail suspension test, mice injected with rAAV-hSYN-TeTXLC-2A-mKO into the left hemisphere turned contralaterally to the injected brain hemisphere while the control mice had no special preference to any side. Post-hoc analysis of the control (rAAV-hSYN-Venus injected mice) indicated broad infection in the striatum. (C) Western blot analysis with antibodies against VAMP1, VAMP2 and β-tubulin indicated the TeTxLC cleaves both VAMP1 and VAMP2.

Venus injected control on the other hand displayed no preferential direction (Fig. 2.14 B, M 4). To demonstrate that the TeTxLC-2A-mKO also cleaves VAMP1 and VAMP2, rat organotypic slices were infected for two weeks and the tissues were harvested and lysed for Western blot with antibodies against VAMP1 and VAMP2 (Fig. 2.14 C). From the Western bIot data, it was observed that the bands corresponding to both VAMP1 and VAMP2 in the infected slices disappeared (Fig. 2.14 C). This result clearly demonstrates that the constitutively expressed TeTxLC also cleaves its target proteins.

2.3.3 tTA- and rtTA-dependent reversible silencing of synaptic transmission in freely behaving mice

To investigate reversible silencing of synaptic transmission, rAAV-hSYN-tTA and rAAV-P_{tet}bi-TeTxLC/tdTOM were injected unilaterally into the striatum of four wild-type mice (Fig. 2.15 A, lower left). For a control, three wild-type mice were also injected with rAAV-hSYN-Venus into the striatum. To assess rotational behavior, all infected mice were injected with a single intraperitonial dose of amphetamine (5 mg/kg) and placed in a square open-field box (50 cm x 50 cm) for 10 minutes. The locomotor activity with and without amphetamine treatment (Fig. 2.15 A, upper-right) was video-recorded and the number of 360^0 cycles completed by the mice were manually counted (Movies M 2 A and B). After amphetamine injection, the total number of ipsilateral rotational cycles completed by mice injected with the TeTxLC-virus was 350 in 10 min (35 rotations/minute) (Fig. 2.15 B). To ruled-out the effect of viral injection as being the cause of the observed rotation, rAAV-hSYN-Venus was injected as a control into three wild type mice (Fig. 2.15 A, top-left). In the control mice, amphetamine injection resulted in a large increase in motor activity with rapid movements around the four corners of the field, but 360^0 rotational behavior was not observed (Fig. 2.15 A, right, M 1A and B). The TeTxLC infected mice upon amphetamine injection turn to explore little space in the open field box compared to the Venus injected mice.

To switch-off TeTxLC expression, the infected mice were treated with 2 mg/ml Dox in their drinking water supplemented with 5 % sucrose. Amphetamine-induced

rotational behavior was recorded over the period of Dox treatment, which lasted for 12 weeks. It was observed that the rotation scores decreased but very gradually, reaching half the initial value after 5 weeks of Dox treatment (Fig. 2.15). The rotation score reached basal level and plateau after more than 8 weeks of being put on Dox. The rotation score was about 50 per 10 min (5 rotations /min) (about 5-fold decrease) in 10 weeks, which is consistent with previously published data (Lerchner et al., 2007, Auer et al., 2010). However, complete reversal of rotation was not achieved (Fig. 2.15 B). This is in conformity with previous findings (Lerchner et al., 2007). However, the mice return to almost the maximum observed rotation score when Dox was withdrawn for one week (Fig. 2.15 B, week 11). Post-mortem analysis of Dox-treated TeTxLC-injected mice showed that gene expression was indeed switched-off as judged by the absence of tdTOM expression in the infected striatum (Fig. 2.15 C, left panel). Also there was no observed morphological damage to structures in the striatum of both control and TeTxLC infected mice. This could be an indication that the neurons of the striatum remained active and functional, however, this need to be confirm with apoptosis markers. Because the TeTxLC protein has a long half-life (6 days), it was most likely that the TeTxLC was not completely depleted and this might have accounted for the low rotation observed even after 10 weeks of Dox treatment.

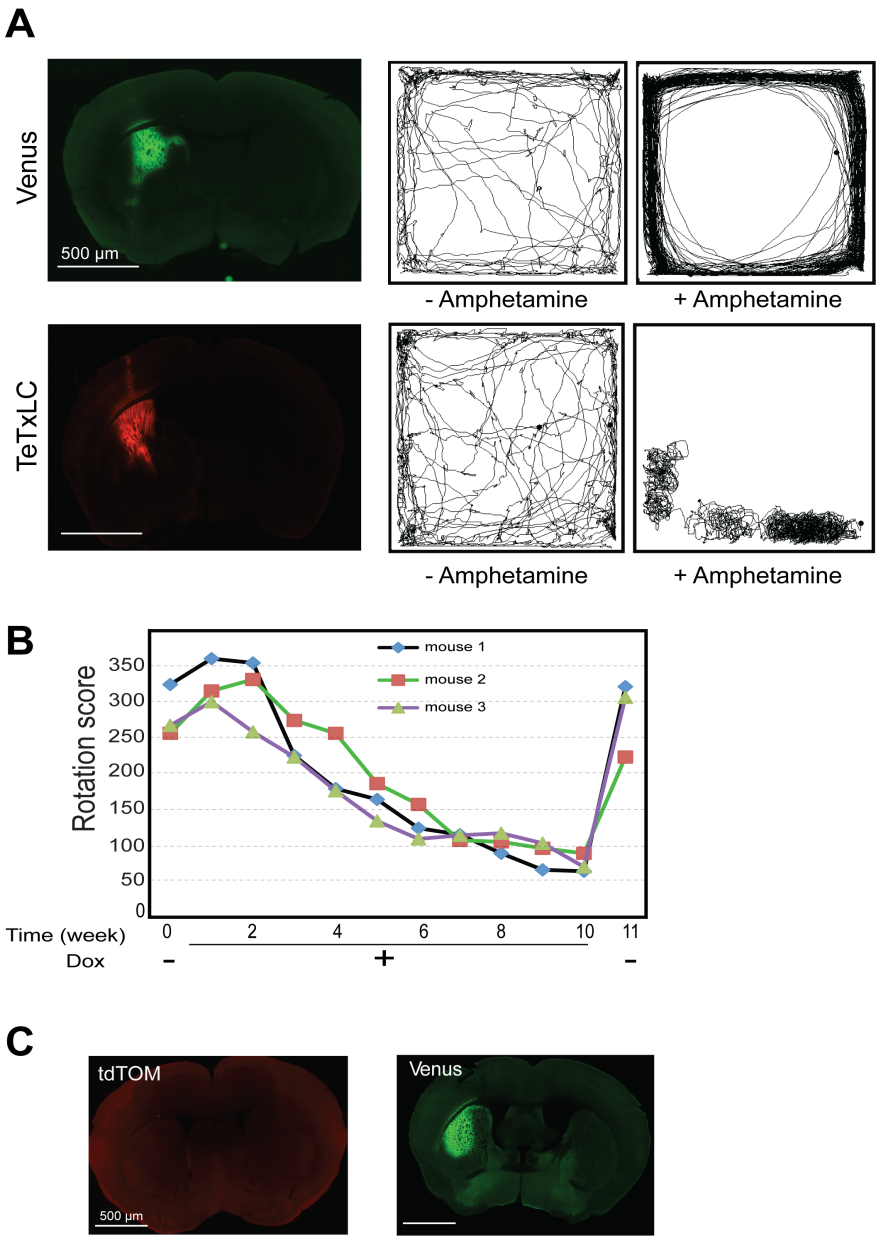

Figure 2.15 Amphetamine-induced rotational behavior-test upon unilateral silencing of synaptic transmission in the striatum

(A) Mice unilaterally infected with viruses into the striatum: rAAV-hSYN-Venus (upper left panel) and rAAV-hSYN-tTA + rAAV-P_{tet}bi-TeTxLC/tdTOM (lower left panel). Ten minutes of locomotor activity trace in the open field without (middle panel) and with (right panel) amphetamine. (B) Mice infected with rAAV-hSYN-tTA and rAAV-P_{tet}bi-TeTxLC/tdTOM were put on Dox in the drinking water (2 mg/ml) for up to 12 weeks and rotational scores were determined. (C) Post-mortem analyses of rAAV-hSYN-tTA and rAAV-P_{tet}bi-TeTxLC/tdTOM mice on Dox (left) and rAAV-hSYN-Venus infected mice as a control (right).

2.3.4 Dox-controlled, rtTA-dependent TeTxLC expression induces rotational behavior

To test the rtTA system for rapid expression of TeTxLC, rat hippocampal organotypic slices were infected with rAAV-hSYN-rtTA and rAAV-P_{tet}bi-TeTxLC/tdTOM. Two weeks after virus infection, when stimulating the mossy fiber pathway (Fig. 2.16 A, upper panel), slices treated with Dox for 48 hours showed reduced f-PSPs compared to untreated slices (Fig. 2.16 A, bottom panel). This is an indication that Dox inducibly caused expression of rtTA and TeTxLC leading to silencing of synaptic transmission.

To test for motor behavior in the open field, two wild-type mice were injected into the striatum with rAAV-hSYN-rtTA and rAAV-P_{tet}bi-TeTxLC/tdTOM and two control mice with rAAV-hSYN-Venus. Motor activity was assessed by amphetamine injection before Dox injection (Movies M3 A and B). Locomotor activities of TeTxLC infected mice were similar to wild-type mice before Dox injection (Fig. 2.16 C). Four days after a single i.p Dox injection, the TeTxLC infected mice showed ipsilateral rotation behavior (Fig. 2.16 D, M 3C). The graph in figure 2.16 E shows the rotation score before and after Dox injection. After almost 11 weeks of Dox withdrawal the rotation scores reduced to nearly the same level as the starting rotation score without Dox (Fig. 2.16 E). The observed initial rotation scores (without Dox) could be due to leaky expression of the responder virus. However, when Dox was again injected, reactivation of TeTxLC took place leading to rapid increase in the rotation scores to levels comparable to the rotation scores at the beginning when a single dose of Dox was injected (Fig. 2.16 E). Post-hoc anatomical analysis indicate reactivation of tdTOM and also no visible structural damage to tissues of the striatum of TeTxLC infected mice compared to the Venus injected control (Fig. 2.16 F).

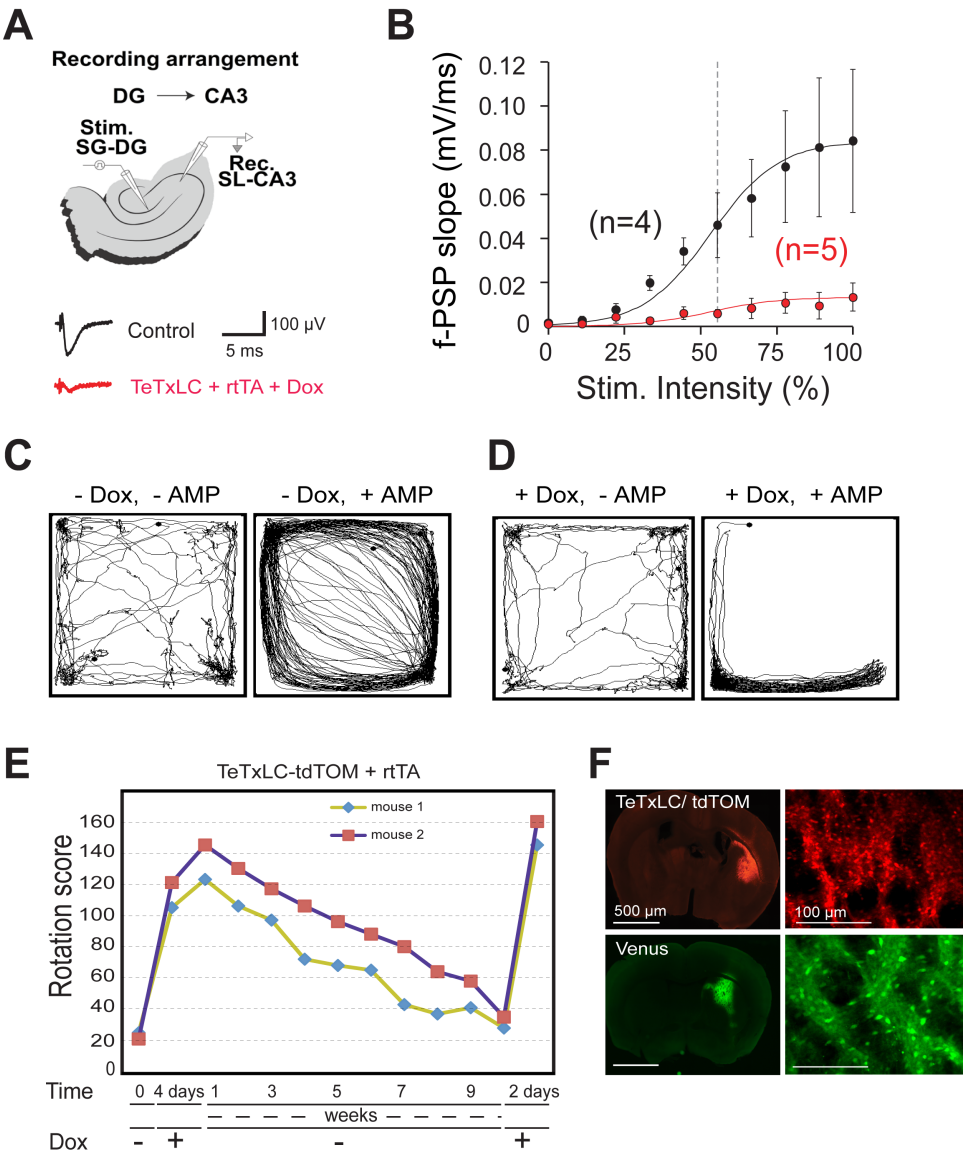

Figure 2.16 Inducible rotational behavior in rtTA- and TeTxLC-infected mice

(A) A schematic of the electrophysiological recording. A single trial field potential (f-PSP) from control and TeTxLC-infected slices (lower panel). (B) Slope of f-PSP in CA3 regions after mossy fiber stimulation with increasing stimulation intensities in uninfected (4 slices) and TeTxLC-infected (5 slices) rat organotypic hippocampal slices. (C, D) Mice were infected with rAAV-hSYN-rtTA and rAAV-P_{tet}bi-TeTxLC/tdTOM. Open field rotational traces with and without Dox treatment and before and after amphetamine injection. (E) Rotational scores before and after Dox treatment and scores after Dox withdrawal. The large increase in rotational score after 10 weeks of Dox withdrawal is due to reactivtion after 2 days of Dox treatment. (F) Post-hoc analysis after Dox reactivation indicates the expression of tdTOM in the striatum. The lower panel is the constitutive Venus control.

2.3.5 Generation of fast TeTxLC constructs

With an estimated half-life of six days for the TeTxLC, it was expected that reversibility of synaptic silencing would take at least several weeks (Fig. 2.15 B and Fig. 2.16 E). It was therefore necessary to develop new TeTxLC-variants with shorter half-lives. To achieve this, two new TeTxLC variants were designed. In the first case, a degradation sequence rich in **p**roline **a**spartic acid, **s**erine and **t**hreonine (**PEST**) derived from the mouse ornithine decarboxylase gene was used (Li et al., 1998, Yamamoto et al., 2003).

Naturally occurring proteins with PEST domains are usually unstable proteins and are rapidly degraded. Deletion of the PEST domain from these proteins dramatically increase their half-lives (Ghoda et al., 1989), therefore these regions act as a degradation domain. It is now well known that PEST-containing proteins have short half-lives, from 30 minutes to two hours (Li et al., 1998). It was previously shown that introduction of a PEST-containing sequence to the green fluorescent protein reduced its half-life from 24 hours to 1 hour (Li et al., 1998, Yamamoto et al., 2003). Proteins with PEST sequences use the calpain protease system for degradation and also ubiquitin-mediated degradation pathways (Fig. 2.17 A) (Bercovich et al., 1989, Rosenberg-Hasson et al., 1989, Murakami et al., 1992, Spencer et al., 2004). Taking advantage of this finding (Li et al., 1998), the PEST sequence was fused to the C-terminus of the TeTxLC to generate a TeTxLC-variant called Fast1-TeTxLC (F1-TeTxLC) (Fig. 2.18).

In a second TeTxLC construct, the N-end rule was applied to further shorten the half-life of the TeTxLC and this construct is named Fast2-TeTxLC (F2-TeTxLC) (Fig. 2.18). The N-end rule states that the N-terminal amino acid of a protein is an important factor in determining the half-life of the protein (Varshavsky, 1997a). This is applicable to eukaryotic and prokaryotic systems (Varshavsky, 1997a). Previously, it was found that on average, a protein's half-life is correlated with its N-terminal residue. Proteins with methionine, serine, alanine, threonine, valine or glycine have half-lives of more than 20 hours (Varshavsky, 1997a). However, if the N-terminal amino acid is phenylalanine, leucine, aspartic acid, lysine or arginine, protein half-lives can be as low as 3 minutes (Taxis et al., 2009). Proteins that follow the N-terminal rule are recognized and degraded

by the ubiquitin-mediated pathway (Fig. 2.17 B) (Varshavsky, 1997a, b, Taxis et al., 2009).

To generate a new TeTxLC with shorter half-life, an N-degron was fused to the N-terminus of the TeTxLC. The N-degron is protected at its N-terminus by an amino acid sequence recognized by the tobacco etch virus protease (TEV). The TEV recognition site contains seven amino acids (ENLYFQ-X). The protease cleaves between positions 6 and 7 of the recognition site. Residue X then becomes the new amino terminal upon cleavage (in this case, X = phenylalanine) (Taxis et al., 2009). Thus, in this system, cleavage of the TEV recognition sequence by TEV would expose the susceptible N-degron for rapid protein degradation (Fig. 2.17 B). To make TEV protease mediated cleavage of the N-degron more efficient, an amino acid sequence from the splicing factor 3b155 ($SF3b155^{381-424}$) was introduced in the TeTxLC. The 3b155 domain is recognized by the spliceosome subunit p14, which is linked to the TEV (named TEV-p14) (Suzuki and Varshavsky, 1999, Spadaccini et al., 2006, Taxis et al., 2009) (Fig. 2.17 B). Thus, TEV-p14, by binding to 3b155 deprotects N-degron, and therefore targeting the fusion protein (F2-TeTxLC) for rapid degradation (Fig. 2.17 B). In summary, a new TeTxLC construct was generated called F2-TeTxLC by attaching N-degron and a TEV protease recognition site, under the control of a P_{tet}bi promoter. The other half of the promoter is occupied by the TEV protease fused to p14 (the spliceosome subunit). The N-degron can be exposed by the expression of the p14-TEV leading to ubiquitination and degradation in the proteasome.

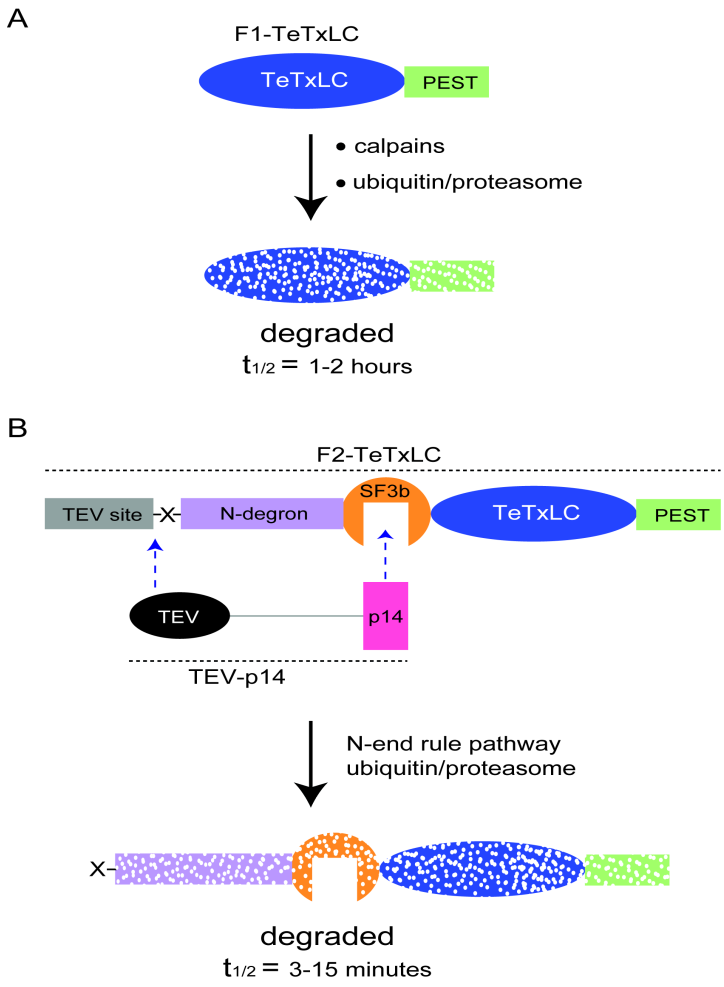

Figure 2.17 Schematics of the PEST and TEV induced protein instability

(A) Schematic of calpain and ubiquitin mediated protein degradation involving PEST sequence. (B) TEV protease induced protein instability system. The N-degron containing the TEV recognition site with the SF3b155$^{381-424}$ was fused to the N-terminus of the HA-tagged-TeTxLC. Spacers were introduced at specific points to allow for proper protein folding. p14 is fused to the N-terminus of the TEV protein. The TEV is FLAG tagged at the C-terminus for immunodetection. The construct is under the control of the P_{tet}bi promoter. When TEV is expressed, it binds to the target TeTxLC protein, binding is aided by the interaction of p14 with a 40 amino acid fragment (381-424) derived from SF3b155. The interaction directs the efficient cleavage of the N-degron by the TEV at the TEV recognition site (ENLYFQ-X). Cutting of the N-degron at the TEV recognition site leads to the deprotection of the N-degron, the N-terminus is now the newly exposed amino acid (X). The exposed amino acid is ubiquitinated and the fate of the protein is determine by the nature of X (X= A, C, G, M, P, S, T and V leads to stable proteins, where as X =D, E, F, H, I, K, L, N, Q, R, W and Y render the protein unstable (half-lives =2-30 minutes) (Suzuki and Varshavsky, 1999, Taxis et al., 2009). The target protein is poly-ubiquitinated by Ubr1p and degraded by the proteasome (Modified from Taxis et al., 2009).

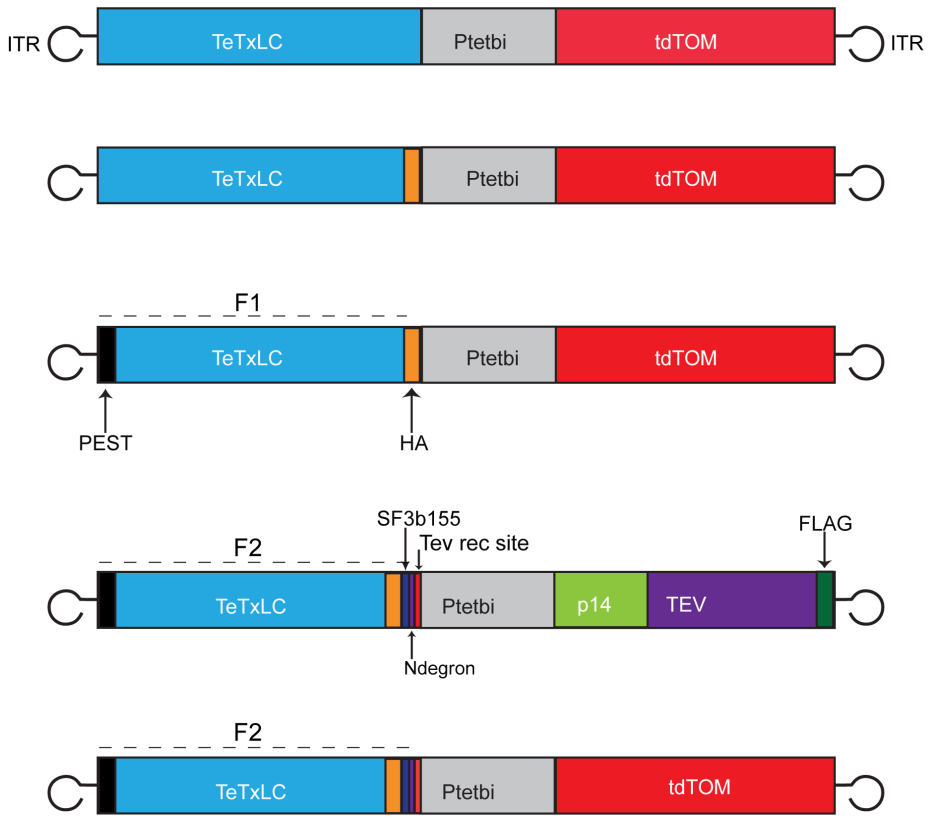

Figure 2.18 The different rAAV based TeTxLC constructs

The first construct is the original TeTxLC with tdTOM for fluorescent imaging, the second construct is also the original TeTxLC with C-terminus HA-tag. The third construct is F1-TeTxLC a PEST domain (in black) and HA-tag (orange) for immunodetection. The fourth construct is the F2-TeTxLC with TEV in a bidirectional cassette expressing both proteins. The last construct is also F2-TeTxLC with tdTOM for imaging. All five constructs are under the control of the P_{tet}bi promoter.

2.3.6 Functional expression of fast TeTxLC variants in HEK293 cells and in organotypic brain slices

To test whether the newly generated TeTxLC constructs can be expressed in mammalian cells, HEK293 cells were transfected with the new constructs and cell lysates were used for Western blot analysis with a mouse monoclonal HA antibody (Fig. 2.19 A). Both fusion proteins (F1-TeTxLC and F2-TeTxLC) were detected on a Western blot with exp-

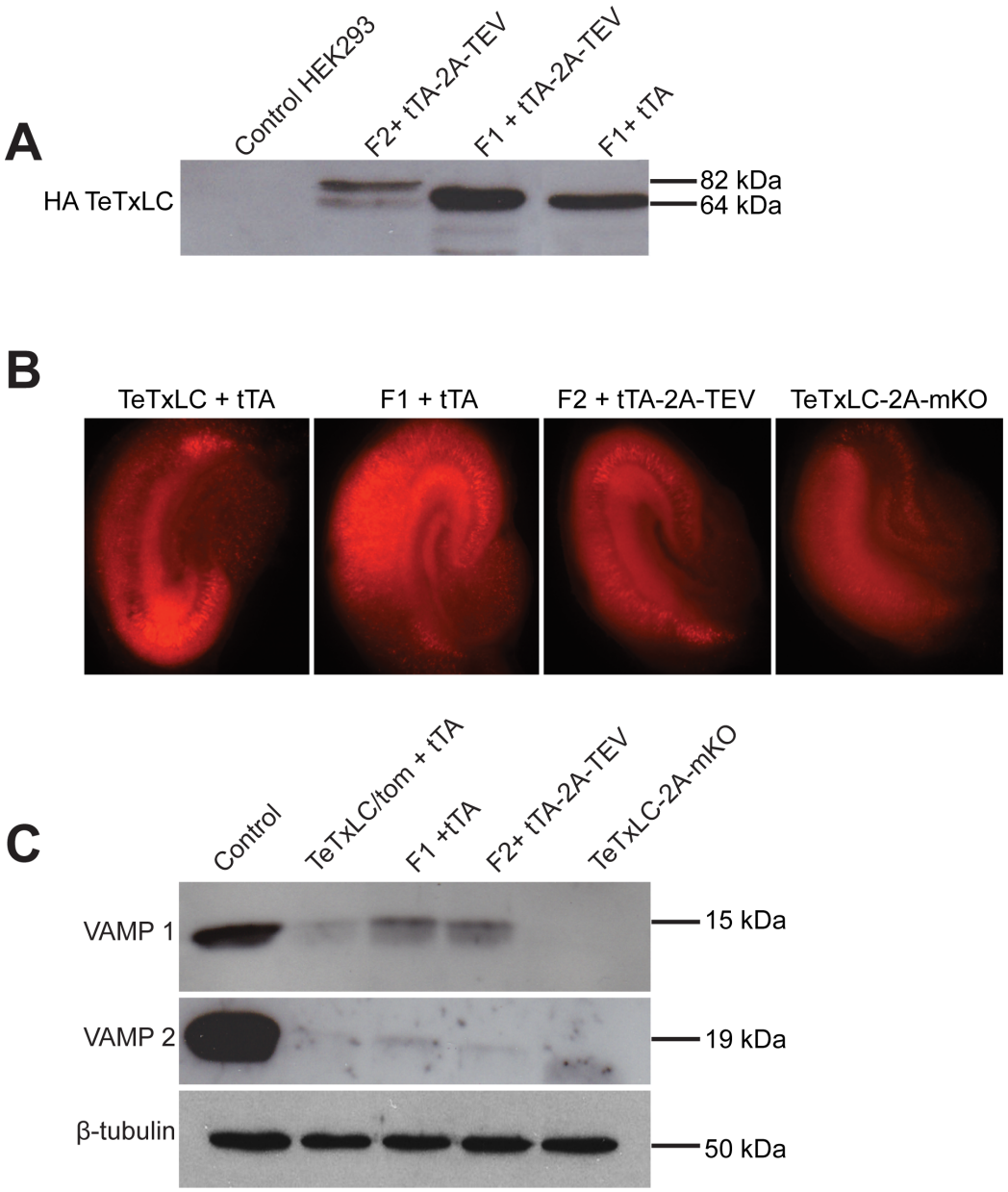

Figure 2.19 Expression of F1- and F2-TeTxLC constructs

(A) HEK293 cells were transfected with F1- and F2-TeTxLC with tTA. Cell lysates were run on SDS gel and blotted onto nitrocellulose membrane. Immunodetection was done with mouse monoclonal HA antibody. The control is an uninfected HEK293 cells. The 88 kDa protein band correspond to the approximate molecular weight of F2-TeTxLC and the 75 kDa protein correspond to the estimated molecular weight of F1-TeTxLC. (B) Rat hippocampal organotypic slices were infected with the original TeTxLC construct (far left), F1- and F2-TeTxLC constructs (middle) and TeTxLC-2A-mKO (far right) with hSYN-tTA for two weeks. (C) Cell lysates from the infected organotypic slices were run on SDS page and blotted with antibodies against VAMP1, VAMP2 and ß-tubulin. The control slices were uninfected.

ected molecular weights of approximately 75 kDa and 88 kDa, respectively (Fig. 2.19 A). For a functional assay rat organotypic slices were infected with viruses of F1- and F2-TeTxLC in addition to tTA (Fig. 2.19 B). The infected tissues were imaged first for fluorescence detection of tdTOM and later harvested two weeks after infection and the lysates used for Western blot analysis with antibodies against VAMP 1 and VAMP 2. β-tubulin was used as a control (Fig. 2.19 C). The result of the Western blot clearly indicates that F1-TeTxLC and F2-TeTxLC proteins were able to cleave both VAMP 1 and VAMP 2 (Fig. 2.19 C).

2.3.7 tTA- and rtTA-dependent induction of F1- and F2-TeTxLC

In order to demonstrate that the new TeTxLC variants are inducible, dissociated primary neurons were infected with either rAAV-P_{tet}bi-F1-TeTxLC/tdTOM only (Fig. 2.20 A, upper left panel) or with rAAV-P_{tet}bi-F1-TeTxLC/tdTOM + rAAV-hSYN-tTA (Fig.2.20 A, upper right panel) for two weeks. The same experiment was repeated with the rAAV-P_{tet}bi-F2-TeTxLC/tdTOM with or without tTA. The results indicate that gene expression occurred only in the presence of tTA as measured by tdTOM expression.

To show Dox dependent gene activation, dissociated primary neurons were infected with rAAV-P_{tet}bi-F1-TeTxLC/tdTOM + rAAV-hSYN-rtTA for two weeks in the absence of Dox (Fig. 2.20 B, upper left panel) and in the presence of 1 µg/ml Dox for forty-eight hours (Fig. 2.20 B, upper right panel). The same experiment was repeated with rAAV-P_{tet}bi-F2-TeTxLC/tdTOM + rAAV-hSYN-rtTA (Fig. 2.20 B lower panel). The results indicate that both systems are tTA and rtTA-dependent and therefore regulatable.

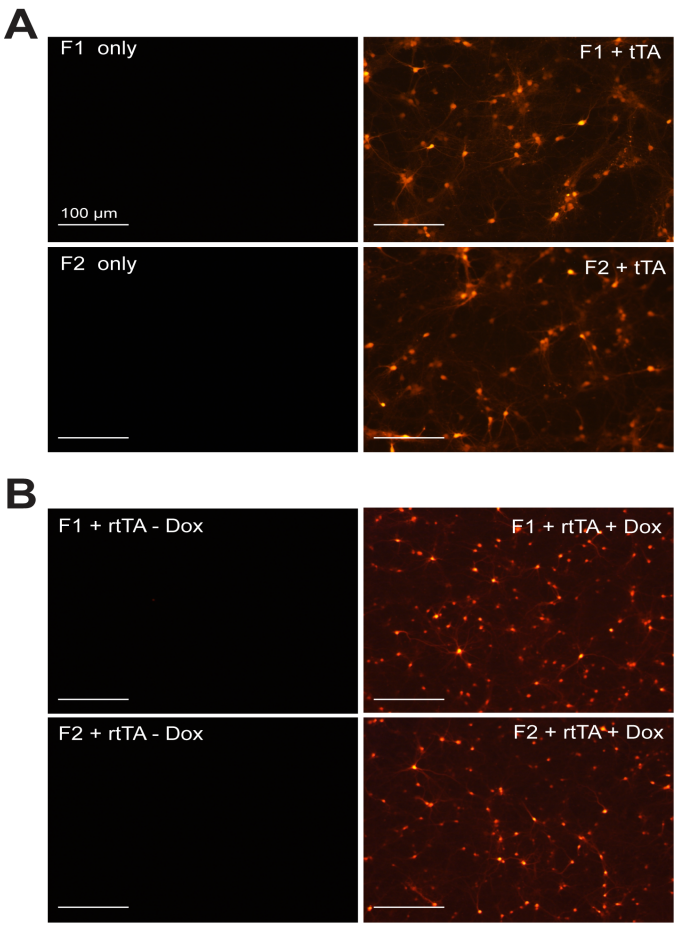

Figure 2.20 tTA- and rtTA-dependent induction of F1 and F2-TeTxLC

(A) Dissociated primary neurons infected with rAAV-P_{tet}bi-F1- and F2-TeTxLC only (left panels), and with rAAV-hSYN-tTA (right panels) for two weeks indicate gene expression only in the presence of the activator. (B) Dissociated neurons infected with rAAV-P_{tet}bi-F1- and F2-TeTxLC + rAAV-hSYN-rtTA in the absence of Dox (left panels) and in the presence of Dox for 48 hours indicate rtTA-dependent gene activation only in the presence of Dox.

2.3.8 Repeated cycles of silencing and un-silencing of synaptic transmission using F1- and F2-TeTxLC, assessed by amphetamine-induced rotational behavior

In the previous amphetamine-induced rotational behavior with the original TeTxLC, it was observed that the behavior phenotype can be reversed, however, reversal took more

than 8 weeks to complete. This therefore makes the system unsuitable for rapid reversible silencing of synaptic transmission. To overcome this, new TeTxLC variants were generated as described above (Fig. 2.17 and 2.18). To test the applicability of the new TeTxLC variants for rapid reversible silencing of synaptic transmission, wild type mice (3) were injected with rAAV-P_{tet}bi-F1-TeTXLC/tdTOM + rAAV-hSYN-tTA into the striatum. Two weeks after virus injection, the mice were subjected to amphetamine-induced rotational behavior test in the open field as described above. The total number of rotations made was recorded as rotation scores (Fig. 2.21 A). After the first recording, the mice were put on Dox in the drinking water to shut down the expression of tTA. The rotation behavior experiment was repeated over the period of Dox treatment. It was observed that the rotation score decreased by about 50 % (from 150 rotation to around 75 rotations) within two weeks of Dox treatment (Fig. 2.21 A). And within three weeks, the rotation score decreased to 45 and remained fairly constant by the 4th week. Reactivation took place when the mice were withdrawn from Dox within a week (Fig. 2.21 A). A second cycle of reversible silencing was repeated and the results nearly the same as the first cycle. It therefore implies that a complete cycle of silencing and un-silencing of synaptic transmission is possible with the F1-TeTxLC/tdTOM within 3 weeks. However, there is a significant rotational behavior after the three weeks, which may be due to the leakiness of the responder.

A similar experiment was repeated with F2-TeTxLC by injecting rAAV-P_{tet}bi-F2-TeTxLC/TEV in combination with either rAAV-hSYN-tTA or rtTA into the striatum. With the tTA system (Fig. 2.21 B), it was observed that the rotation score decreased by more than half within two weeks, and almost to the basal level by the 3rd week. On reactivation by Dox withdrawal at the end of the fourth week, rotation scores returned to maximum within a week. However, when Dox was again administered, the decrease in rotational score was more dramatic. Within a week after the mice were put back on Dox, the rotation score decreased from 150 to about 75 (Fig. 2.21 B, week 6). This was not observed with the F1-TeTxLC on reactivation, instead, F1-TeTxLC showed a marginal increase in rotation score on Dox administration (150 to 160) (Fig. 2.21 A, week 6). By the end of the 2nd week of Dox administration, the rotation score decreased to the basal level (Fig. 2.21 B).

With the rtTA system, the mice displayed some amphetamine-induced rotation behavior without Dox administration (Fig. 2.21 C). However, two days after a single i.p. injection of Dox, the mice displayed robust amphetamine-induced rotation behavior reaching as high as 180 rotation scores in 10 minutes from the basal value of 25. This is more than 7 fold increase in rotation score. When no Dox was administered for a week, the rotation score decreased sharply in two of the mice to almost baseline level (34 rotations in 10 minutes). The decrease in the observable rotations in the 3rd mice also reached the basal level within two weeks (Fig. 2.21 C, day 16). This remained constant for one more week. Upon reactivation, the rotation score increased to the maximum level and within another one week of Dox withdrawal, the rotation score of one mouse was back to the basal level while the other two also showed significant decrease in rotation scores. By the end of the second week of Dox withdrawal, the rotation scores of all three mice decrease to the baseline. From the rtTA and the tTA data, it is possible to complete a cycle of reversible silencing and un-silencing of synaptic transmission within two weeks or even less with the F2-TeTxLC. To conclude from this results, the F1-TeTxLC and F2-TeTxLC can be used for rapid reversible silencing of synaptic transmission within 3 weeks and 2 weeks respectively.

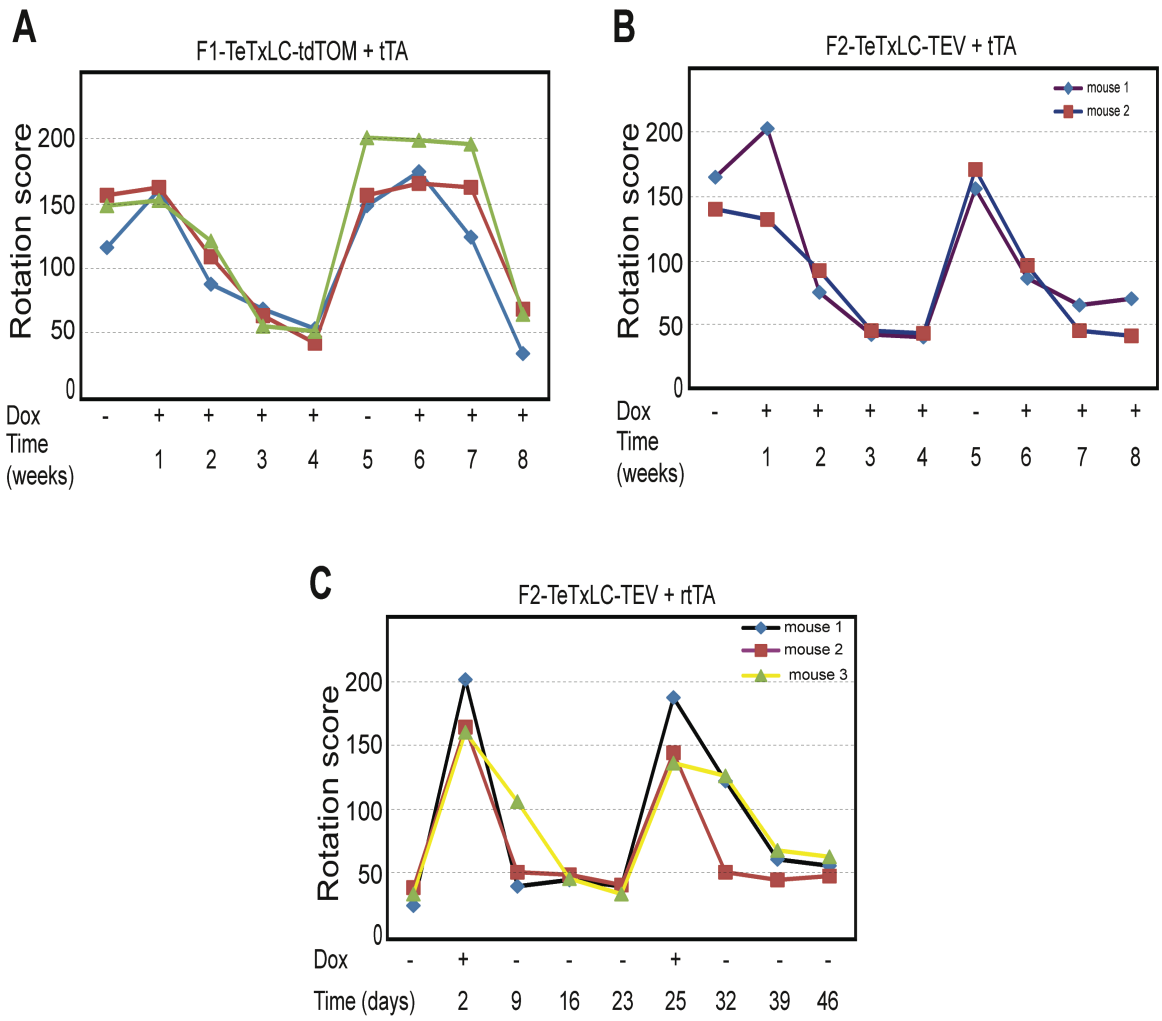

Figure 2.21 Repeated cycles of amphetamine-induced rotational behavior in F1- and F2-TeTxLC injected mice. (A) Three wild-type mice injected into the striatum with rAAV-P_{tet}bi-F1-TeTxLC/tdTOM + rAAV-hSYN-tTA and subjected to repeated cycles of amphetamine induced rotational behavior. Rotation was reversed after 3 weeks of Dox treatment in the drinking water. (B) Cycles of amphetamine-induced rotational behavior in 2 wild-type mice injected with rAAV-P_{tet}bi-F2-TeTxLC/TEV + rAAV-hSYN-tTA. Rotation behavior is reversed after two and a half week of Dox treatment. (C) Amphetamine induced rotational behavior analysis in 3 wild-type mice injected with rAAV-P_{tet}bi-F2-TeTxLC/TEV + rAAV-hSYN-rtTA. These mice showed rotational behavior before Dox administration. However, rotational scores increased to as high as 200, and reversed to almost basal level after one and a half weeks of Dox withdrawal.

2.3.9 Application of a genetic mosaic technique to inducibly express TeTxLC in selected neurons

In order to make the inducible expression of TeTxLC a more versatile tool, a new Cre-dependent genetic switch called the Flip-Excision (FLEX) cassette was generated (Schnutgen et al., 2003, Atasoy et al., 2008). In this system, Tag-RFP (red fluorescence protein) was fused to rtTA via a 2A peptide linker. This DNA fragment was cloned in between 2 *lox*P sites oriented in opposite direction (*lox* 2722) (Fig. 2.23) in a reverse sense with a cytomegalovirus early enhancer/chicken β actin (CAG) promoter. The fusion gene sequences (rtTA-2A-Tag-RFP) will only be expressed when the Cre-recombinase protein is expressed (Fig. 2.23, middle). In the absence of Cre, there will be no gene inversion and therefore no expression of rtTA and Tag-RFP, and the system will remain shut. However, in the presence of Cre-recombinase, there will be an inversion at the *lox*P sites and the genes will be oriented under the CAG promoter, leading to expression of rtTA and Tag-RFP (Fig. 2.23 B).

The advantage of this system is that it can be applied in a combinatorial approach using the inducible bidirectional F2-TeTxLC and the Cre transgenic mice to specifically silenced selected type of neurons only in the presence of Dox (Fig. 2.23, lower section). This combinatorial approach will allow for the conditional expression of rtTA in only Cre positive cells and therefore only these cells will be silenced on Dox administration.

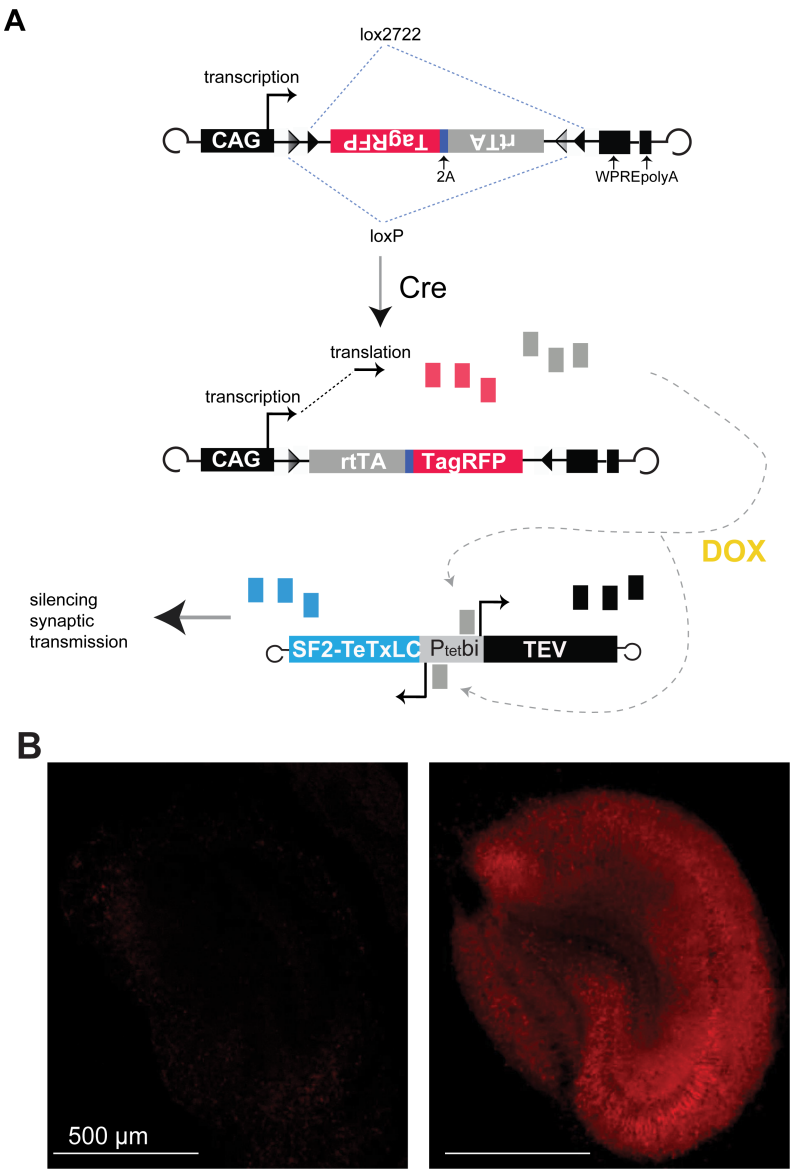

Figure 2.23 Mechanism of action of the FLEX cassette

(A) rtTA and Tag-RFP were cloned (in a reverse sense) between two *lox*P sites oriented in opposite directions under the control of the CAG promoter and the Woodchuck Posttranscriptional Regulatory Element (WPRE) with SV40 polyA. Cre recombinase will cause gene inversion at the *lox*P sites leading to the expression of rtTA and the Tag-RFP protein. A combinatorial expression of Cre, FLEX cassette and TeTxLC will lead to silencing of only Cre positive neurons in the presence of Dox. (B) Rat organotypic slices infected with only rAAV-FLEX-rtTA-2A-Tag-RFP (left panel) and in the right panel is a combination of rAAV-FLEX-rtTA-2A-Tag-RFP and Cre. The red fluorophore is the expressed Tag-RFP after Cre- mediated excision.

3. DISCUSSION

3.1 Manipulating gene expression and neuronal circuits in the mouse brain

Brain circuits are composed of different neuronal types with diverse functions (Druga, 2009). Neurons are connected with each other via synapses, and they form complex synaptic circuits (Chklovskii et al., 2004). In different brain regions, functional neuronal circuits are dedicated for specific functions, such as assembling and integrating sensory signals into meaningful relationships, decision-making and motor output responses (O'Connor et al., 2009). There is compelling evidence that distributed neuronal circuit encompassing different brain regions are involved in learning and also forming memory representations, which are encoded in spatiotemporal neuronal activity patterns. There are a large number of proteins, which are critically needed in strengthening and weakening functional synaptic connections (Luscher et al., 2000).To understand their function, it is important to develop genetic tools to inducibly inactivate genes of interest in specific brain regions (Mayford et al., 1996). Moreover, silencing synaptic transmission between synaptically connected neurons can help to reveal their role in learning and memory (Yamamoto et al., 2003, Nakashiba et al., 2008).

In my PhD study, I focused on two major goals: (1) to develop a novel genetic approach for inducible, cell-type-specific gene deletion in the brain and (2) reversible silencing of synaptic transmission. Recombinant adeno-associated viruses were developed, which were equipped with the tetracycline (Tet)-controlled genetic switches to investigate the role of specific genes and cell types in learning and memory consolidation processes.

3.2 The rAAV gene delivery system

Our study has demonstrated the usefulness of the recombinant adeno-associated virus (rAAV) for gene expression *in vitro* and *in vivo*. Unlike the transgenic approach, the

rAAV system has several advantages such as easy production and handling (Grimm et al., 1998). It permits excellent infection of neurons *in vitro* and *in vivo* within two weeks and guarantees expression *in vivo* for many years (Klein et al., 2002). By stereotaxic injection, the virus can be targeted to any brain region. The extent of infection can be controlled by decreasing the number of virus particles injected in the brain. The use of D-mannitol by intraperitoneal injection creates a hyperosmotic condition in the brain, facilitating virus diffusion, thus increasing the infection diameter (Fig. 2.10).

One major limitation of the rAAV system is the cloning capacity of the virus. For maximum gene expression, it has been shown that 4.7 kb of DNA between the two ITRs is sufficient for effective packaging. Therefore genes larger than 4.7 kb are poorly packaged, with generally poor expressions. However, in this study, we cloned a gene of about 5.2 kb between the two ITRs and still obtained good expression. The other disadvantage of the rAAV is the loss of ITR sites when expressed in *E. coli*. The repetitive nature of the ITR sequences makes them unstable when propagated in *E.coli*. Since the ITRs are vital for virus packaging, it is important to ensure that they remain intact. To overcome this, *E coli* strains defective in recombination such as SURE competent Cells (Stratagene, La Jolla, California, USA) have been found to maintain stable ITRs. However, it is important to check the presence of the ITR sites for every transformation by restriction digest with Sma I.

3.3 rAAV-mediated gene expression in the mouse nervous system

rAAV2 has been used predominantly to demonstrate infectivity in the CNS in regions such as hippocampus, striatum, globus pallidus, substantia nigra and spinal cord (Wang et al., 1998, Alisky et al., 2000). In this study, however, a cross-packaging of AAV1 and AAV2 was used. In rat dissociated neuron cultures and organotypic slices, we observed strong expression by rAAV1/2. In many instances, using a neuron specific promoter such as the human synapsin promoter, besides neurons, we unexpectedly also observed expression in glia cells *in vitro*. However, in different brain regions *in vivo*, we observed expression, which was neuron-specific. Interestingly, expression was largely restricted to

neurons in cortical layer 2/3 and layer 5, but no expression in layer 4 and 6 (Fig. 2.6, 2.9 and 2.11). This interesting feature of rAAV1/2 can be advantageous to selectively target layer 2/3 and layer 5 cortical neurons. In deeper brain regions, strong expression was observed in the granule cells of the dentate gyrus including the mossy fibers and CA1 and CA3 pyramidal neurons. In the striatum, medium spiny neurons and interneurons also showed good expression. This demonstrates that AAV1/2 can be used effectively for targeting gene expression in different brain regions.

3.4 Inducible gene expression: kinetics of gene regulation in neurons

The Tet-inducible gene expression systems have been used extensively in eukaryotic systems. In this investigation, we have demonstrated the use of the Tet-inducible systems for *in vitro* and *in vivo* long-term gene expression in the mouse brain. In combination with reporters such as the firefly luciferase under control of the Tet promoter, we elucidated the time course of tTA/rtTA-dependent gene activation/inactivation in the mammalian brain. The kinetics of the tTA system in this study looked nearly the same as that of the rtTA (Fig. 2.1-2.4). With both tTA and rtTA systems, an approximately 200 fold increase in gene regulation was observed. However, the Tet promoter showed basal expression in the absence of the activators (tTA/rtTA), which could be due to the ITR enhancer activity onto the Tet promoter (Fig. 2.1- 2.4) (Hatfield and Hearing, 1991).

When the systems were used with luciferase for repeated cycle of gene regulation, it was observed that at the end of each 'OFF' state, there was a residual luciferase activity. This observation could be due to the fact that gene expression was not completely switched-off. This activity was carried onto the next cycle, giving an impression of higher basal levels of luciferase activity at the subsequent 'OFF state (Fig. 2.2 B). With the *in vivo* Dox-dependent gene regulation, Dox efflux was found to play a crucial role in the length of period of each activation/inactivation cycle. Dox gets trapped in fatty tissues in the brain and its clearance takes longer in the brain than in tissue culture medium. Therefore, with the tTA and the rtTA systems, it takes longer time to reactivate (6 days) and inactivate (6 days) Dox-dependent gene expression, respectively. Decreasing

Dox concentration should help to shorten the gene regulation cycle times. In summary, *in vivo* gene expression cycles with the Tet systems can be applied to control many other genes. It is important to bear in mind that the off-rate of gene expression is in part also strongly dependent on the half-life of the regulated protein. Proteins with shorter half-lives such as firefly luciferase (3 hours) or specially engineered proteins with shorter half-lives can be used for rapid cycles of gene regulation.

Comparative analysis of firefly luciferase (*Photinus pyralis* fLUC) and the Brazilian luciferase (*Cratomorphus distinctus* bLUC) in this study showed that bLUC emits more photons (by about 60 times) than the fLUC (Fig. 2.5). It was expected that the regulatory factor of the bLUC should be similar to that of the fLUC. However, a 1000 fold increase in regulation of the bLUC was observed compared to 300 fold of the fLUC (Fig. 2.5 B). One possibility is that the transcriptional units in the two Tet responder vectors were modestly affected by the cloned genes.

It is clear from these studies that both the tTA and the rtTA systems can be effectively used for inducible and reversible control of gene expression. However, the rtTA system has a key advantage in that it can be switched-on rapidly, within hours, thus providing a great possibility to investigate neurophysiology and behavior before and after gene deletion. With the tTA system, however, gene expression must be kept off by Dox, and upon Dox removal, it takes several days for gene re-activation. Importantly, if gene expression is kept off by Dox during prenatal development, re-activation of gene expression upon Dox removal can take several months (Bejar et al., 2002, Zhu et al., 2007).

3.5 Inducible, cell type-specific gene knockout

In this current study, the versatility of Dox-induced, rtTA-dependent Cre-mediated gene recombination and deletion was demonstrated. It was shown that a combination of rAAVs expressing the Cre-recombinase and rtTA could be used for conditional, site-specific gene recombination in targeted brain regions in the mouse nervous system. Expression of Cre and rtTA in the presence of Dox showed robust gene recombination in

the transgenic Rosa26R mice only in regions infected with the viruses (Fig. 2.7 and 2.8). However, the observed very low basal recombination in control mice without Dox could be due to leakiness of the responder viruses (iCre/tdTOM). With multiple viruses infecting each neuron, low basal activity by P_{tet}bi also accumulates and this could lead to recombination in the absence of Dox. This leakiness could also be due to the proximity of the viral ITRs to the responder genes. It has been reported that ITRs in some instances act as enhancers to nearby genes (Hatfield and Hearing, 1991). This basal leakiness could be reduced by a number of ways; the first possibility is by titrating the responder virus to the activator, in this case, the number of responder particles are reduced significantly thus, decreasing the cumulative effect of multiple virus infection. This was clearly demonstrated in this study when the responder virus was diluted (Fig. 2.8). The second possibility is to use genetic insulators, which acting as a barrier to the ITR, can reduce the enhancer activity of the ITR (Burgess-Beusse et al., 2002).

Using the rAAV systems with Cre and rtTA we have demonstrated knockout of the NMDA receptor 1 gene in the barrel cortex of NR1-2*lox* mice within a week of putting the virus-injected mice on Dox. With this approach, we electrophysiologically demonstrated loss of NMDA charge transfer as a result of functional loss of the NMDA receptor gene. This method provides a powerful approach to selectively target a specific brain region for cell type-specific inducible gene knockout.

The role of motor cortex NMDA receptors in associative learning and memory was investigated in this study using the Tet-inducible system and NR1-2*lox* transgenic mice. rAAV expressing the activator (rtTA) and the responder (iCre/tdTOM) were injected into the mouse motor cortex. We demonstrated that Dox treatment for 1 week was sufficient for complete knockout of the NMDA receptor in the barrel cortex, leading to a significant reduction in NMDA current. This combinatorial approach was also applied to the motor cortex of NR1-2*lox* transgenic mice. One issue was that the motor cortex is very large (about 3 mm in length and 0.5-1.5 mm wide) and therefore a D-mannitol procedure was applied to increase the expression diameter (Fig. 2.10). We successfully targeted 70 % of the motor cortical region, with 90 % of the neurons within this region. After Dox treatment, we expect efficient deletion of the NMDA receptor 1 gene. Would this extent of knockout give us a behavioral phenotype? It was shown

previously that a little over 30 % of deletion of the NMDA receptor and between 10-20 % deletion of AMPA receptor in the lateral amygdala was sufficient to cause memory deficit in fear related learning (Rumpel et al., 2005). We therefore conjectured that more than 70 % of NMDA receptors knocked out in the motor cortex should be sufficient to produce behavioral phenotypes in the Skinner box test and classical conditioning of vibrissae responses (Thompson and Disterhoft, 1997).

3.6 Constitutive expression of TeTxLC-2A-mKO

In the current investigation, we showed that the TeTxLC and a red fluorescent protein variants, mKO, could be expressed constitutively with the 2A peptide (Tang et al., 2009) leading to the generation of two functional proteins (Fig. 2.14). With this approach, we confirmed that the 2A peptide fused to the C-terminus did not affect the TeTxLC functional activity and both proteins were expressed at nearly equal levels (Tang et al., 2009). The 2A approach offers a versatile tool for multiple gene expression from a single promoter. The TeTxLC-2A expression was easily detectable by both Western blot and immunofluorescence using the 2A-specific antibody (Fig 2.12 and 2.14). TeTxLC expressing neurons can be easily identified because they also express mKO. The disadvantage of this approach is that the system cannot be regulated.

3.7 Reversible silencing of synaptic transmission with TeTxLC

Genetic tools provide a potent approach to establishing the relationship between the activity of specific neuronal circuits and behavior. Several genetic strategies for reversible silencing of synaptic transmission have been described (Karpova et al., 2005, Lerchner et al., 2007). In this study, we have expressed the tetanus toxin light chain (TeTxLC) either constitutively (human synapsin promoter) or inducibly (P_{tet}bi promoter), for permanent and reversible silencing of synaptic transmission, respectively. TeTxLC is known to selectively cleave the synaptic vesicle protein VAMP2, thus leading to

abrogation of Ca^{2+}-induced fusion of synaptic vesicles, the result of which is the termination of neurotransmitter release at the presynaptic terminals. In this study, we have confirmed by Western blot that TeTxLC specifically cleaves VAMP2 (Schiavo et al., 1992a, Sweeney et al., 1995). However, to our surprise, VAMP1 also disappeared (Fig. 2.12). Electrophysiologically, we demonstrated that the TeTxLC silenced neurons were capable of generating action potentials, which were blocked by tetrodotoxin. We also demonstrated that the postsynaptic cells responded to exogenous glutamate application. This confirmed that the TeTxLC preferentially blocks presynaptic transmission without affecting the neuronal viability.

Behaviorally, we also showed that injection of a TeTxLC expressing virus into the striatum of living mice produced a behavioral phenotype in amphetamine-induced rotational studies as well as in tail suspension tests (Fig. 2.14 and 2.15). The silencing in the striatum by TeTxLC mainly involves dopaminergic neurons. The dopaminergic neurons of the striatum relay dopaminergic signals from the *substantia nigra* to the motor and sensory neurons of the cortex. These neurons were unilaterally silenced with the inducible TeTxLC. The amphetamine-induced rotation behavior observed with the Tet-inducible systems was reversed after more than 10 weeks of Dox treatment or withdrawal, with the tTA and rtTA systems, respectively. Post-hoc analysis by fluorescent imaging indicated that the medium spiny neurons of the striatum remained morphologically unchanged. There were also no observable 'holes' in the brain regions infected with the virus, indicating that there were no lesions in the striatum. This is an indication that the neurons are likely alive. Rotation scores (number of rotations made in 10 minutes) of as high as 350 were observed with the tTA system, while up to 160 were observed with the rtTA system (Fig. 2.15 and 2.16). The apparent difference in the rotation score between the tTA and the rtTA mice could be due to the quality of the tTA and the rtTA viruses since the responder virus was the same. The basal rotation observed with the rtTA system is most likely due to the leakiness of the responder.

The long period taken to observe a decrease in rotation behavior of the TeTxLC injected mice to the basal level upon Dox administration (tTA) and Dox withdrawal (rtTA) was most likely due to the long half-life of the TeTxLC of approximately six days (Habig et al., 1986). We thus sought to generate TeTxLC variants with reduced half-life.

3.8 TeTxLC variants with short half-life

To decrease the half-life of the TeTxLC protein, two different approaches were employed. The first approach involved the use of the PEST sequence fused to the C-terminus of the TeTxLC. With this, the half-life of the TeTxLC decreased significantly, as judged from the amphetamine-induced rotation behavior. In this study using the F1-TeTxLC (PEST), the rotation scores decreased to less than half of the initial value (150 to about 70 rotations in 10 minutes) within two weeks compared to the over 6 weeks taken by the original TeTxLC to decrease to half of the original rotation score (Fig. 2.21). With the F1-TeTxLC, the rotation returned to basal levels within 3 weeks of Dox administration.

This finding is a confirmation of the outcome reported by Yamamoto et al., 2003. Using the PEST sequence in transgenic mice, the authors demonstrated the reversal of rotation behavior in the mice after 3 weeks of Dox treatment. In a previous study, 100 % reversal of rotation could not be achieved (Lerchner et al., 2007). The reason for this residual rotational behavior could be due to leakiness of the responder, to the prolonged silencing of neurons by the TeTxLC, or the effects of repeated injections of amphetamine, leading to a directional bias in the rotational behavior test. This could be investigated further by virus titration of the responder. The rapid reversibility of the system was confirmed when Dox was withdrawn within one week, with the rotation score returning to the initial value of about 150 rotations in 10 minutes.

To improve the system further and make it faster for rapid reversible silencing, a second approach was used, called the TEV protease induced protein instability (TIPI) method (Fig. 2.17) (Taxis et al., 2009). TIPI is used to decrease the abundance of proteins expressed in cells. In this method, N-degron (Spadaccini et al., 2006, Taxis et al., 2009) with a TEV recognition site was fused to the N-terminus of TeTxLC while the C-terminus was fused to a PEST sequence. The resulting TeTxLC variant was named F2-TeTxLC. Amphetamine-induced rotational behavior with this new TeTxLC variant showed a rapid decrease in rotation score. Upon injection of a single dose of Dox, the rotation score increased to a peak of 160 rotations in 10 minutes within 2 days (Fig. 2.21 C). This value decreased to baseline within a week of Dox withdrawal, though a residual

baseline rotation was still observed. The decline in rotation score may even be faster if the experiments were done on a daily basis for two weeks. However, one has to take into account that repeated injection of amphetamine on such short time scale could present other problems such as anxiety, pain and edema, thus leading to sluggishness in motor activity.

Another factor, which could affect the rapidity of the system, could be Dox efflux. As shown earlier in this study with firefly luciferase, it took approximately 6 days for Dox to be cleared from the brain tissues (Fig. 2.3). Judging from this, the half-life of the F2-TeTxLC could be shorter but other factors also play a role in determining the half-life. A different way to determine quantitatively the half-life of the F1-TeTxLC and F2-TeTxLC is via Western blot. The main pitfall in this approach is the leakiness of the responder with plasmid DNA transfection into HEK cells, which in small quantities can greatly influence the result of the degradation experiment. A serial titration of the responder plasmid DNA against the activator could overcome this problem.

In this study, it was found that tagging of the TeTxLC at both terminals had no effect on the functionality of the protein (Fig. 2.19 and 2.21). Cleavage of VAMP1 and VAMP2 was observed in all instances of the tagged TeTxLC expression *in vitro* (with organotypic slices) and *in vivo* in the striatum. TIPI could be a great tool to strongly decrease the half-lives of proteins and, in combination, with the Tet-inducible gene expression system could be used for conditional control of protein levels (Taxis et al., 2009).

3.9 Flip-Excision (FLEX) vector / Cre transgenic mice allow for cell type-specific inducible control of TeTxLC expression

Genetic mosaic techniques provide powerful tools for investigating gene functions in the nervous system of mammals and other eukaryotic organisms. For example, the genetic mosaic techniques make it possible to investigate homozygosity of mutations at defined points in an organisms' development (Zugates and Lee, 2004). One such tool is the Flip Excision switch inversion technique (FLEX) (Schnutgen et al., 2003, Atasoy et al., 2008).

This system takes advantage of the ability of the Cre recombinase to excise or invert a DNA fragment flanked by *lox*P sites and also the availability of wild-type and spacer variant *lox*P sites. In this study, we have developed a FLEX vector, which expresses two genes (rtTA/TagRFP) linked by a 2A peptide in an antisense orientation. The FLEX vector expresses the desired gene products only in Cre positive cells. This tool can be used in a combinatorial approach with the Tet-inducible systems to express TeTxLC in only Cre positive neurons. In this case, with Dox administration, only the Cre-positive neurons will be silenced.

3.10 Future perspective

This study was largely focused on engineering novel genetic tools for reversible manipulation of gene expression and silencing of synaptic transmission. In combination with the transgenic mice, the rAAV systems can be used to delete any gene of choice. The inducible expression of TeTxLC is a promising tool to study how silencing of defined neural circuits in the mammalian brain affect animal behavior. These tools can be applied to investigate a wide variety of neurobiological questions, including learning and memory consolidation processes. With the FLEX vector and Cre transgenic mice combined, it should be possible to target the TeTxLC expression in specified neuron types, such as dopaminergic and different inhibitory neurons. The rAAV systems described here can be used successfully for precise targeting of different brain regions, with a possibility to even deliver gene-products with therapeutic potentials to treat some neurological conditions such as the Parkinson's disease.

4. MATERIALS AND METHODS

4.1 Materials

4.1.1 List of mouse lines

C57BL/6 wild-type, NMRI albino mice, Rosa26R (Soriano, 1999) and NR1-2*lox* (Niewoehner et al., 2007) transgenic mice were housed under standard conditions in a 12 hr light/dark cycle in Makrolon cages type 2A with food and water. All procedures were performed in accordance with governmental regulation, German law for animal protection.

4.1.2 Reagents

Agarose	Invitrogen
APS	Sigma
Aquamount	Polysciences
5-bromo-4-chloro-3-indolyl- beta-D-galactopyranoside (X-gal)	Gerbu
Bromophenol blue	IBI
BenchMark™ Pre-Stained Protein Ladder	Invitrogen
Bovine serum albumin (BSA)	Sigma
Dual-Luciferase® reporter 1000 assay system	Promega
3,3'-Diaminobenzidine (DAB)	Fluka
DMSO	Sigma
EDTA	Merck
Ethanol	Roth
Ethidium bromide	Serva
Glycerol	Merck
Hydrogen peroxide (H_2O_2) (30 %)	Fluka

Heparin column	Amersham
Isofluran	Baxter
Isopropanol	Fluka
Ketamine	Inversa
Licain (Lidocain)	Delta select
β-Mercaptoethanol	Sigma
Normal goat serum	Vector
Penicillin/Streptomycin	Gibco
Polyacrylamide	Bio Rad
Paraformaldehyde (PFA), 37 %	Merck
Potassiumferrocyanid ($K_6Fe(CN)_6$)	Sigma
Potassiumferricyanid ($K_3Fe(CN)_6$)	Sigma
Phenol/Chloroform	Roth/Merck
Sodium dodecyl sulfate (SDS)	Serva
Sodium acetate	Merck
Salmon sperm DNA	Roche
Triton X-100	Merck
TEMED	Bio Rad
Trizma	Sigma
Xylazine	Bayer
ECL kit,	Amersham

4.1.3 Antibiotics

Ampicillin	Sigma
Doxycycline	Sigma
Kanamycin	Sigma
Penicillin/Streptomycin	Gibco

4.1.4 Enzymes

Unless otherwise stated, all restriction endonucleases from New England Biolabs

Benzonase	Sigma
E.coli DNA-polymerase1 (Klenow fragment)	Roche
T4-DNA ligase	Roche
Taq-DNA-Polymerase	Gibco BRL
Phusion® High-Fidelity DNA Polymerase	NEB

4.1.5 Antibodies

Anti-2A peptide (Rabbit polyclonal)	Millipore
Anti-β-tubulin (Mouse monoclonal)	Millipore
Anti-Cellubrevin (Rabbit polyclonal)	abcam
Anti-Cre (Rabbit polyclonal/ mouse monoclonal)	Convance
Anti-Flag (Rabbit polyclonal)	abcam
Anti-GFP (Mouse)	Clontech
Anti-HA (Mouse monoclonal)	abcam
Anti-NeuN (Mouse)	Chemicon
Anti-rabbit FITC secondary antibody	Jackson Immuno Research
Anti-Synaptophysin (Goat polyclonal)	Santa Cruz
Anti-Synaptotagmin II (Goat polyclonal)	Santa Cruz
Anti-VAMP1 (Rabbit polyclonal)	abcam
Anti-VAMP2 (Rabbit polyclonal)	abcam

4.1.6 Primers/Nucleotides

Deoxyribonucleotide (dNTP)	MBI

(1) Primers for cloning pAAV-hSYN-TeTxLC-2AKO

GD_TTx-2A-KO EcoR1 S	ATAATGAATTCAGGTATGCCGATCACCATCA
GD_TTx-2A-KO Xho1 AS	TTAAATCTCGAGTAAGCGGTACGGTTGTA

(2) Primers for cloning pCAG-itTA

GD_CAGitTABamH_S	AGAAGGGATCCCTTACCATGTCTAGACTGG
GD_CAGitTAXhoAS	AGATCCTCGAGCATCACAGCATATCCAGGT

(3) Primers for cloning pFLEX_CAG_rtTA-2A-TagRFP

GD_RFPBamHI_S	GCTCGGATCCATGGTGTCTAAGGGCGA
GD_RFPHindIII_AS	TGCAAAGCTTGAATTCTTACTTGTACAGC

(4) Primers for cloning pAAV-P_{tet}bi-bluc/Venus

GD_ElucHind3_S	CGATAAGCTTACGCGTGCTAGCGCATGCAGA
GD_ElucSpeI_AS	TGTCTGACTAGTGGCGGCCGCTCTAGATTA

4.1.7 *Escherichia coli* Strains

DH10B	Invitrogen
SURE cells	Stratagene
Top 10	Invitrogen

4.1.8 Equipments

Amicon Ultracel	Millipore
Biofuge fresco Centrifuge	Hereaus
Biophotometer	Eppendorf
Biotic® Lumi-10 luminometer	Macherey-Nagel
Concentrator 5301 (SpeedVac)	Eppendorf

Cover slips (24x50 mm)	Roth
DC Temperature control Unit	FHC
Falcon tubes	Nalgene
Heating Pad	FHC
Kopf Stereotaxic Instrument	Kopf Instruments
Labofuge 400L Centrifuge	Hereaus
LSM-Pascal Confocal Microscope	Zeiss
Leica MZ6 stereo Microscope	Leica
MicroAmp tubes (200 µl)	Perkin Elmer
Micropipette Puller p-97	Sutter Instrument
Maxi and mini prep kits	Qiagen
Optimal LE 80K ultra centrifuge	Bechman
PCT Thermocycler GeneAmp PCR-System 9600	Perkin Elmer
Safe-lock eppendorf tubes (1.5 and 2 ml)	Eppendorf
TSE VideoMot	TSE systems
Spritzenpump LA-100	Landgraf Laborsysteme
Thermistor Probe	FHC
UV-Spectrophotometer Ultrospec 3000	Pharmacia
Uvette	Eppendorf
Vibratom VT1000S	Leica
Whatman paper 3 MM	Whatman
Zeiss Axiovert 200 M	Zeiss

4.1.9 Special software

Adobe Illustrator CS4	Adobe Systems
Adobe Photoshop CS4	Adobe Systems
DNA Strider 1.4	CEA
Gene Construction kit 3.0	Textco

Microsoft Word for Mac	Microsoft Corp.
Microsoft Excel for Mac	Microsoft Corp.
Microsoft PowerPoint for Mac	Microsoft Corp.
Editseq	DNASTAR
ImageJ	NIH, USA
VideoMot	TSE System
iMovie	Apple

4.1.10 Solutions

1 x PBS:	123 mM NaCl 2.7 mM KCl 1.4 mM KH_2PO_4 4.3 mM Na_2HPO_4, pH pH 7.4, 1 liter H_2O
1 x PBS-T:	1x PBS, 0.05 % Tween20
1 x PBS-MK:	1xPBS, 1mM $MgCl_2$ 2.5 mM KCl
10 x DNA loading buffer:	30 % Glycerol 0.25 % Bromophenol blue 0.25 % Xylencyanol 25 mM EDTA
1x TAE Buffer:	40 mM Tris 5 mM Sodium acetate 2 mM EDTA, pH 8.3

	1 liter H_2O
Day 1 Buffer:	1 % BSA 0.3-0.5 % Triton X-100 1 x PBS
Day 2 buffer:	Day 1 buffer diluted 1:3 in 1x PBS
DAB staining solution:	0.04 % DAB 20 mM Tris, pH 7.6 7.5 x 10^{-3} % H_2O_2
SDS-Gel:	
a) Separation gel (10 %):	4.1 ml H_2O 3.3 ml polyacrylamide 2.5 ml Tris-HCl (1.5M) pH 8.8, 100 µl of 10 % SDS 10 µl TEMED 32 µl of 10 % APS
b) Stacking gel (4 %):	6.1 ml H_2O 1.3 ml Polyacrylamide 2.5 ml Tris HCl (0.5 M) pH 6.8, 100 µl of 10 % SDS 10 µl TEMED, 100 µl APS
WB-Running buffer (10x):	250 mM Trizma base 1.92 M Glycine 1 % SDS 1 liter dH_2O, pH 8.3

WB-Blotting buffer (1x):	25 mM Trizma base 192 mM Glycine 10 % (v/v) Methanol
WB-Sample (Lämli) buffer (5x):	500 mM DTT 10 % (w/v) SDS 50 % (v/v) Glycerol 250 mM Tris/HCl pH 6.8 0.5 % bromophenol blue 10 % 2-Mercaptoethanol just before use
Coomassie staining solution:	2.5 % (w/v) Coomassie-Brilliant-Blue 4 % (v/v) Methanol 45 % dH_2O 10 % (v/v) Acetic acid
Coomassie destaining solution:	7.5 % glacial acetic acid 5 % Methanol, 1 liter H_2O
4 % Paraformaldehyde:	200 g paraformaldehyde 2.5 liter dH_2O, 10 M NaOH until solution becomes clear add 2x PBS 1:1, pH 7.3
LB medium:	1 % (w/v) Bacto-Trypton, 0.5 % (w/v) Yeast extract 1 % NaCl, 1liter H_2O

2YT medium:	2.6 % (w/v) Bacto-Trypton 1.6 % (w/v) Yeast extract 0.8 % NaCl, 3 liter dH_2O, pH 7.5

4.2 Methods

4.2.1 Standard molecular biology methods

All standard molecular biology procedures used in this study including cloning, transformation of competent *E.coli* cells and culturing of bacteria, transfection of HEK293 cells, gel electrophoresis and PCR techniques were derived from already published protocols (Ausubel et al., 1989, Sambrook and Russell, 2001)

4.2.2 rAAV plasmids

Table 1 List of plasmids used in this study

pAAV-hSYN-itTA	(Zhu et al., 2007)
pAAV-CMV-tTA	Rolf Sprengel
pAAV-P_{tet}bi-iCre-tdTOM	(Zhu et al., 2007, Cambridge et al., 2009)
pAAV-P_{tet}bi-fLUC-tdTOM	Dogbevia, G
pAAV-hSYN-rtTA	Hasan, M.T
pAAV-hSYN-tTA-2A-mKO	(Tang et al., 2009)
pAAV-hSYN-TeTxLC-2A-mKO	Dogbevia, G
pAAV-P_{tet}bi-TeTxLC-tdTOM	Spieler, K
pAAV-P_{tet}bi-F1TeTxLC-tdTOM	Dogbevia, G
pAAV-P_{tet}bi-F2TeTxLC-tdTOM	Dogbevia, G and Kneisel, N
pAAV-P_{tet}bi-HATeTxLC-tdTOM	Dogbevia, G and Kneisel, N

pAAV-P_{tet}bi-F2TeTxLC-TEV	Dogbevia, G and Kneisel, N
pAAV-hSYN-rLUC	Dogbevia, G
pAAV-CAG-itTA	Dogbevia, G
pAAV-hSYN-bLUC	Dogbevia, G and Kneisel, N
pAAV-P_{tet}bi-bLUC-Venus	Dogbevia, G and Kneisel, N
pAAV-hSYN-tTA-2A-TEV	Dogbevia, G and Kneisel, N
pAAV-CAG-FLEX-rtTA-2A-TagRFP	Dogbevia, G and Kneisel, N
pAAV-CAG-TetR-Pro-2A-RFP	Dogbevia, G
pAAV-hSYN-TetR-Pro-2A-mKO	Dogbevia, G
pAAV-hSYN-TetR-Pro	Dogbevia, G
pAAV-hSYN-TetR-SP1	Dogbevia, G
pAAV-hSYN-TetR-Oct1	Dogbevia, G

4.2.3 Construction of F1-TeTxLC plasmid

The F1TeTxLC was designed as an improved variant of the original TeTxLC construct (pAAV-P_{tet}bi-TeTxLC/tdTOM). The construct was designed by introducing 122 bp sequence of the hemagglutinin tag (3x HA) to the N-terminus and 121 bp PEST sequence to the C-terminus. For easy cloning into the original vector backbone, a Pme1 restriction site was introduced at the N-terminus and a HindIII at the C-terminus. The entire sequence (1740 bp) was synthesized by GENEART into a kanamycin resistant vector (pMK-RQ) using SFiI cloning sites and named 1049267_TeTxLC-SF_pMK-RQ. The synthesized TeTxLC (1740 bp) was cut out with PmeI and HindIII and cloned into the vector pAAV-P_{tet}bi-TeTxLC/tdTOM in which the original TeTxLC was cut out with EcoRV/HindIII. The new plasmid generated was called pAAV-P_{tet}bi-F1TeTxLC/tdTOM.

4.2.4 Construction of F2-TeTxLC plasmid

The F2TeTxLC construct was designed by introducing a spacer (2x, 64 bp) linked to a TEV protease recognition site (21 bp) and an N-degron (41 bp) followed by another spacer sequence (26 bp). SF3b155 (143) sequence was also fused to this and linked to the

N-terminus of the F1TeTxLC sequence. The new sequences were derived from the plasmid pCT251 (Taxis et al., 2009). The first Xcm1 site in F1TeTxLC was removed for easy cloning. The 825 bp long sequence was ordered from GENEART and the generated sequence was cloned into a kanamycin resistance vector backbone called pMK-RQ to generate the plasmid named 1077563_F2-TeTxLC_pMK-RQ. The engineered gene fragment was cut out with Pme1/EcoN1 and sub-cloned into the vector pAAV-P_{tet}bi-F1TeTxLC/tdTOM in which part of the F1TeTxLC was cut out with Pme1/EcoN1. The new construct was named pAAV-P_{tet}bi-F2TeTxLC/tdTOM.

By replacing tdTOM with TEV protease sequence by a directional BamH1/Xho1 cloning strategy, an additional F2TeTxLC was generated with the TEV in the same bidirectional cassette.

4.2.5 Other rAAV constructs used in this study

The plasmid pAAV-hSYN-TeTxLC-2A-mKO was created by PCR amplification of the 1.3 kb TeTxLC fragment with 5^1EcoR1 and 3^1 Xho1 from the plasmid pAAV-P_{tet}bi-TeTxLC/tdTOM. The fragment was cloned into pAAV-hSYN-tTA-2A-mKO (Tang et al., 2009) by 5^1 EcoR1 and 3^1 Xho1 sticky end ligation, by replacing tTA.

To generate the plasmid pAAV-P_{tet}bi-fLUC/tdTOM, firefly luciferase was excised from the plasmid pB1-5 (Baron et al., 1995) with Pst1/Xba1. The 1.6 kb fragment was blunted and ligated into the vector pAAV-P_{tet}bi-iCre/tdTOM (by the removal of iCre with HindIII/SphI followed by blunting). Likewise the plasmid pAAV-hSYN-rLUC was generated by excising the 947 bp fragment from the plasmid pRL-CMV with Nhe/Xba1. The fragment was cloned by blunt-end ligation into pAAV-hSYN-EGFP (by the removal of EGFP with BamHI/HindIII).

4.2.6 Preparation and purification of recombinant adeno-associated viruses (rAAVs)

4.2.6 .1 Transfection of HEK293 cells for virus production

HEK293 cells were grown in DMEM supplemented with 10 % FCS and 50 mg/l penicillin/streptomycin in 5 % CO_2 at 37 ^{o}C. Transfection was performed by calcium phosphate method with 50 µg total DNA per 15 cm plate.

4.2.6 .2 Virus harvesting and purification via Heparin column

Plasmids corresponding to rAAV constructs were individually co-transfected with pDp1 and pDp2 (ratio 2:1:1) helper plasmids in HEK293 cells (Grimm et al., 2003, Zhu et al., 2007). Forty-eight hours after transfection, cells were harvested by scraping and pulled into 50 ml falcon tubes. The cells were resuspended in 45 ml of 20 mM Tris 150 mM NaCl buffer (pH 8.0), frozen immediately in liquid nitrogen and stored overnight at -70 ^{o}C. Cells were thawed at room temperature (RT) and incubated at 37 ^{o}C with 40 U/ml of Benzonase (for the degradation of unpacked DNA) and 0.5 % NaDOC for 60 minutes with frequent mixing. Lysed cells were spin at 3900 rpm for 15 minutes and the supernatant collected into new falcon tube and frozen at -70 ^{o}C overnight. The next day, the supernatant was thawed and spin for 15 minutes at 3900 rpm. The supernatant was run through a pre-equilibrated 1 ml heparin column (from Amersham, Freiburg, Germany). The column was serially washed with 20 ml of 100 mM NaCl 20 mM Tris (pH 8), 1 ml of 200 mM NaCl 20 mM Tris (pH 8) and 1 ml of 300 mM NaCl 20 mM Tris (pH 8). The virus was eluted serially with 1.5 ml of 400 mM NaCl 20 mM Tris, 3 ml of 450 mM NaCl 20 mM Tris (pH 8) and 1.5 ml of 500 mM NaCl 20 mM Tris (pH 8). The eluted virus solution was collected into a 15 ml Amicon Ultra concentrator. The virus was washed at least two times with PBS by filling the tubes and spinning at 3200 rpm for 2 minutes. The virus was concentrated further into a final volume of 250 µl and filtered through 0.2 µm Acrodisc column. 10 µl of the purified virus was loaded on 10 % SDS gel. Purified viruses were stored at -80 ^{o}C for long-term storage in 10 µl volumes.

To determine the functional virus titer, dissociated neurons were infected with serially diluted viruses and fluorescently labeled cells were counted. For more details on virus preparation, see (Heindorf and Hasan, 2011).

4.2.7 Coomassie Blue staining of proteins

10 µl of purified virus was loaded onto a 10 % SDS PAGE with 2.5 µl of 5x Lämli buffer. The gel was run at 130 V and 400 mA for about an hour. The gel was stained for 45 minutes with Coomassie blue and destained for another 45 minutes. Successful virus purification resulted in the observation of 3 bands on the gel corresponding to the viral proteins 87 kDa VP1, 73 kDa VP2 and 62 kDa VP3.

4.2.8 Infectious virus titer determination

Primary hippocampal neurons were prepared from E18 rat embryos according to the protocol designed by (Brewer et al., 1993) and plated at $5x10^4$ in 24 well plates were infected *in vitro* four days after preparation, with different volumes of rAAVs. Two weeks after infection, the highest dilution at which fluorescent cells were present was used for titer determination by counting. Six 10 x magnification fields were photographed and the number of fluorescent neurons counted. This number was multiplied by the ratio of the total well surface area to the 10 x field area and divided by the volume of virus applied. This yielded the number of neurons infected per microliter of virus.

4.2.9 Infection of rat organotypic brain slice culture and dissociated neurons with rAAVs

Organotypic brain slices were prepared from rat embryo according to an existing protocol (Stoppini et al., 1991). Slices were infected with different rAAVs by directly dropping 0.5-1 µl of the viral cocktail onto the tissue. Tissue media were changed at least 5 days after infection and subsequent media changes were done every 2-3 days. After two weeks of virus infection, tissues were either harvested for Western blotting, quantitative luciferase assay or fluorescent microscopy. Dissociated neurons on the other hand were

infected by adding 1 µl of virus cocktail into the media. Two weeks after virus addition, cells were lysed for quantitative luciferase assay or used for viral titer determination.

4.2.10 Quantifying gene activity and expression pattern

4.2.10 .1 Dual luciferase assay

Dissociated primary neurons (or rat organotypic slices) derived from rat embryos were infected with rAAV-P_{tet}bi fLUC/tdTOM and rAAV-hSYN-rLUC. Two weeks later, cells in 24-well plates were lysed with 100 µl of passive lysis buffer (Promega, Madison, USA) per well. Twenty microliter of cell lysates were used for the measurement of the firefly and renilla luciferase activities using the Dual-Luciferase® reporter 1000 assay system (Promega, Madison, USA). In brief, the firefly luciferase and renilla luciferase assay were performed sequentially in one reaction tube. 100 µl of Luciferase Assay Reagent II (LAR II) was dispensed into all tubes sufficient for the total number of assay to be performed. The luminometer was programmed to perform a 5-sec premeasurement delay, followed by a 10 second measurement period for every reporter assay. 20 µl of the cell lysates was carefully transferred into the tube containing the 100 µl of LAR II and mixed gently by pipetting 3 times. The firefly luciferase activity measured was manually recorded. This was followed by the immediate addition of Stop and Glow reagent and vortexing. The tube was returned into the luminometer and the renilla luciferase activity measured.

Luciferase activity was measured for 15 seconds using the Biotic® Lumi-10 luminometer (Macherey-Nagel). Inducible firefly luciferase activity was normalized with the renilla luciferase activity from the same cell lysate and Dox-controlled gene expression was quantified as fLUC/rLUC.

For detailed dual luciferase reporter assay protocol, refer to Dual-Luciferase® Reporter Assay System protocol instructions for use of products e1910 and e1960 (Promega USA).

4.2.10 .2 Time course of Dox dependent gene activation by firefly luciferase

Dissociated primary neurons were infected with rAAV-P_{tet}bi fLUC/tdTOM, rAAV-hSYN-tTA and rAAV-hSYN-rLUC for two weeks in 24 well plates. Wells were put into groups of four. To each group was added 1 µg/ml of Dox to shut down tTA dependent gene activation. The different groups were harvested over a period of time spanning 0 minute (-Dox) to 2880 minutes (48 hours of Dox). Quantitative firefly/ renilla luciferase activities were measured as described above. The same experiment was performed with the rtTA system. In brief, dissociated neurons were infected with rAAV-P_{tet}bi fLUC/tdTOM, rAAV-hSYN-rtTA and rAAV-hSYN-rLUC for two weeks, followed by incubation with 1 µg/ml Dox. Cells were harvested for luciferase activity measurement over a period of 0 to 48 hours.

4.2.10 .3 Repeated cycles of Dox-dependent gene activation and inactivation

To investigate repeated cycles of gene activation, dissociated primary neurons were infected with either rAAV-P_{tet}bi fLUC/tdTOM, rAAV-hSYN-tTA and rAAV-hSYN-rLUC or rAAV-P_{tet}bi fLUC/tdTOM, rAAV-hSYN-rtTA and rAAV-hSYN-rLUC. Wells of cell were grouped as before and each group was incubated with or without Dox over 48 hours. The Dox treated medium was replaced with another conditioned medium without Dox also for another 48 hours. This was repeated for five cycles of Dox addition or withdrawal. The removal of Dox was done by washing three times with conditioned medium without Dox. At the end of the cycles, cells were harvested for luciferase assay.

4.2.10 .4 *In vivo* luciferase assay with brain lysates

To measure luciferase activities from brain lysates, wild-type mice were injected with either rAAV-P_{tet}bi fLUC/tdTOM + rAAV-hSYN-tTA and rAAV-hSYN-rLUC or rAAV-P_{tet}bi fLUC/tdTOM + rAAV-hSYN-rtTA and rAAV-hSYN-rLUC. Two weeks after virus

infection, mice were either injected with Dox (rtTA injected mice) or without (tTA injected mice) for forty-eight hours. The mice were anaesthetized with isofluran and decapitated. Brain regions infected with the viruses were carefully dissected and frozen in liquid nitrogen. These brain extracts were later sonicated and 20 µl of each extract was used to measure firefly luciferase and renilla luciferase activities as described above.

4.2.10 .5 Bioluminescence *in vivo* imaging in the living mouse

Wild-type mice were injected with the viruses: rAAVP_{tet}bi-bLUC + rAAV-hSYN-tTA into the cortex of one brain hemisphere while the other hemisphere was injected with rAAV-hSYN-bLUC. Two weeks after virus injection, mice were anesthetized with ketamine/xylazine, injected with an aqueous solution of D-luciferin (100 mg/g) and placed into a light-tight chamber. The emitted photons were acquired by a photon counting camera (2-stage ICCD C2400-47) fitted with a Nikon lens (35 mm/f1.2) and a computer with image analysis capabilities (Contag et al., 1997). Ten minutes after D-luciferin injection, the chamber was closed and the photon counting program was initiated for a periods of 1–5 min. Photons were collected over time and the generated images converted to pseudocolor, digitized with the Argus 20 image processor (Hamamatsu). The intensity of acquired images was calculated as relative luminescent units per minute (rlu/min).

4.2.11 β-galactosidase assay

Transgenic Rosa26R mice were injected with rAAV-P_{tet}bi-iCre/tdTOM and hSYN-rtTA for two weeks. Paraformaldehyde fixed brain slices (100 µm) were prepared by vibratome sectioning. To visualize β-galactosidase activity, fixed brain slices were incubated in X-gal solution (5 mM $K_4Fe(CN)_6$, 5 mM $K_3Fe(CN)_6$, 2 mM $MgCl_2$, 2 mg/ml X-Gal in dimethylformamide / 1x PBS) at room temperature for 30-60 minutes. Sections were washed three times in 1x PBS, once in 10 mM Tris-HCl pH 7.5, mounted on glass

slides with Aqua Poly/Mount (Polysciences, Inc., Warrington, PA, USA) and protected with cover slips.

4.2.12 Immunohistochemistry

Immunostaining was carried out on wild-type mice (infected with rAAV-hSYN-TeTxLC-2A-mKO), NR1-2*lox* transgenic mice (infected with rAAV-P_{tet}bi-iCre/tdTOM and rAAV-hSYN-rtTA). In brief, mice were anesthetized by isoflurane inhalation followed by intracardial perfusion with warm 1x PBS (137 mM NaCl, 2.7 mM KCl, 4.3 mM $Na_2HPO_4/2H_2O$, 1.4 mM KH_2PO_4) and 4 % paraformaldehyde (PFA) in 1x PBS prior to decapitation. Brains were removed and post-fixed in 4 % PFA at 4 ^oC overnight, followed by embedding in 2.5 % agarose (in PBS). 60-100µm vibratome coronal sections were prepared (VT1000S, Leica, Wetzlar, Germany) and stored in PBS supplemented with 0.01 % sodium azide at 4 ^oC. Some sections were directly analyzed by fluorescent imaging after mounting with Aqua Poly/Mount (Polysciences, Inc., Warrington, PA, USA) and covered with cover slips.

Tissues for immunostaining were blocked in 4 % normal goat serum (supplemented with 1 % bovine serum albumin (BSA), 0.3 % Triton X-100). Sections were incubated overnight at room temperature in primary antibodies diluted in 1x PBS/ 1 % BSA/ 1 % normal goat serum/ 0.3 % Triton X-100. The antibodies used were anti 2A 1:2000 (rabbit polyclonal, Millipore), anti-Cre 1:1000 (rabbit polyclonal or mouse monoclonal, Covance, Germany), and anti-NeuN (mouse monoclonal, Chemicon, California USA). The next day, sections were washed twice in 1x PBS/ 0.3 % BSA/ 0.1 % Triton X-100 (D2) followed by anti-rabbit or anti mouse FITC secondary antibody (1:200, Jackson Immuno Research) for 1 hour at RT. Slices were washed in 1x D2 buffer followed by 1x wash in PBS and mounted with Aqua Poly/Mount on glass slides with cover slips. Immunostained sections were analyzed with an Axiovert 200 M confocal microscope with LSM 5 PASCAL (Zeiss, Jena, Germany) coupled to 543 nm HeNe and 450-530 nm Argon lasers (Lasos Lasertechnik GmbH, Germany).

4.2.13 Protein extraction and Western blot analysis

Protein analyses by Western blot were done by either transfecting HEK293 cells for 48 hours or by infecting rat organotypic slices for two weeks with viruses. HEK293 cells were transfected with the following plasmids: pAAV-hSYN-TeTxLC-2A-mKO, pAAV-P_{tet}bi-HATeTxLC/tdTOM + pAAV-hSYN-tTA, pAAV-P_{tet}bi-F1TeTxLC/tdTOM + pAAV-hSYN-tTA, pAAV-P_{tet}bi-F2TeTxLC/tdTOM + pAAV-hSYN-tTA and pAAV-hSYN-EGFP. 48 hours after transfection, cells were harvested in lysis buffer (50 mM Tris-HCl, pH 7.6; 5 mM $MgCl_2$; 130 mM NaCl; 10 mM KCl; 1 % Triton X-100; 5 % Glycerin supplemented with protease inhibitor complex, (CompleteTM, Roche, Mannheim). In the case of infection, rat organotypic slices were infected with the following viruses: rAAV-hSYN-TeTxLC-2A-mKO, rAAV-P_{tet}bi-TeTxLC/tdTOM + rAAV-hSYN-tTA, rAAV-P_{tet}bi-F1TeTxLC/tdTOM + rAAV-hSYN-tTA and rAAV-P_{tet}bi-F2TeTxLC/tdTOM + rAAV-hSYN-tTA.

Rat organotypic slices were harvested in cold lysis buffer, two weeks after virus infection and homogenized by sonication. Protein concentrations were determined by Bradford assay. 15 µg of the protein lysates from both rAAV infected and uninfected tissues and lysates from HEK293 transfected cells were separated by SDS-PAGE (15 % separating and 6 % stacking gels) then transferred onto nitrocellulose membranes. Transfer onto membranes was done overnight at 30 V and 90 mA followed by blocking of the membrane in 5-10 % fat-free milk in 1x PBS for 1 hour. Western blots were probed with the following primary antibodies either overnight at 4 ^{o}C or 2 hours at RT: polyclonal rabbit anti-2A-peptide, (1:2000, Millipore), VAMP-2 (1:1000, rabbit polyclonal, abcam), cellubrevin (1:1000, rabbit polyclonal, abcam). Polyclonal goat anti-synaptotagmin (1:500, Santa Cruz), synaptophysin (1:500, goat polyclonal, Santa Cruz), monoclonal mouse anti- β-tubulin (1:1000, Millipore), VAMP1 (rabbit polyclonal, abcam), mouse monoclonal anti-GFP (1: 1000, Clontech) and monoclonal mouse anti-HA (1:1000, abcam). The secondary antibodies used were; horseradish peroxidase-linked anti-rabbit, anti-goat or anti-mouse (1:15000, Vector Laboratories, Peterborough, UK). Western blots were detected by enhanced chemiluminescence kit (ECL kit, Amersham Pharmacia Biotech, Freiburg, Germany).

4.2.14 Stereotactic virus injection into the mouse brain

Six weeks old mice (C57BL/6), Rosa26R and NR1-2*lox*, were deeply anesthetized (Ketamine 100 mg/kg, and Xylazine 5 mg/kg), and secured in a Kopf stereotaxic setup (Kopf Instruments, California, USA). The foreskin on the skull was cut open to expose the skull. With the help of a drill, small holes (about 50-100 µm) were drilled into the head of the mice at different coordinates as stated below. Approximately 300 nl volume of viral suspension was stereotaxically injected via glass pipette (tip diameter 10-20 µm) into each spot chosen to be injected. The ~300 nl virus was injected in a total time of at least 2-5 minutes and a waiting period of 5 minutes before the next injection or the withdrawal of the injection needle. After injection, the skin was sutured and the wound disinfected. Newly injected mice were kept on heating blocks at 37 ^{o}C until they woke up and were fed on wet food. For details on injection, see (Cetin et al., 2006).

The coordinates used for the different injections with reference to the bregma were (Paxinos and Franklin, 2001):

(1) Somatosensory cortex:	-1.70 mm bregma
	1.5 mm lateral
	500 µm deep
(2) Hippocampus	-1.70 mm bregma
	1.5 mm lateral
	1.5 mm deep
(3) Barrel Cortex	-1.5 mm bregma
	3 mm lateral
	500 µm deep
(4) Striatum (unilateral)	0 mm bregma
	2.2mm lateral
	1.7mm deep

(5) Medial septum (bilateral)	0.5 and 1.2 mm bregma ± 0 mm lateral 4 and 4.5 mm deep
(6) Motor cortex (bilateral)	+ 0.1, + 1.0, and + 1.9 mm bregma ± 1, ± 1.5, and ± 1.75 mm lateral 0.6 mm deep

4.2.15 Fluorescence and confocal imaging

Light and fluorescence imaging were performed with Zeiss Axioplan2 (Carl Zeiss, Jena, Germany) with the camera system AxioCam HRC with magnifications ranging from 2.5x to 40x dry or 63x oil immersion objectives (software: Axiovision 4.8.1). A compact light source (Leistungselectronic Jena, Germany) with 488 nm and 568 nm filters. Confocal images were acquired with Zeiss LSM PASCAL confocal laser scanning microscope equipped with an Argon laser (457,476, 488 and 514 nm) and a Helium Neon laser (543 nm) with objectives 5x-40x dry and 63x oil-immersion objective. Images were analyzed with ImageJ and LSM image browser.

4.2.16 Amphetamine-induced rotational behavior in mice

D-amphetamine (AMP) sulfate was dissolved in sterile 1x PBS at 10 mg/ml and further diluted to 0.5 mg/ml (working concentration) in sterile saline for intraperitoneal injections (i.p.) (5 mg/kg). TeTxLC virus injected mice and control virus (hSYN-Venus) injected mice were later injected with a single i.p. of amphetamine (5 mg/kg body weight). Ten minutes after amphetamine injection, mice were placed in an open field box (50 x 50 cm) for locomotor activity studies. Locomotor activity was recorded with a top-mounted camera connected to a video tracking system. Each mouse was allowed to move

freely in the open field for 10 minutes. Recordings were done before and after amphetamine injection. The movie files were analyzed using the VideoMot software. The total number of 360^{o} rotations made by the animals was manually counted and mice tracking paths were also documented. A rotation was scored when the mouse make a continuous 360 ^{o} circle without change in direction. Only ipsilateral rotations were counted. Movements made around the periphery of the box were not counted as a rotation.

4.2.17 Tail suspension test (TST)

Tail suspension test is one of the commonly used test to study antidepressant behavior in mice (rodents) (Steru et al., 1985). In this work, I used a modified version of the TST to investigate the behavior of mice with unilateral lesion to the striatum. Mice with virus injected unilaterally to the striatum were suspended by the tail for one minute and their twitching behavior monitored by video recording and visual observation for one minute.

5. REFERENCES

Abremski K, Hoess R (Bacteriophage P1 site-specific recombination. Purification and properties of the Cre recombinase protein. J Biol Chem 259:1509-1514.1984).

Alisky JM, Hughes SM, Sauter SL, Jolly D, Dubensky TW, Jr., Staber PD, Chiorini JA, Davidson BL (Transduction of murine cerebellar neurons with recombinant FIV and AAV5 vectors. Neuroreport 11:2669-2673.2000).

Atasoy D, Aponte Y, Su HH, Sternson SM (A FLEX switch targets Channelrhodopsin-2 to multiple cell types for imaging and long-range circuit mapping. J Neurosci 28:7025-7030.2008).

Atchison RW, Casto BC, Hammon WM (Electron microscopy of adenovirus-associated virus (AAV) in cell cultures. Virology 29:353-357.1966).

Auer S, Sturzebecher AS, Juttner R, Santos-Torres J, Hanack C, Frahm S, Liehl B, Ibanez-Tallon I (Silencing neurotransmission with membrane-tethered toxins. Nat Methods 7:229-236.2010).

Auricchio A, Hildinger M, O'Connor E, Gao GP, Wilson JM (Isolation of highly infectious and pure adeno-associated virus type 2 vectors with a single-step gravity-flow column. Hum Gene Ther 12:71-76.2001).

Ausubel FM, Brent R, Kingston RE, Moore DD, Seidman JG, Smith JA, Struhl K (Current Protocols in Molecular Biology. Wiley Interscience.1989).

Bannerman DM, Good MA, Butcher SP, Ramsay M, Morris RG (Distinct components of spatial learning revealed by prior training and NMDA receptor blockade. Nature 378:182-186.1995).

Baron U, Freundlieb S, Gossen M, Bujard H (Co-regulation of two gene activities by tetracycline via a bidirectional promoter. Nucleic Acids Res 23:3605-3606.1995).

Baron U, Gossen M, Bujard H (Tetracycline-controlled transcription in eukaryotes: novel transactivators with graded transactivation potential. Nucleic Acids Res 25:2723-2729.1997).

Bartlett JS, Samulski RJ, McCown TJ (Selective and rapid uptake of adeno-associated virus type 2 in brain. Hum Gene Ther 9:1181-1186.1998).

Bartlett JS, Wilcher R, Samulski RJ (Infectious entry pathway of adeno-associated virus and adeno-associated virus vectors. J Virol 74:2777-2785.2000).

Beard C, Hochedlinger K, Plath K, Wutz A, Jaenisch R (Efficient method to generate single-copy transgenic mice by site-specific integration in embryonic stem cells. Genesis 44:23-28.2006).

Bejar R, Yasuda R, Krugers H, Hood K, Mayford M (Transgenic calmodulin-dependent protein kinase II activation: dose-dependent effects on synaptic plasticity, learning, and memory. J Neurosci 22:5719-5726.2002).

Bercovich Z, Rosenberg-Hasson Y, Ciechanover A, Kahana C (Degradation of ornithine decarboxylase in reticulocyte lysate is ATP-dependent but ubiquitin-independent. J Biol Chem 264:15949-15952.1989).

Berens C, Hillen W (Gene regulation by tetracyclines. Genet Eng (N Y) 26:255-277.2004).

Berger SL, Pina B, Silverman N, Marcus GA, Agapite J, Regier JL, Triezenberg SJ, Guarente L (Genetic isolation of ADA2: a potential transcriptional adaptor required for function of certain acidic activation domains. Cell 70:251-265.1992).

Betz AL, Shakui P, Davidson BL (Gene transfer to rodent brain with recombinant adenoviral vectors: effects of infusion parameters, infectious titer, and virus concentration on transduction volume. Exp Neurol 150:136-142.1998).

Blacklow NR (Adeno-associated viruses of human. In Parvoviruses and Human Disease . (Pattison JR Ed) CRC Press: Boca Raton, FL 165-174.1988).

Bliss TV, Collingridge GL (A synaptic model of memory: long-term potentiation in the hippocampus. Nature 361:31-39.1993).

Bocker R, Estler CJ, Maywald M, Weber D (Comparative evaluation of the effects of tetracycline and doxycycline on blood and liver lipids on male and female mice. Arzneimittelforschung 31:2118-2120.1981).

Bohenzky RA, LeFebvre RB, Berns KI (Sequence and symmetry requirements within the internal palindromic sequences of the adeno-associated virus terminal repeat. Virology 166:316-327.1988).

Brewer GJ, Torricelli JR, Evege EK, Price PJ (Optimized survival of hippocampal neurons in B27-supplemented Neurobasal, a new serum-free medium combination. J Neurosci Res 35:567-576.1993).

Buller RM, Rose JA (Characterization of adenovirus-associated virus-induced polypeptides in KB cells. J Virol 25:331-338.1978).

Buning H, Perabo L, Coutelle O, Quadt-Humme S, Hallek M (Recent developments in adeno-associated virus vector technology. J Gene Med 10:717-733.2008).

Burger C, Gorbatyuk OS, Velardo MJ, Peden CS, Williams P, Zolotukhin S, Reier PJ, Mandel RJ, Muzyczka N (Recombinant AAV viral vectors pseudotyped with viral capsids from serotypes 1, 2, and 5 display differential efficiency and cell tropism after delivery to different regions of the central nervous system. Mol Ther 10:302-317.2004).

Burgess-Beusse B, Farrell C, Gaszner M, Litt M, Mutskov V, Recillas-Targa F, Simpson M, West A, Felsenfeld G (The insulation of genes from external enhancers and silencing chromatin. Proc Natl Acad Sci U S A 99 Suppl 4:16433-16437.2002).

Callaway EM (A molecular and genetic arsenal for systems neuroscience. Trends Neurosci 28:196-201.2005).

Cambridge SB, Geissler D, Calegari F, Anastassiadis K, Hasan MT, Stewart AF, Huttner WB, Hagen V, Bonhoeffer T (Doxycycline-dependent photoactivated gene expression in eukaryotic systems. Nat Methods 6:527-531.2009).

Carty N, Lee D, Dickey C, Ceballos-Diaz C, Jansen-West K, Golde TE, Gordon MN, Morgan D, Nash K (Convection-enhanced delivery and systemic mannitol increase gene product distribution of AAV vectors 5, 8, and 9 and increase gene product in the adult mouse brain. J Neurosci Methods 194:144-153.2010).

Cetin A, Komai S, Eliava M, Seeburg PH, Osten P (Stereotaxic gene delivery in the rodent brain. Nat Protoc 1:3166-3173.2006).

Chang CC (Looking back on the discovery of alpha-bungarotoxin. J Biomed Sci 6:368-375.1999).

Chen ZY, Yant SR, He CY, Meuse L, Shen S, Kay MA (Linear DNAs concatemerize in vivo and result in sustained transgene expression in mouse liver. Mol Ther 3:403-410.2001).

Chklovskii DB, Mel BW, Svoboda K (Cortical rewiring and information storage. Nature 431:782-788.2004).

Christian KM, Thompson RF (Neural substrates of eyeblink conditioning: acquisition and retention. Learn Mem 10:427-455.2003).

Contag CH, Spilman SD, Contag PR, Oshiro M, Eames B, Dennery P, Stevenson DK, Benaron DA (Visualizing gene expression in living mammals using a bioluminescent reporter. Photochem Photobiol 66:523-531.1997).

Conway JE, Zolotukhin S, Muzyczka N, Hayward GS, Byrne BJ (Recombinant adeno-associated virus type 2 replication and packaging is entirely supported by a herpes simplex virus type 1 amplicon expressing Rep and Cap. J Virol 71:8780-8789.1997).

Cryan JF, Mombereau C, Vassout A (The tail suspension test as a model for assessing antidepressant activity: review of pharmacological and genetic studies in mice. Neurosci Biobehav Rev 29:571-625.2005).

Davidson BL, Stein CS, Heth JA, Martins I, Kotin RM, Derksen TA, Zabner J, Ghodsi A, Chiorini JA (Recombinant adeno-associated virus type 2, 4, and 5 vectors: transduction of variant cell types and regions in the mammalian central nervous system. Proc Natl Acad Sci U S A 97:3428-3432.2000).

Di Pasquale G, Davidson BL, Stein CS, Martins I, Scudiero D, Monks A, Chiorini JA (Identification of PDGFR as a receptor for AAV-5 transduction. Nat Med 9:1306-1312.2003).

Druga R (Neocortical inhibitory system. Folia Biol (Praha) 55:201-217.2009).

During MJ (Adeno-associated virus as a gene delivery system. Adv Drug Deliv Rev 27:83-94.1997).

Eckenstein FP, McGovern T, Kern D, Deignan J (Neuronal vulnerability in transgenic mice expressing an inducible dominant-negative FGF receptor. Exp Neurol 198:338-349.2006).

Epe B, Woolley P (The binding of 6-demethylchlortetracycline to 70S, 50S and 30S ribosomal particles: a quantitative study by fluorescence anisotropy. EMBO J 3:121-126.1984).

Flotte TR, Carter BJ (Adeno-associated virus vectors for gene therapy. Gene Ther 2:357-362.1995).

Foran PG, Mohammed N, Lisk GO, Nagwaney S, Lawrence GW, Johnson E, Smith L, Aoki KR, Dolly JO (Evaluation of the therapeutic usefulness of botulinum neurotoxin B, C1, E, and F compared with the long lasting type A. Basis for distinct durations of inhibition of exocytosis in central neurons. J Biol Chem 278:1363-1371.2003).

Gao G, Vandenberghe LH, Wilson JM (New recombinant serotypes of AAV vectors. Curr Gene Ther 5:285-297.2005).

Gaur RK (RNA interference: a potential therapeutic tool for silencing splice isoforms linked to human diseases. Biotechniques Suppl:15-22.2006).

Ghoda L, van Daalen Wetters T, Macrae M, Ascherman D, Coffino P (Prevention of rapid intracellular degradation of ODC by a carboxyl-terminal truncation. Science 243:1493-1495.1989).

Gill G, Ptashne M (Negative effect of the transcriptional activator GAL4. Nature 334:721-724.1988).

Gingrich JR, Roder J (Inducible gene expression in the nervous system of transgenic mice. Annu Rev Neurosci 21:377-405.1998).

Gordon JW, Ruddle FH (Germ line transmission in transgenic mice. Prog Clin Biol Res 85 Pt B:111-124.1982).

Gossen M, Bujard H (Tight control of gene expression in mammalian cells by tetracycline-responsive promoters. Proc Natl Acad Sci U S A 89:5547-5551.1992).

Gossen M, Bujard H (Studying gene function in eukaryotes by conditional gene inactivation. Annu Rev Genet 36:153-173.2002).

Gossen M, Freundlieb S, Bender G, Muller G, Hillen W, Bujard H (Transcriptional activation by tetracyclines in mammalian cells. Science 268:1766-1769.1995).

Grimm D, Kay MA, Kleinschmidt JA (Helper virus-free, optically controllable, and two-plasmid-based production of adeno-associated virus vectors of serotypes 1 to 6. Mol Ther 7:839-850.2003).

Grimm D, Kern A, Rittner K, Kleinschmidt JA (Novel tools for production and purification of recombinant adenoassociated virus vectors. Hum Gene Ther 9:2745-2760.1998).

Habig WH, Bigalke H, Bergey GK, Neale EA, Hardegree MC, Nelson PG (Tetanus toxin in dissociated spinal cord cultures: long-term characterization of form and action. J Neurochem 47:930-937.1986).

Hamilton DL, Abremski K (Site-specific recombination by the bacteriophage P1 lox-Cre system. Cre-mediated synapsis of two lox sites. J Mol Biol 178:481-486.1984).

Hasan MT, Friedrich RW, Euler T, Larkum ME, Giese G, Both M, Duebel J, Waters J, Bujard H, Griesbeck O, Tsien RY, Nagai T, Miyawaki A, Denk W (Functional fluorescent Ca2+ indicator proteins in transgenic mice under TET control. PLoS Biol 2:e163.2004).

Hasan MT, Schonig K, Berger S, Graewe W, Bujard H (Long-term, noninvasive imaging of regulated gene expression in living mice. Genesis 29:116-122.2001).

Hatfield L, Hearing P (Redundant elements in the adenovirus type 5 inverted terminal repeat promote bidirectional transcription in vitro and are important for virus growth in vivo. Virology 184:265-276.1991).

Hauck B, Chen L, Xiao W (Generation and characterization of chimeric recombinant AAV vectors. Mol Ther 7:419-425.2003).

Hecht B, Muller G, Hillen W (Noninducible Tet repressor mutations map from the operator binding motif to the C terminus. J Bacteriol 175:1206-1210.1993).

Heindorf M, Hasan MT (Imaging in Neuroscience, A Laboratory Manual. Cold Spring Harbor Laboratory Press 583-609.2011).

Herculano-Houzel S (The human brain in numbers: a linearly scaled-up primate brain. Front Hum Neurosci 3:31.2009).

Hermens WT, Verhaagen J (Viral vectors, tools for gene transfer in the nervous system. Prog Neurobiol 55:399-432.1998).

Hermonat PL, Muzyczka N (Use of adeno-associated virus as a mammalian DNA cloning vector: transduction of neomycin resistance into mammalian tissue culture cells. Proc Natl Acad Sci U S A 81:6466-6470.1984).

Hillen W, Berens C (Mechanisms underlying expression of Tn10 encoded tetracycline resistance. Annu Rev Microbiol 48:345-369.1994).

Hoggan MD, Blacklow NR, Rowe WP (Studies of small DNA viruses found in various adenovirus preparations: physical, biological, and immunological characteristics. Proc Natl Acad Sci U S A 55:1467-1474.1966).

Ibanez-Tallon I, Wen H, Miwa JM, Xing J, Tekinay AB, Ono F, Brehm P, Heintz N (Tethering naturally occurring peptide toxins for cell-autonomous modulation of ion channels and receptors in vivo. Neuron 43:305-311.2004).

Iyer M, Salazar FB, Lewis X, Zhang L, Carey M, Wu L, Gambhir SS (Noninvasive imaging of enhanced prostate-specific gene expression using a two-step transcriptional amplification-based lentivirus vector. Mol Ther 10:545-552.2004).

Jay FT, Laughlin CA, Carter BJ (Eukaryotic translational control: adeno-associated virus protein synthesis is affected by a mutation in the adenovirus DNA-binding protein. Proc Natl Acad Sci U S A 78:2927-2931.1981).

Jeltsch H, Bertrand F, Lazarus C, Cassel JC (Cognitive performances and locomotor activity following dentate granule cell damage in rats: role of lesion extent and type of memory tested. Neurobiol Learn Mem 76:81-105.2001).

Kaludov N, Brown KE, Walters RW, Zabner J, Chiorini JA (Adeno-associated virus serotype 4 (AAV4) and AAV5 both require sialic acid binding for hemagglutination and efficient transduction but differ in sialic acid linkage specificity. J Virol 75:6884-6893.2001).

Kao CY, Levinson SR (Tetrodotoxin, saxitoxin, and the molecular biology of the sodium channel. New York Academy of Sciences ISBN 0897663543. 1986).

Karpova AY, Tervo DG, Gray NW, Svoboda K (Rapid and reversible chemical inactivation of synaptic transmission in genetically targeted neurons. Neuron 48:727-735.2005).

Kim J (Improvement and establishment of the tTA dependent inducible system in the mouse brain. Max-Planck-Institute for Medical Research, Molecular Neurobiology University of Heidelberg p.80 2001).

Kistner A, Gossen M, Zimmermann F, Jerecic J, Ullmer C, Lubbert H, Bujard H (Doxycycline-mediated quantitative and tissue-specific control of gene expression in transgenic mice. Proc Natl Acad Sci U S A 93:10933-10938.1996).

Klein RL, Hamby ME, Gong Y, Hirko AC, Wang S, Hughes JA, King MA, Meyer EM (Dose and promoter effects of adeno-associated viral vector for green fluorescent protein expression in the rat brain. Exp Neurol 176:66-74.2002).

Koeberl DD, Alexander IE, Halbert CL, Russell DW, Miller AD (Persistent expression of human clotting factor IX from mouse liver after intravenous injection of adeno-associated virus vectors. Proc Natl Acad Sci U S A 94:1426-1431.1997).

Krestel HE, Shimshek DR, Jensen V, Nevian T, Kim J, Geng Y, Bast T, Depaulis A, Schonig K, Schwenk F, Bujard H, Hvalby O, Sprengel R, Seeburg PH (A genetic switch for epilepsy in adult mice. J Neurosci 24:10568-10578.2004).

Laughlin CA, Tratschin JD, Coon H, Carter BJ (Cloning of infectious adeno-associated virus genomes in bacterial plasmids. Gene 23:65-73.1983).

Lederer T, Kintrup M, Takahashi M, Sum PE, Ellestad GA, Hillen W (Tetracycline analogs affecting binding to Tn10-Encoded Tet repressor trigger the same mechanism of induction. Biochemistry 35:7439-7446.1996).

Lerchner W, Xiao C, Nashmi R, Slimko EM, van Trigt L, Lester HA, Anderson DJ (Reversible silencing of neuronal excitability in behaving mice by a genetically targeted, ivermectin-gated Cl- channel. Neuron 54:35-49.2007).

Li X, Zhao X, Fang Y, Jiang X, Duong T, Fan C, Huang CC, Kain SR (Generation of destabilized green fluorescent protein as a transcription reporter. J Biol Chem 273:34970-34975.1998).

Lindeberg J, Mattsson R, Ebendal T (Timing the doxycycline yields different patterns of genomic recombination in brain neurons with a new inducible Cre transgene. J Neurosci Res 68:248-253.2002).

Linden RM, Berns KI (Molecular biology of adeno-associated viruses. Contrib Microbiol 4:68-84.2000).

Louboutin JP, Chekmasova AA, Marusich E, Chowdhury JR, Strayer DS (Efficient CNS gene delivery by intravenous injection. Nat Methods 7:905-907.2010).

Luscher C, Nicoll RA, Malenka RC, Muller D (Synaptic plasticity and dynamic modulation of the postsynaptic membrane. Nat Neurosci 3:545-550.2000).

Mann JR, McMahon AP (Factors influencing frequency production of transgenic mice. Methods Enzymol 225:771-781.1993).

Manno CS, Chew AJ, Hutchison S, Larson PJ, Herzog RW, Arruda VR, Tai SJ, Ragni MV, Thompson A, Ozelo M, Couto LB, Leonard DG, Johnson FA, McClelland A, Scallan C, Skarsgard E, Flake AW, Kay MA, High KA, Glader B (AAV-mediated factor IX gene transfer to skeletal muscle in patients with severe hemophilia B. Blood 101:2963-2972.2003).

Mansuy IM, Winder DG, Moallem TM, Osman M, Mayford M, Hawkins RD, Kandel ER (Inducible and reversible gene expression with the rtTA system for the study of memory. Neuron 21:257-265.1998).

Martin JR, Keller A, Sweeney ST (Targeted expression of tetanus toxin: a new tool to study the neurobiology of behavior. Adv Genet 47:1-47.2002).

Mastakov MY, Baer K, Xu R, Fitzsimons H, During MJ (Combined injection of rAAV with mannitol enhances gene expression in the rat brain. Mol Ther 3:225-232.2001).

Mayford M, Bach ME, Huang YY, Wang L, Hawkins RD, Kandel ER (Control of memory formation through regulated expression of a CaMKII transgene. Science 274:1678-1683.1996).

McCarty DM, Young SM, Jr., Samulski RJ (Integration of adeno-associated virus (AAV) and recombinant AAV vectors. Annu Rev Genet 38:819-845.2004).

Mendelson E, Trempe JP, Carter BJ (Identification of the trans-acting Rep proteins of adeno-associated virus by antibodies to a synthetic oligopeptide. J Virol 60:823-832.1986).

Michel G, Mosser J, Olle J (Pharmacokinetics and tissue localization of doxycycline polyphosphate and doxycycline hydrochloride in the rat. Eur J Drug Metab Pharmacokinet 9:149-153.1984).

Monyer H, Sprengel R, Schoepfer R, Herb A, Higuchi M, Lomeli H, Burnashev N, Sakmann B, Seeburg PH (Heteromeric NMDA receptors: molecular and functional distinction of subtypes. Science 256:1217-1221.1992).

Mori S, Wang L, Takeuchi T, Kanda T (Two novel adeno-associated viruses from cynomolgus monkey: pseudotyping characterization of capsid protein. Virology 330:375-383.2004).

Morris RG, Anderson E, Lynch GS, Baudry M (Selective impairment of learning and blockade of long-term potentiation by an N-methyl-D-aspartate receptor antagonist, AP5. Nature 319:774-776.1986).

Murakami Y, Matsufuji S, Kameji T, Hayashi S, Igarashi K, Tamura T, Tanaka K, Ichihara A (Ornithine decarboxylase is degraded by the 26S proteasome without ubiquitination. Nature 360:597-599.1992).

Muzyczka N (Use of adeno-associated virus as a general transduction vector for mammalian cells. Curr Top Microbiol Immunol 158:97-129.1992).

Nagy A (Cre recombinase: the universal reagent for genome tailoring. Genesis 26:99-109.2000).

Nakashiba T, Young JZ, McHugh TJ, Buhl DL, Tonegawa S (Transgenic inhibition of synaptic transmission reveals role of CA3 output in hippocampal learning. Science 319:1260-1264.2008).

Nakazawa K, Quirk MC, Chitwood RA, Watanabe M, Yeckel MF, Sun LD, Kato A, Carr CA, Johnston D, Wilson MA, Tonegawa S (Requirement for hippocampal CA3 NMDA receptors in associative memory recall. Science 297:211-218.2002).

Niemann H, Blasi J, Jahn R (Clostridial neurotoxins: new tools for dissecting exocytosis. Trends Cell Biol 4:179-185.1994).

Niewoehner B, Single FN, Hvalby O, Jensen V, Meyer zum Alten Borgloh S, Seeburg PH, Rawlins JN, Sprengel R, Bannerman DM (Impaired spatial working memory but spared spatial reference memory following functional loss of NMDA receptors in the dentate gyrus. Eur J Neurosci 25:837-846.2007).

O'Connor DH, Huber D, Svoboda K (Reverse engineering the mouse brain. Nature 461:923-929.2009).

O'Keefe J, Nadel L (The Hippocampus as a Cognitive Map. Oxford University Press, Oxford.1978).

Orth P, Schnappinger D, Hillen W, Saenger W, Hinrichs W (Structural basis of gene regulation by the tetracycline inducible Tet repressor-operator system. Nat Struct Biol 7:215-219.2000).

Paxinos G, Franklin JL (The Mouse Brain in Stereotaxic Coordinates.2001).

Pelvig DP, Pakkenberg H, Stark AK, Pakkenberg B (Neocortical glial cell numbers in human brains. Neurobiol Aging 29:1754-1762.2008).

Qing K, Mah C, Hansen J, Zhou S, Dwarki V, Srivastava A (Human fibroblast growth factor receptor 1 is a co-receptor for infection by adeno-associated virus 2. Nat Med 5:71-77.1999).

Richter M, Iwata A, Nyhuis J, Nitta Y, Miller AD, Halbert CL, Allen MD (Adeno-associated virus vector transduction of vascular smooth muscle cells in vivo. Physiol Genomics 2:117-127.2000).

Rosenberg-Hasson Y, Bercovich Z, Ciechanover A, Kahana C (Degradation of ornithine decarboxylase in mammalian cells is ATP dependent but ubiquitin independent. Eur J Biochem 185:469-474.1989).

Rumpel S, LeDoux J, Zador A, Malinow R (Postsynaptic receptor trafficking underlying a form of associative learning. Science 308:83-88.2005).

Russell DW, Kay MA (Adeno-associated virus vectors and hematology. Blood 94:864-874.1999).

Rutledge EA, Halbert CL, Russell DW (Infectious clones and vectors derived from adeno-associated virus (AAV) serotypes other than AAV type 2. J Virol 72:309-319.1998).

Sakimura K, Kutsuwada T, Ito I, Manabe T, Takayama C, Kushiya E, Yagi T, Aizawa S, Inoue Y, Sugiyama H, et al. (Reduced hippocampal LTP and spatial learning in mice lacking NMDA receptor epsilon 1 subunit. Nature 373:151-155.1995).

Sambrook J, Russell DW (Molecular Cloning: a Laboratory Manual
. Cold Spring Harbor Laboratory Press 3rd Edition 2001).

Samulski RJ, Berns KI, Tan M, Muzyczka N (Cloning of adeno-associated virus into pBR322: rescue of intact virus from the recombinant plasmid in human cells. Proc Natl Acad Sci U S A 79:2077-2081.1982).

Sanlioglu S, Benson PK, Yang J, Atkinson EM, Reynolds T, Engelhardt JF (Endocytosis and nuclear trafficking of adeno-associated virus type 2 are controlled by rac1 and phosphatidylinositol-3 kinase activation. J Virol 74:9184-9196.2000).

Sauer B, Henderson N (Cre-stimulated recombination at loxP-containing DNA sequences placed into the mammalian genome. Nucleic Acids Res 17:147-161.1989).

Schiavo G, Benfenati F, Poulain B, Rossetto O, Polverino de Laureto P, DasGupta BR, Montecucco C (Tetanus and botulinum-B neurotoxins block neurotransmitter release by proteolytic cleavage of synaptobrevin. Nature 359:832-835.1992a).

Schiavo G, Poulain B, Rossetto O, Benfenati F, Tauc L, Montecucco C (Tetanus toxin is a zinc protein and its inhibition of neurotransmitter release and protease activity depend on zinc. EMBO J 11:3577-3583.1992b).

Schnutgen F, Doerflinger N, Calleja C, Wendling O, Chambon P, Ghyselinck NB (A directional strategy for monitoring Cre-mediated recombination at the cellular level in the mouse. Nat Biotechnol 21:562-565.2003).

Schultz BR, Chamberlain JS (Recombinant adeno-associated virus transduction and integration. Mol Ther 16:1189-1199.2008).

Schwarcz R, Fuxe K, Agnati LF, Hokfelt T, Coyle JT (Rotational behaviour in rats with unilateral striatal kainic acid lesions: a behavioural model for studies on intact dopamine receptors. Brain Res 170:485-495.1979).

Seisenberger G, Ried MU, Endress T, Buning H, Hallek M, Brauchle C (Real-time single-molecule imaging of the infection pathway of an adeno-associated virus. Science 294:1929-1932.2001).

Shevtsova Z, Malik JM, Michel U, Bahr M, Kugler S (Promoters and serotypes: targeting of adeno-associated virus vectors for gene transfer in the rat central nervous system in vitro and in vivo. Exp Physiol 90:53-59.2005).

Sollner T, Whiteheart SW, Brunner M, Erdjument-Bromage H, Geromanos S, Tempst P, Rothman JE (SNAP receptors implicated in vesicle targeting and fusion. Nature 362:318-324.1993).

Soriano P (Generalized lacZ expression with the ROSA26 Cre reporter strain. Nat Genet 21:70-71.1999).

Spadaccini R, Reidt U, Dybkov O, Will C, Frank R, Stier G, Corsini L, Wahl MC, Luhrmann R, Sattler M (Biochemical and NMR analyses of an SF3b155-p14-U2AF-RNA interaction network involved in branch point definition during pre-mRNA splicing. RNA 12:410-425.2006).

Spencer ML, Theodosiou M, Noonan DJ (NPDC-1, a novel regulator of neuronal proliferation, is degraded by the ubiquitin/proteasome system through a PEST degradation motif. J Biol Chem 279:37069-37078.2004).

Sprengel R, Hasan MT (Tetracycline-controlled genetic switches. Handb Exp Pharmacol 49-72.2007).

Stephenson FA (Structure and trafficking of NMDA and GABAA receptors. Biochem Soc Trans 34:877-881.2006).

Steru L, Chermat R, Thierry B, Simon P (The tail suspension test: a new method for screening antidepressants in mice. Psychopharmacology (Berl) 85:367-370.1985).

Stoppini L, Buchs PA, Muller D (A simple method for organotypic cultures of nervous tissue. J Neurosci Methods 37:173-182.1991).

Strand AD, Aragaki AK, Baquet ZC, Hodges A, Cunningham P, Holmans P, Jones KR, Jones L, Kooperberg C, Olson JM (Conservation of regional gene expression in mouse and human brain. PLoS Genet 3:e59.2007).

Sudhof TC (The synaptic vesicle cycle: a cascade of protein-protein interactions. Nature 375:645-653.1995).

Summerford C, Bartlett JS, Samulski RJ (AlphaVbeta5 integrin: a co-receptor for adeno-associated virus type 2 infection. Nat Med 5:78-82.1999).

Summerford C, Samulski RJ (Membrane-associated heparan sulfate proteoglycan is a receptor for adeno-associated virus type 2 virions. J Virol 72:1438-1445.1998).

Summerford C, Samulski RJ (Viral receptors and vector purification: new approaches for generating clinical-grade reagents. Nat Med 5:587-588.1999).

Sun JY, Anand-Jawa V, Chatterjee S, Wong KK (Immune responses to adeno-associated virus and its recombinant vectors. Gene Ther 10:964-976.2003).

Sutherland RJ, Whishaw IQ, Kolb B (A behavioural analysis of spatial localization following electrolytic, kainate- or colchicine-induced damage to the hippocampal formation in the rat. Behav Brain Res 7:133-153.1983).

Suzuki T, Varshavsky A (Degradation signals in the lysine-asparagine sequence space. EMBO J 18:6017-6026.1999).

Sweeney ST, Broadie K, Keane J, Niemann H, O'Kane CJ (Targeted expression of tetanus toxin light chain in Drosophila specifically eliminates synaptic transmission and causes behavioral defects. Neuron 14:341-351.1995).

Sweeney TJ, Mailander V, Tucker AA, Olomu AB, Zhang W, Cao Y, Negrin RS, Contag CH (Visualizing the kinetics of tumor-cell clearance in living animals. Proc Natl Acad Sci U S A 96:12044-12049.1999).

Tang W, Ehrlich I, Wolff SB, Michalski AM, Wolfl S, Hasan MT, Luthi A, Sprengel R (Faithful expression of multiple proteins via 2A-peptide self-processing: a versatile and reliable method for manipulating brain circuits. J Neurosci 29:8621-8629.2009).

Taxis C, Stier G, Spadaccini R, Knop M (Efficient protein depletion by genetically controlled deprotection of a dormant N-degron. Mol Syst Biol 5:267.2009).

Thompson LT, Disterhoft JF (N-methyl-D-aspartate receptors in associative eyeblink conditioning: both MK-801 and phencyclidine produce task- and dose-dependent impairments. J Pharmacol Exp Ther 281:928-940.1997).

Thompson LT, Moskal JR, Disterhoft JF (Hippocampus-dependent learning facilitated by a monoclonal antibody or D-cycloserine. Nature 359:638-641.1992).

Trempe JP, Carter BJ (Alternate mRNA splicing is required for synthesis of adeno-associated virus VP1 capsid protein. J Virol 62:3356-3363.1988).

Trimble WS, Cowan DM, Scheller RH (VAMP-1: a synaptic vesicle-associated integral membrane protein. Proc Natl Acad Sci U S A 85:4538-4542.1988).

Uchida S, Sakai S, Furuichi T, Hosoda H, Toyota K, Ishii T, Kitamoto A, Sekine M, Koike K, Masushige S, Murphy G, Silva AJ, Kida S (Tight regulation of transgene expression by tetracycline-dependent activator and repressor in brain. Genes Brain Behav 5:96-106.2006).

Urlinger S, Baron U, Thellmann M, Hasan MT, Bujard H, Hillen W (Exploring the sequence space for tetracycline-dependent transcriptional activators: novel mutations yield expanded range and sensitivity. Proc Natl Acad Sci U S A 97:7963-7968.2000).

Varshavsky A (The N-end rule pathway of protein degradation. Genes Cells 2:13-28.1997a).

Varshavsky A (The ubiquitin system. Trends Biochem Sci 22:383-387.1997b).

Wallace DJ, Meyer zum Alten Borgloh S, Astori S, Yang Y, Bausen M, Kugler S, Palmer AE, Tsien RY, Sprengel R, Kerr JN, Denk W, Hasan MT (Single-spike detection in vitro and in vivo with a genetic Ca2+ sensor. Nat Methods 5:797-804.2008).

Walters RW, Yi SM, Keshavjee S, Brown KE, Welsh MJ, Chiorini JA, Zabner J (Binding of adeno-associated virus type 5 to 2,3-linked sialic acid is required for gene transfer. J Biol Chem 276:20610-20616.2001).

Wang XS, Khuntirat B, Qing K, Ponnazhagan S, Kube DM, Zhou S, Dwarki VJ, Srivastava A (Characterization of wild-type adeno-associated virus type 2-like particles generated during recombinant viral vector production and strategies for their elimination. J Virol 72:5472-5480.1998).

Wehr M, Hostick U, Kyweriga M, Tan A, Weible AP, Wu H, Wu W, Callaway EM, Kentros C (Transgenic silencing of neurons in the mammalian brain by expression of the allatostatin receptor (AlstR). J Neurophysiol 102:2554-2562.2009).

Witt A, Macdonald N, Kirkpatrick P (Memantine hydrochloride. Nat Rev Drug Discov 3:109-110.2004).

Wortge S, Eshkind L, Cabezas-Wallscheid N, Lakaye B, Kim J, Heck R, Abassi Y, Diken M, Sprengel R, Bockamp E (Tetracycline-controlled transgene activation using the ROSA26-iM2-GFP knock-in mouse strain permits GFP monitoring of DOX-regulated transgene-expression. BMC Dev Biol 10:95.2010).

Xavier GF, Oliveira-Filho FJ, Santos AM (Dentate gyrus-selective colchicine lesion and disruption of performance in spatial tasks: difficulties in "place strategy" because of a lack of flexibility in the use of environmental cues? Hippocampus 9:668-681.1999).

Xiao W, Chirmule N, Berta SC, McCullough B, Gao G, Wilson JM (Gene therapy vectors based on adeno-associated virus type 1. J Virol 73:3994-4003.1999).

Yamaguchi A, Udagawa T, Sawai T (Transport of divalent cations with tetracycline as mediated by the transposon Tn10-encoded tetracycline resistance protein. J Biol Chem 265:4809-4813.1990).

Yamamoto M, Wada N, Kitabatake Y, Watanabe D, Anzai M, Yokoyama M, Teranishi Y, Nakanishi S (Reversible suppression of glutamatergic neurotransmission of cerebellar granule cells in vivo by genetically manipulated expression of tetanus neurotoxin light chain. J Neurosci 23:6759-6767.2003).

Yang GS, Schmidt M, Yan Z, Lindbloom JD, Harding TC, Donahue BA, Engelhardt JF, Kotin R, Davidson BL (Virus-mediated transduction of murine retina with adeno-associated virus: effects of viral capsid and genome size. J Virol 76:7651-7660.2002).

Yu TS, Dandekar M, Monteggia LM, Parada LF, Kernie SG (Temporally regulated expression of Cre recombinase in neural stem cells. Genesis 41:147-153.2005).

Zeltner N, Kohlbrenner E, Clement N, Weber T, Linden RM (Near-perfect infectivity of wild-type AAV as benchmark for infectivity of recombinant AAV vectors. Gene Ther 17:872-879.2010).

Zeng H, Horie K, Madisen L, Pavlova MN, Gragerova G, Rohde AD, Schimpf BA, Liang Y, Ojala E, Kramer F, Roth P, Slobodskaya O, Dolka I, Southon EA, Tessarollo L, Bornfeldt KE, Gragerov A, Pavlakis GN, Gaitanaris GA (An inducible and reversible mouse genetic rescue system. PLoS Genet 4:e1000069.2008).

Zhou X, Muzyczka N (In vitro packaging of adeno-associated virus DNA. J Virol 72:3241-3247.1998).

Zhu P, Aller MI, Baron U, Cambridge S, Bausen M, Herb J, Sawinski J, Cetin A, Osten P, Nelson ML, Kugler S, Seeburg PH, Sprengel R, Hasan MT (Silencing and un-silencing of tetracycline-controlled genes in neurons. PLoS ONE 2:e533.2007).

Zolotukhin S, Potter M, Zolotukhin I, Sakai Y, Loiler S, Fraites TJ, Jr., Chiodo VA, Phillipsberg T, Muzyczka N, Hauswirth WW, Flotte TR, Byrne BJ, Snyder RO (Production and purification of serotype 1, 2, and 5 recombinant adeno-associated viral vectors. Methods 28:158-167.2002).

Zugates CT, Lee T (Genetic mosaic analysis in the nervous system. Curr Opin Neurobiol 14:647-653.2004).